الجمهورية الجزائرية الديموقراطية الشعبية
PEOPLE'S DEMOCRATIC REPUBLIC OF ALGERIA
Ministry of Higher Education and Research

UNIVERSITY OF BLIDA 1
Institute of Aeronautics and Space Studies

Avionics Major

Memory Submitted
In partial fulfillment of the requirements
for Master's degree of Science

Theme:

Enhancing the stabilization of the F-16 fighter aircraft pitch motion control via intelligent and classical method

Under supervision of :

CHEGRANI Ahmed

Presented by:

SAADA Nourhane

Academic Year 2020 - 2021

Dedication

I dedicate this work to my parents 'Hamid and 'Amel' , to my family

and to anyone helped me during my academic career from near or far.

Acknowledgements

First and foremost, I would like to address my thanks to the institute of aeronautics and space studies of Saad Dahlab Blida, that I spent five years of university studies there and continuous successes in it, and today I am reaping the efforts and researches of all these years.

I could never overstate my gratitude towards Professor CHEGRANI Ahmed, for his support, ideas, guidance and encouragement. I have been fortunate to have a supervisor who gave me the freedom to explore on my own, and at the same time thought me how to do research and helped me focus my ideas.

My thanks go out to all my teachers, I express my gratitude and my acknowledgments to them for providing me with all these knowledge throughout my studies. It's thanks to them that I got to this point.

I also would like to thank all the amazing people and my colleagues - far too numerous to name them all - that I have meet over the years. A special thank you goes to 'Chakib'.

I am forever indebted to my parents 'Hamid' and 'Amel' to whom this thesis is dedicated to. They gave me the unconditional love and were a source of my strength and courage all these years. Thank you for being the most amazing parents and for giving me more than I could ask for, all the love from your one and only daughter.

Last but not least, I would like to express a heart-felt gratitude to my family with a special mention to my grandmothers ' Laitmas' and 'Tounes' God rest there souls and pit them in paradise.

ملخص

تقدم هذه الأطروحة في إطارها التصميمي حيث قمنا بخطوات تسلسلية لتنفيذ محاكاة نموذج الطائرة المقاتلة F-16 باستخدام بيئة MATLAB / Simulink. وتم تقديم دراسة نظرية على طائرة F-16 للحصول على نموذج رياضي باستخدام صيغة نيوتن أويلر. وقمنا بتحويل النموذج غير خطي إلى نموذج خطي وفصلنا كل من الاتجاهات الطولية والجانبية حول نقاط التوازن بمراعاة شروط معينة للتعديل وهذا للحصول على نموذج حالة الفضاء. يهدف هذا العمل إلى دراسة وتحليل وتصميم ومراقبة أداء كاملة لوحدات التحكم الكلاسيكية (LQR, PID, FLC) والجديدة (GA-PID, Self-tuning Fuzzy PID , $H2/H\infty$)من حيث التتبع المرجعي لمسار الرحلة وزيادة الاستقرار لحركة الخطران. بناء على النتائج المحققة سيتم إجراء تحليل مقارن.

الكلمات الرئيسية: النماذج غير الخطية / الخطية، المحاكاة، أدوات التحكم الكلاسيكية/القوية، الاستقرار، حركة الخطران.

Abstract

This thesis presents within the framework of a conceptual context simulation of our F-16 fighter aircraft model using the MATLAB/Simulink environment. A theoretical study on the aircraft F-16 will be presented in which a mathematical model was obtained using Newton-Euler formulism. The non-linear model was linearized and decoupled for both longitudinal and lateral directions around equilibrium points at certain trim conditions to obtain state space models. This work aims at a complete study, analysis, design and performance monitoring of the classical (LQR, PID, FLC) and the new robust generation controllers (Self-tuning Fuzzy PID, GA-PID, $H2/H\infty$) in terms of flight trajectory reference tracking and stability augmentation of the pitch motion. From the results achieved a comparative analysis will be investigated.

Keywords: Non-linear/linear models, Simulation, classical/robust controllers, stability, pitch motion.

Résumé

Cette thèse présente dans le cadre d'un contexte conceptuel, un enchainement des étapes pour réaliser la simulation de notre modèle d'avion de chasse F-16 à l'aide de l'environnement MATLAB/Simulink. Une étude théorique sur l'avion F-16 sera présentée dans laquelle un modèle mathématique a été obtenu en utilisant le formalisme de Newton-Euler. Le modèle non linéaire a été linéarisé et découplé pour les directions longitudinale et latérale autour des points d'équilibre à certaines conditions d'ajustement pour obtenir des modèles d'espace d'état. Ce travail vise à une étude complète, une analyse, une conception et un suivi des performances des contrôleurs classiques (LQR, PID, FLC) et de nouvelle génération robuste (Self-tuning Fuzzy PID, GA-PID, $H2/H\infty$) en termes de suivi de référence de trajectoire de vol et d'augmentation de la stabilité du mouvement de tangage. À partir des résultats obtenus, une analyse comparative sera faite.

Mots clés : Modèles non-linéaires/linéaires, Simulation, contrôleurs classiques/robustes, stabilité, mouvement de tangage.

Contents

List of tables

List of figures

Notations and acronyms

USAF	United States Air Force.
UHF	Ultra High Frequency.
VHF	Very High Frequency.
HUD	Head-Up Display.
ASRAAM	Advanced Short Range Air-to-Air Missile.
HARM	High-speed Anti-Radiation Missile.
JASSM	Joint Air-to-Surface Stand-off Missile.
JDAM	Joint Direct Attack Munition.
JSOW	Joint Stand-Off Weapon.
WCMD	Wind-Corrected Munitions Dispenser.
SLAM	Stand-Off Land-Attack Missile.
XR	extended Range.
FLIR	Forward-looking Infrared.
CCD	Charge-Coupled Device.
GPS	Global Positioning System.
TACAN	Tactical Air Navigation System.
IFF	Identification Friend or Foe.
CFT	Conformal Fuel Tanks.
EOM	Equations of motion.
LTI	Linear Time Invariant.

Notations and acronyms

SSC	Side-Stick Controller.
FBW	Fly-By-Wire
RSS	Relaxed Static longitudinal Stability.
AOA	Angle Of Attack.
SM	Static Margin.
MAC	Mean Aerodynamic Chord.
CAP	Control Anticipation Parameter.
LQR	Linear Quadratic Regulator.
PID	Proportional Integral Derivative.
FLC	Fuzzy Logic Controller.
RF	Reference frame.
m	Aircraft mass (Kg).
b	Reference wing span (m).
S	Reference wing area (m^2).
$\bar{c}$	Mean aerodynamic chord (m).
ρ	Atmospheric density.
I_x	Roll moment of inertia (Kg. m^2).
I_y	Pitch moment of inertia (Kg. m^2).
I_z	Yaw moment of inertia (Kg. m^2).
I_{xz}, I_{xy} , I_{yz}	Products moment of inertia (Kg. m^2).
x_{cg}	c.g. location (m).
x_{ac}	Aerodynamic location (m)

Notations and acronyms

x_{cgr}	Reference c.g. location (m).
h_E	Engine angular momentum (Kg. m² /s).
cg	Center of Gravity
$x\ , y\ , z$	Coordinate axes in right-handed coordinate system.
L, M, N	Components of aerodynamic moment in (roll, pitch, yaw) respectively.
$u, v\ , w$	Components of absolute linear velocity vector V expressed in the body coordinate system.
$p, q\ , r$	Components of angular rate vector ω expressed in the body.
$\Phi\ , \theta\ , \psi$	Euler angles rotations in roll, pitch and yaw respectively.
L_A, M_A, N_A	Components of aerodynamic moment vector expressed in body coordinate system (roll, pitch, and yaw) respectively.
$\mathrm{F_E}$	Earth-fixed inertial reference frame.
$\mathrm{F_B}$	Body-fixed reference frame.
$\mathrm{ox_b, y_b, z_b}$	Coordinates of the generalized body axes.
ox_w, y_w, z_w	Coordinates of the wind axes.
x_e, y_e, z_e	Coordinates of earth coordinate system.
V_0	Steady equilibrium velocity.
β	Slide slip angle.
α	Angle of attack.
$U_e\ , V_e\ ,\ W_e$	(Axial, Lateral, Normal) components of steady equilibrium velocity respectively.
θ_e	Steady pitch attitude of the aircraft.
θ	Pitch attitude.

Notations and acronyms

$\mathrm{ox_0, y_0, z_0}$	Orientation of the body coordinate frame before Euler rotations (aligned with the earth reference frame).
ox_1, y_1, z_1	Intermediate orientation of the body coordinate frame after the first Euler rotation.
ox_2, y_2, z_2	Intermediate orientation of the body coordinate frame after the second Euler rotation.
ox_3, y_3, z_3	Intermediate orientation of the body coordinate frame after the third Euler rotation.
δ_ξ	Roll control stick angle.
δ_η	Pitch control stick angle.
δ_ζ	Rudder pedal control angle.
$\mathrm{\delta_e}$	Elevator control input.
δ_{th}	Thrust control input.
$\mathrm{\delta_a}$	Aileron control input.
$\mathrm{\delta_r}$	Rudder control input.
τ	Engine thrust perturbation: Time parameter.
ε	Throttle lever.
ζ	Rudder.
η	Elevator.
ξ	Ailerons.
τ	Thrust.
k_τ	Gain constant.

Notations and acronyms

T_τ	Lag time constant.
W	Total normal velocity.
V	Perturbed total velocity: Total lateral velocity.
U	Total axial velocity.
a'_x, a'_y, a'_z	Inertial or absolute accelerations along the three axes of body coordinate system.
$\dot{p},\ \dot{q},\ \dot{r}$	Components of angular acceleration $\dot{\omega}$ expressed in body coordinate system (roll, pitch, and yaw, respectively).
$\dot{U},\ \dot{V}, \dot{W}$	Components of linear acceleration expressed in the body coordinate system.
X_a, Y_a, Z_a	Components of aerodynamic force vector.
L_a, M_a, N_a	Components of aerodynamic moment vector.
X_g, Y_g, Z_g	Components of gravitational force vector.
L_g, M_g, N_g	Components of gravitational moment vector.
X_c, Y_c, Z_c	Components of aerodynamic control force vector.
L_c, M_c, N_c	Components of aerodynamic control moment vector.
X_p, Y_p, Z_p	Components of power effects force vector.
L_p, M_p, N_p	Components of power effects moment vector.
X_d, Y_d, Z_d	Components of atmospheric disturbances effects force vector.
L_d, M_d, N_d	Components of atmospheric disturbances effects moment vector.
X_u	A shorthand notation to denote the dimensionless derivative $\partial \hat{X}/\partial \hat{u}$.
$\mathring{X}_u$	A shorthand notation to denote the dimensional derivative $\partial X/\partial u$.

Notations and acronyms

$\mathrm{X_u}$	A shorthand notation to denote the American normalised dimensional derivative $\mathring{\mathrm{X}}_u/m$.
L'_v	A shorthand notation to denote a modified North American lateral–directional derivative
$\hat{u}$	A shorthand notation to denote that the variables u is dimensionless.
(◦)	A dressing to denote a dimensional derivative in British notation.
(ˆ)	A dressing to denote a dimensionless parameter.
C_m	Aerodynamic pitch moment coefficient about center of mass.
C_n	Aerodynamic yaw moment coefficient about center of mass.
C_L	Aerodynamic roll moment coefficient about center of mass.
C_D	Aerodynamic drag coefficient.
C_{D_α}	Slope of curve formed by drag coefficient C_D versus angle of attack α.
L	Magnitude of aerodynamic lift force vector.
D	Magnitude of aerodynamic drag force vector.
C_{m_α}	Slope of curve formed by pitch moment coefficient C_m versus angle of attack α.
C_{m_0}	Pitch moment coefficient at zero AOA.
$C_{m_{\delta e}}$	Slope of curve i.e pitching moment coefficient C versus control-surface deflection δ_e.
C_{D_u}	Drag coefficient variation versus velocity.
C_{L_α}	Slope of curve formed by lift coefficient C_L versus angle of attack α.
C_l	Aerodynamic roll moment coefficient about center of mass.

Notations and acronyms

C_{l_β}	Roll damping derivative relative to angle-of sideslip rate.
$C_{l_{\delta a}}$	Slope of curve i.e rolling moment coefficient C versus control-surface deflection δ_a.
C_{l_v}	Lift coefficient for vertical tail .
$C_{L_{max}}$	Maximum lift coefficient.
τ_a	Aileron control surface effectiveness parameter.
C_{n_β}	Slope of curve formed by yawing moment coefficient Cn versus angle of sideslip.
A	State matrix.
B	Input matrix.
I	Identity matrix.
u(t)	Input vector.
x(t)	State vector.
$\mathrm{y}(t)$	column vector of r output variables called the output vector.
C	$(r \times n)$ output matrix.
D	$(r \times m)$ direct matrix.
M	Mass matrix.
K	LQR gain matrix.
Q	LQR weight matrix.
R	The weighing matrix of control variables.
K_p	Proportional gain.
K_I	Integral gain.
K_D	Derivative gain.
k_d	Derivative gain.
T_d	Derivative time.

General Introduction

The F-16 is a fighter aircraft requires a high stability in flight for both offensive and defensive purposes. The military aircrafts demand a high performances, it has introduced areas of concern associated with the aircraft's handling qualities, control and safety. Studies conducted previously show that there are two types of control problems when flying at high angles of attack, these are the 'pitch departures' caused by coupling and the 'deep stall trim'. However avoidance of these problems requires that the airplane have sufficient pitch and roll control. In this approach the introduction of autopilots was one of the great step in aviation development, they were used with the purpose to replace the human pilot during cruise modes , When an aircraft had a deviation form a particular flight path, the autopilots alter the roll, pitch and heading angles of an aircraft.

In recent decades, enormous techniques including linear and non-linear approaches are investigated to propose control schemes for F-16, such as proportional-integral-derivative (PID), linear quadratic regulator (LQR) and fuzzy logic; they have been studied to stabilize the aircraft during flight operations. The LQR is a well-known controller for minimizing cost functions. Indeed PID controller is another commonly used controller, implemented successfully to enhance the response times of systems, popular by it simple structure that can be easily applied with sufficient performance. Fuzzy logic controllers fall into the class of intelligent control systems; it's a mathematical tool for dealing with uncertainty by providing a technique to deal with imprecision and information granularity.

As aircraft handling and performance requirements increased so did the complexity of the flight control system, now the big question to ask is: *"Can the classical controllers keep the aircraft stable in critical situations?"* Of course, the short answer is that technology does not stand still: new solution capabilities are always emerging. The focus of this study is to develop the design of mixed controllers, in addition to that, our main problematic is based on the following questions: *"will these controllers be reliable to meet the required stability?"*, "*will they be able to guarantee control adaptive convergence must occur in less than 8.5 seconds", "*will it be possible to maintain the pitch control under a variety of complex maneuvers conditions including approach, subsonic cruise and supersonic cruise?".

Therefore this project proposes three robust controllers based on combining different design schemes and new algorithms such as genetic algorithm assuring better optimization

for the PID controller. The objective of this thesis is to demonstrate and present a comparative study of the proposed new technology by completing the conceptual design with simulation results using MATLAB/Simulink environment, and all the conclusions and hypotheses achieved will be discovered later during this scientific research.

This thesis is organized as follows:

Firstly**, Chapter 1** provides a brief description about our aircraft model F-16 Fighter Falcon.

Then, **Chapter 2** introduces the development of the equations of motion considering the main moments and forces acting on the aircraft, stating some assumptions, presenting the coordinate systems and then developing the mathematical non-linear dynamic model, after that we introduce the linearization method based on small perturbations theory , finally the decoupled equations of motion are determined.

Furthermore, **Chapter 3** discusses the stability and control analysis includes static and dynamic stability for longitudinal, lateral and directional motions. Indeed military flying qualities have been introduced.

Control design constitutes one of the main topics approached in this work and is presented in **chapter 4.** First, a control architecture of the classical controllers PID, LQR , FLC is proposed , followed by the combined architecture of new controllers self-tuning PID , GA-PID and finally mixed $\mathrm{H}_2/\mathrm{H}_\infty$ **.**

Finally, **chapter 5** concludes this work by highlighting the main results and discussing the comparative analysis between the traditional controllers and the mixed robust new controllers.

Chapter 1: An overview about fighter aircraft F-16

Chapter 1: An overview about fighter aircraft F-16

1.1 Introduction

This chapter will cover an overview about the fighter aircraft F-16 which will be applied as a dynamic model of our study in the next chapters. A brief introduction to the technology and flight equipment systems and design history of the aircraft will be discussed.

1.2 Description

The Lockheed F-16 Fighting Falcon which is shown in Figure 1.1 , is a single-engine , supersonic ,multi-role fighter aircraft originally developed by General Dynamics for the United States Air Force (USAF) , It was initially ridiculed and rejected by both the company and the Air Force for being too small and too light to go anywhere or carry anything significant. Nevertheless, the F- 16 has proven to be an extraordinary fighter. The F-16 has been ordered by 24 countries and is operating in the air forces of more than 20 countries.

The F-16 and the F-15 Eagle were the world's first aircraft able to withstand higher g-forces than the pilot's .The judicious application of advanced technologies combined with design innovations gives the airplane its unprecedented combat performance at an affordable cost, designed as an air superiority day fighter, it evolved into a successful all-weather multi-role aircraft. Over 4,500 aircraft have been built since production was approved in 1976. Although no longer being purchased by the U.S. Air Force, improved versions are still being built for export customers. In 1993, General Dynamics sold its aircraft manufacturing business to the Lock-heed Corporation, which in turn became part of Lockheed Martin after a 1995 merger with Martin Marietta.

Figure 0.1: *F-16 aircraft model* [2].

1.3 Design properties

The F-16 is a revolutionary aircraft designed by Harry Hillaker. It represents a major change in fighter design; its fine blend of high technology and common sense requirements emphasizes flight performance-range, persistence, and maneuverability right in the heart of the flight envelope where air combat takes place. The structural criteria were fully compatible with the aerodynamic capacity of the airplane and the pilot's physical tolerance. The structural design which is shown in Figure 1.2 load factor was set at 9.0 g's at start of combat with full internal fuel, as contrasted to the normal military specification of 7.33 g's with only 60 percent internal fuel. F-16 models are denoted by increasing block numbers to denote upgrades. The blocks cover both single- and two-seat versions. A variety of software, hard-ware, systems, weapons compatibility and structural enhancements have been instituted over the years to gradually upgrade production models and retrofit delivered aircraft. While many F-16s were produced according to these block designs, there have been many other variants with significant changes, usually due to modification programs. Other changes have resulted in role-specialization, such as the close air support and reconnaissance variants. Several models were also developed to test new technology. The F-16 design also inspired the design of other aircraft, which are considered derivatives.

The F-16 introduced many successful technologies. Fly-by-wire and relaxed static stability gave the F-16 a quantum leap in air combat capability over other fighters when it was introduced and this technology still makes the aircraft an unmatched competitor today. Its

provides excellent flight control through its “fly-by-wire” system, side-stick controller, highly accurate inertial navigation system, UHF/VHF radios, instrument landing system, AN/APG-66/68 radar warning system, and modular countermeasure pods, a notable product of advanced technology. Flight control system is the link that integrates the pilot and the airframe into a highly responsive and effective combat fighter, this advanced system is a radical departure from previous systems. Indeed With a fly-by-wire system, the pilot commands roll, pitch, or yaw rate—not surface deflection, as in a conventional system. When the pilot makes a roll input, for instance, he commands a roll rate that varies with the force of his input. If he releases his input, the airplane maintains the resultant bank angle until he makes another control input; he doesn’t have to center the “control stick” to maintain the bank angle as he does with a conventional system.

Beyond the necessary control of flight, the pilot has precise response control. The reduced lags and overshoots afforded by the better kinematics of the electronic circuitry results in greatly improved and expanded flying qualities, which, in turn, significantly improve the response and tracking accuracy of the pilot-airframe system. A much higher level of precise, non-varying control response is possible throughout the flight envelope with the fly-by-wire system than with conventional flight control systems. The resulting system is a quad-redundant (fail-operative, fail-safe), high-authority, command-and-stability augmentation system. The system consists of a series of sensors (accelerometers, rate gyros, air data converter), computers, selectors, transducers, and inverters that collectively generate the pitch, roll, and yaw rates that are transmitted as electronic signals to the five triplex electrohydraulic, servo actuators that control the flappers (roll and flaps), elevens (pitch and roll), and rudder.

All F-16s delivered since November 1981 have built-in structural and wiring provisions and systems architecture that permit the multi-role flexibility to perform precision strike, night attack and beyond-visual-range interception missions. The weight saving resulting from the absence of cables, linkages, bell cranks, and the ratio changer was translated into redundancy. The redundancy level and the freedom of routing afforded by wire harnesses improved the reliability and increased the operational survivability of the airplane and contributed to its compactness and small size.

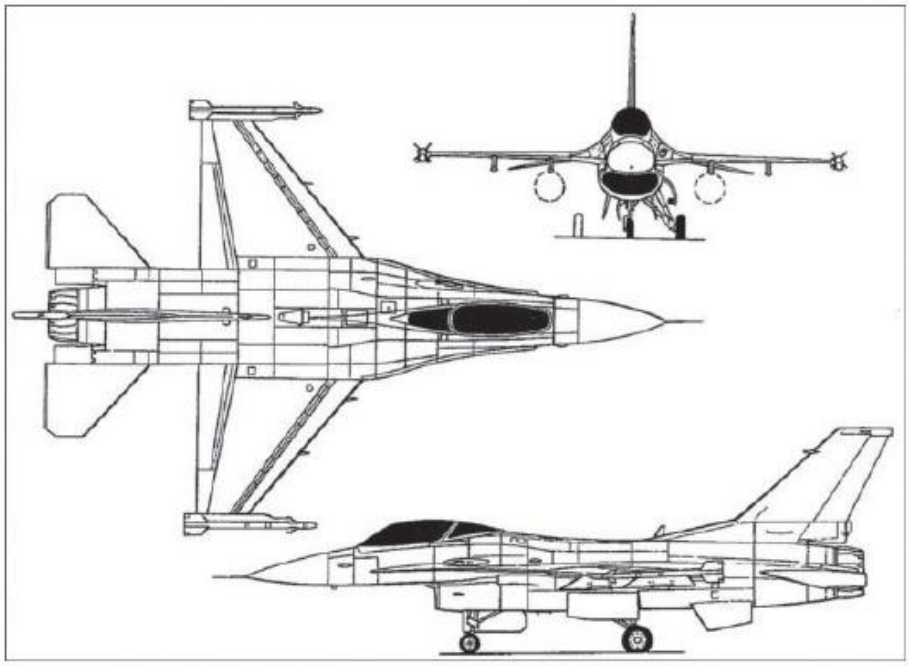

Figure 0.2: *3D view of the General Dynamic F-16 aircraft* [3].

1.4 Flight equipment

1.4.1 F-16 missiles and weapons

The aircraft has nine hard points for weapons payloads: one at each wing tip, three under each wing, and one centerline under the fuselage. The ordnance is launched from Raytheon LAU-88 launchers, MAU-12 and Organ bomb ejector racks. The port wing is fitted with a 20mm General Electric M61A1 multi-barrel cannon and the gunsight is interfaced to the cockpit HUD.

Air-to-air missiles carried on the F-16 include the Lockheed Martin / Raytheon AIM-9 Sidewinder, Raytheon AMRAAM, Raytheon Sparrow, MBDA (formerly Matra BAe Dynamics) Skyflash and ASRAAM, and the MBDA R550 Magic 2. In April 2004, the F-16 first fired the new-generation AIM-9X Sidewinder, which is in full-rate production for the USAF. Air-to-surface missiles carried on the F-16 include Maverick, HARM and Shrike missiles, manufactured by Raytheon, and anti-ship missiles include Boeing Harpoon and Kongsberg

Penguin. Flight tests with the Lockheed Martin joint air-to-surface stand-off missile (JASSM) have been conducted from the F-16.

The first guided launch of the new joint direct attack munition (JDAM) was successfully carried out from an F-16. It was the first USAF aircraft to be fitted with the joint stand-off weapon (JSOW) in April 2000.

The F-16 can be fitted with Lockheed Martin wind-corrected munitions dispenser (WCMD), which provides precision guidance for CBU-87, -89, and 97 cluster munitions. The system corrects for launch transients, ballistic errors, and winds aloft.

The F-16 is the first aircraft to use the USAF's new weapon rack, the Edo Corporation BRU-57. The BRU-57 is a vertical ejection rack which doubles the aircraft's capacity for precision-guided weapons such as the JDAM and WCMD.

All-weather stand-off weapons, such as the AGM-84E stand-off land-attack missile (SLAM) and the AGM-142 Popeye II, are planned to be included in future upgrades to the aircraft. Other advanced weapons include MICA, IRIS-T, Python IV, Active Skyflash air-to-air missile, ALARM anti-radiation missile, Apache multimission stand-off weapon, autonomous free-flight dispenser system and AS30L laser-guided missile.

1.5 Targeting

The F-16 carries the Lockheed Martin LANTIRN infrared navigation and targeting system. This is used in conjunction with a BAE Systems holographic display. Block 50/52 aircraft are equipped with the HARM targeting system, AN/ASQ-213 from Raytheon. US Air National Guard F-16 aircraft are fitted with Northrop Grumman Litening II / Litening ER targeting pods.

In August 2001, Lockheed Martin was selected to provide the Sniper XR as the new advanced targeting pod for USAF F-16 and F-15E aircraft. Sniper XR (extended range) incorporates a high-resolution mid-wave FLIR, dual-mode laser, CCD TV, laser spot tracker and laser marker combined with advanced image processing algorithms , deliveries began in March 2003.

1.6 Radar

The Northrop Grumman AN/APG-68 radar provides 25 separate air-to-air and air-to-ground modes, including long-range, all-aspect detection and tracking, simultaneous multiple-target tracking, and high-resolution ground mapping. The planar antenna array is installed in the nose of the aircraft.

An upgraded version of the radar, AN/APG-68(V)9, has begun flight testing. The upgrade features a 30% increase in detection range, five times increase in processing speed, ten times increase in memory, as well as significant improvements in all modes, jam-resistance and false alarm rate.

1.7 Navigation and communications of F-16 Fighting Falcon

The F-16 was the first operational US aircraft to receive a global positioning system (GPS). The aircraft has an inertial navigation system and either a Northrop Grumman (Litton) LN-39, LN-93 ring laser gyroscope or Honeywell H-423.

Other navigation equipment includes a BAE Systems Terprom digital terrain navigation system, Gould AN/APN-232 radar altimeter, a Rockwell Collins AN/ARN-118 tactical air navigation system (TACAN) and Rockwell Collins AN/ARN-108 instrument landing system.

The communications systems include the Raytheon UHF AN/ARC-164 receiver / transmitter and Rockwell Collins VHF AM/FM AN/ARC-186 together with AN/APX101 identification friend or foe (IFF) and encryption / secure communications systems. The AN/APX-101 is being upgraded with BAE Systems AN/APX-113.

1.8 Engines

The aircraft is powered by a single engine: the General Electric F110-GE-129 or Pratt and Whitney F100-PW-229. The fuel supply is equipped with an inert gas anti-fire system. An inflight refueling probe is installed in the top of the fuselage.

Lockheed Martin completed developmental flight testing on new conformal fuel tanks (CFT) for the F-16, which will significantly add to the aircraft's mission radius. The first flight of the F-16 equipped with the new tanks was in March 2003. Greece is the launch customer for the CFT [2].

1.9 Aircraft Specifications

In this section we will describe the properties used with certain assumptions and indicated values to be able to perform further calculations in further chapters. Table 1.1 shows the assume values of specific parameters.

Table 0.1: Mass and geometric properties of F-16 [7].

Parameter	**Symbol**	**Value**
aircraft mass (Kg)	*m*	9295.44
reference wing span (m)	*b*	9.144
reference wing area (m^2)	*S*	27.87
mean aerodynamic chord (m)	$\bar{c}$	3.45
roll moment of inertia (Kg. m^2)	I_x	12874.8
pitch moment of inertia (Kg. m^2)	I_y	75673.6
yaw moment of inertia (Kg. m^2)	I_z	85552.1
product moment of inertia (Kg. m^2)	I_{xz}	1331.4
product moment of inertia (Kg. m^2)	I_{xy}	0.0
product moment of inertia (Kg. m^2)	I_{yz}	0.0
c.g. location (m)	x_{cg}	0.3$\bar{c}$
reference c.g. location (m)	x_{cgr}	0.35$\bar{c}$
engine angular momentum (Kg. m^2 /s)	h_E	216.9

1.10 Summary

In this chapter we have described the F-16 aircraft, it was designed to be relatively inexpensive to build and simpler to maintain than earlier-generation fighters and it showed advantageous performances effectiveness in completing military missions. One of the revolutionary features of the F-16 is its flight control system, a notable product of advanced technology, “flyby-wire” was the star technology. New versions are improved over years and a large number of variants and derivative designs have been produced significantly influenced by the F-16.

Chapter 2: Aircraft equations of motion

Chapter 2: Aircraft equations of motion

2.1 Introduction

The performance of an aircraft can adequately be described by assuming the aircraft is a point mass concentrated at the aircraft's center of gravity (cg). The flying qualities of an aircraft, on the other hand, cannot be described in such a simple manner. The flying qualities of an aircraft must instead be described analytically as motions of the aircraft's cg as well as motions of the airframe about the cg, both of which are caused by aerodynamic, thrust and other forces and moments.

In addition, the aircraft must be considered a three dimensional body and not a point mass. The applied forces and moments on the aircraft and the resulting response of the aircraft are traditionally described by a set of equations known as the aircraft equations of motion (EOM).

This chapter presents the form of the aircraft equations of motion used in our aircraft dynamic model. The purpose is to provide an understanding of the different sets of equations used for describing the dynamics of the aircraft system and to express them in the state-space form. The equations will be derived with respect to an inertial Earth-based frame as well as a body reference frame.

2.2 Systems of axes and control notation

To build a mathematical model it is necessary to introduce the aircraft axes and notation in which the (EOM) can be developed in an orderly way. As we know aircraft have six degrees of freedom which make the description of their motion more complex. Therefore for analyzing the rigid body dynamics of an airplane, three axis systems have to be defined.

2.2.1 Description of the F-16 model coordinate system (OVERVIEW)

First let introduce the F-16 body axes model which are conventional. The x-axis is positive out the nose of the aircraft. The y-axis is positive out the right wing as you sit in the cockpit and face out the front of the aircraft. The z-axis is positive normal to the x and y axis and points vertically downward when the aircraft is in the level flight. The moment axes obey the right hand rule about each axis. Moments about x, y and z-axis are labeled $M, L,$ and N, respectively. The body rates $(p, q \text{ and } r)$ and Euler angles $(\phi, \theta \text{ and } \psi)$ are also measured positively using the right-hand rule about each axis. The Figure 2.1 describes the F-16 body axes.

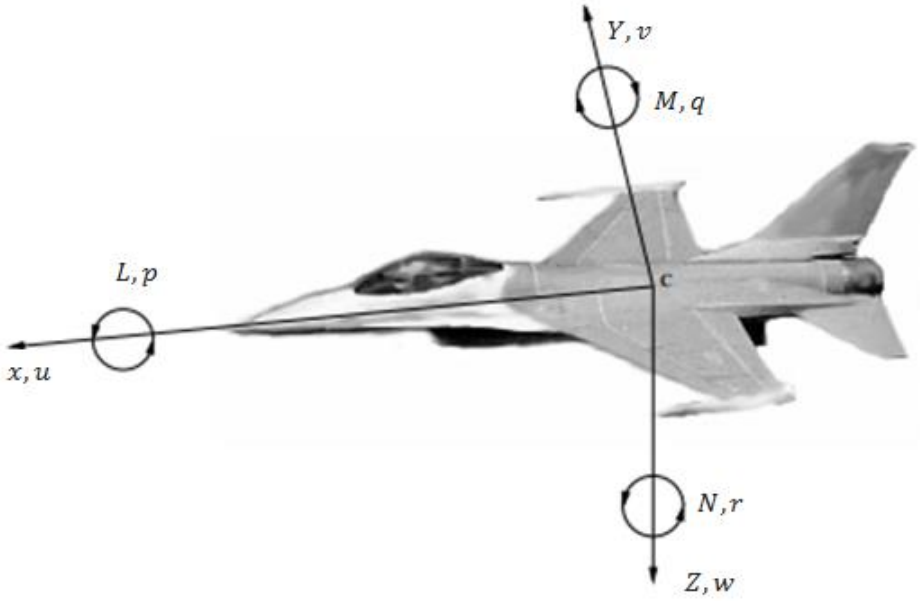

Figure 2.1*: F-16 body axes* [2].

2.2.2 Reference frames and assumptions:

In this section we will produce a development to the reference frames that will be used to determine the equations of motions with listing some assumptions used to facilitate the solution.

2.2.3 Reference frames

When working with a flight dynamics' problem it is crucial to choose a proper reference frame (RF) that specifies the needs of the problem. There is several reference frames, which one is most convenient to use depends on the circumstances. We will examine a few, the most common known frames are the earth-fixed inertial reference frame which is written as $(\mathrm{F_E})$ and the body-fixed reference frame which is noted as $(\mathrm{F_B})$. Both references are shown in Figure 2.2.

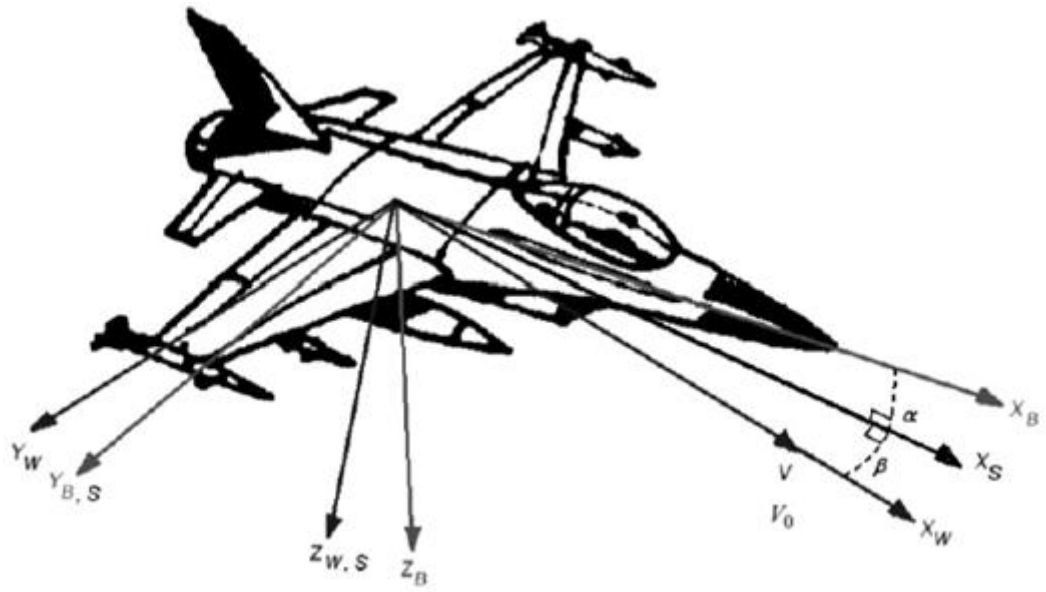

Figure 2.2: *Aircraft reference frames* [5].

Before advancing to the equations of motion (EOM), several reference frames will be presented:

- **Earth-based inertial frame:**

An inertial coordinate system Figure 2.2 is defined as a system in which Newton's second law is valid. The equations of motion must, therefore, be determined in an inertial coordinate system. Another way of defining the inertial coordinate system is to assume it is an axis system fixed in space that has no relative motion.

Experience with physical observations can be used to determine whether a particular reference system can properly be assumed to be an inertial coordinate system for the application of Newton's laws to a particular problem. For space dynamics in our solar system, the sun axis system is a sufficient approximation for an inertial system. For aircraft, the earth axis system is usually a sufficient approximation for an inertial coordinate system. The selection of this frame implies that the effects of the rotational velocity of the earth can be neglected within this context.

- **Aircraft-based body frame:**

  There are many different types of body frame which are used to describe aircraft motion which are:

  - **Generalized body axes:**

The aircraft based body frame $(\mathrm{ox_b}, \mathrm{y_b}, \mathrm{z_b})$ is located at the center of gravity (cg) which is fixed in the aircraft as shown in Figure 2.2. Thus when the aircraft is disturbed from its initial flight condition the axes move with the airframe and the motion is quantified in terms of perturbation variables referred to the moving axes. The $(\mathrm{ox_b}, \mathrm{z_b})$ plane defines the plane of symmetry of the aircraft and the $\mathrm{ox_b}$ axis is arranged such that it is parallel to the geometrical horizontal fuselage datum. Thus in normal flight attitudes the $\mathrm{oy_b}$ axis is directed to starboard and the $\mathrm{oz_b}$ axis is directed downwards. The origin o of the axes is fixed at a convenient reference point in the airframe which is usually, but not necessarily, coincident with the center of gravity (cg).

  - **Aerodynamic, wind or stability axes:**

It is often convenient to define a set of aircraft fixed axes such that the ox axis is parallel to the total velocity vector V_0 as shown in Figure 2.2. Such axes are called aerodynamic, wind or stability axes. In steady symmetric flight wind axes (ox_w, y_w, z_w) are just a particular version of body axes which are rotated about the oy_b axis through the steady body incidence angle α until the ox_w axis aligns with the velocity vector.

The x-stability axis is the projection of the velocity vector of the aircraft on the plane of symmetry. The angle between the velocity vector and the x-stability axis is defined as the slide slip β (beta). The angle between the x-stability axis and the x-body axis is defined as angle of attack angle α (alpha). The z-stability axis is in the plane of symmetry of the aircraft. The stability-axes are used for analyzing the effect of perturbations from steady-state flight.

2.2.4 Steady-state conditions and perturbation variables

Assuming that the airplane to be a rigid body, the motion is described in terms of force, moment, linear and angular velocities and attitude determined into components. Thus initially, the aircraft is assumed to be in steady rectilinear, but not necessarily level, flight when the angle of attack is α and the steady velocity V_0 resolves into components U_e V_e and W_e as indicated in Figure 2.3. The steady-state flight conditions are defined as those conditions where the linear and angular accelerations are zero and it is referred to as trimmed equilibrium.

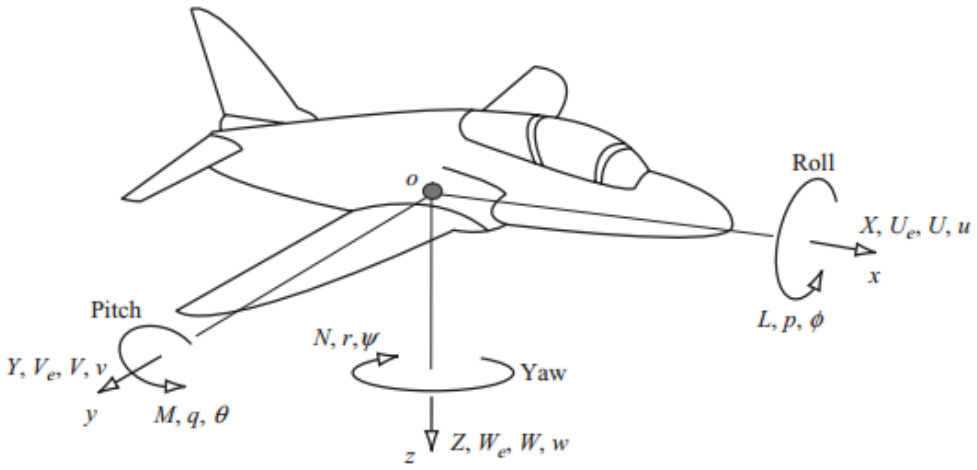

Figure 2.3: *Motion variables notation* [6].

Now the perturbed flight conditions are defined in which all the motion variables of the aircraft dynamics deviate from the steady-state values. The disturbance from the equilibrium is presented by a set of perturbed variables terms that are shown in Figure 2.3 and summarized in Table 2.1.

Table 2.1: *Summary of motion variables* [6].

	Trimmed equilibrium			***Perturbed***		
Aircraft axis	ox	oy	oz	ox	oy	oz
Force	0	0	0	X	Y	Z
Moment	0	0	0	L	M	N
Linear velocity	U_e	V_e	W_e	U	V	W
Angular velocity	0	0	0	p	q	r
Attitude	0	θ_e	0	ϕ	θ	ψ

A simple description of the perturbation variables is given in Table 2.2. Note that the components of the total linear velocity perturbations (U, V, W) are given by the sum of the steady equilibrium components and the transient perturbation components (u, v, w) thus:

$$U = U_e + u$$
$$V = V_e + v$$
$$W = W_e + w \tag{2.1}$$

Table 2.2: *The perturbation variables* [6].

X	Axial "drag" force	Sum of the components of
Y	Side force	aerodynamic , thrust and
Z	Normal "lift" force	weight forces
L	Rolling moment	Sum of the components of
M	Pitching moment	aerodynamic , thrust and
N	Yawing moment	weight forces
p	Roll rate	Component of angular
q	Pitch rate	velocity
r	Yaw rate	
U	Axial velocity	Total linear velocity
V	Lateral velocity	components of the *cg*
W	Normal velocity	

2.2.5 Angular relationships in symmetric flight

With reference to Figure 2.4, the steady velocity vector V_0 defines the flight path and y_e is the steady flight path angle and θ_e is the steady pitch attitude of the aircraft. At a given moment during the disturbance it is clearly seen at the figure that the axes have displaced from its origin, also the relative angular has changed.

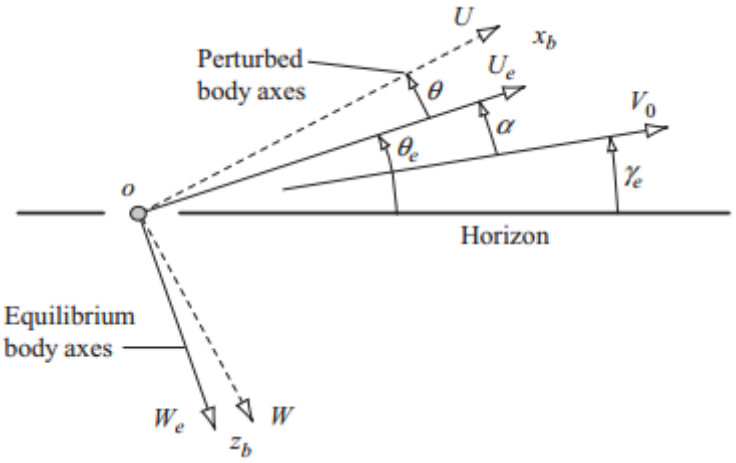

Figure 2.4: *Generalized body axes in symmetric flight* [6].

Thus the steady flight path angle is given by:

$$y_e = \theta_e - \alpha \tag{2.2}$$

In the case when the aircraft fixed axes are wind axes rather than body axes, then:

$$\alpha = 0 \tag{2.3}$$

and in the special case when the axes are wind axes and when the initial condition is level flight,

$$\alpha = \theta_e = 0 \tag{2.4}$$

It is also useful to note that the perturbation in pitch attitude θ and the perturbation in the angle of attack α are the same thus:

$$\tan(\alpha_e + \theta) = \frac{W}{U} = \frac{W+w}{U_e + u} \tag{2.5}$$

2.2.6 Choice of axes

As we have seen before there are many coordinate systems , now the most frequent question to ask is : *what axe is the most appropriate to use for analyzing aircraft motion ?* The answer to this question depends on which axe facilitates the analysis of the (EOM), so it is preferable to use the generalized body axes. While Wind axes are not generally used in the analysis of the motion of a rigid body, because, as in the case of the earth axes, the moment of inertia and product of inertia terms in the three rotational equations of motion vary with time, α and β.

Aerodynamic measurements are referenced to the free stream velocity vector and the measuring equipment is installed in the aircraft, its location is precisely known in terms of body axis coordinates, which therefore determines the best choice of axis system.

Thus, to summarize, we don't really interest particularly to which axis system is chosen. So it becomes necessary to have the mathematical tools to transform data between different reference axes.

2.2.7 Assumptions

The aircraft mass is subjected to the gravity acceleration. According to the "flat-Earth"; assumption, the g vector is aligned with the Z axis of the Earth-based reference frame. In addition, the following assumptions are in place for the derivation of the aircraft equations of motion:

- We consider the aircraft as a rigid-body, where a rigid body is is a system of particles for which the distances between the particles and the angle between the lines remain unchanged. Thus, if each particle of such a body is located by a position vector from reference axes attached to and rotating with the body, there will be no change in any position vector as measured from these axes. Of course this is an idealization since all

solid materials change shape to some extent when forces are applied to them. This assumption is quite valid for fighter aircrafts.

- The earth is at and non-rotating and regarded as an inertial reference, this is valid when dealing with control design of aircraft, but not when analyzing inertial guidance systems.
- The mass is constant during the time interval over which the motion is considered that is, the fuel consumption is neglected during this time-interval.
- The mass distribution is assumed to be time constant with time. This implies that the inertial characteristics of the aircraft (that is, the moments and the products of inertia) can be assumed constant over a limited amount of time. In reality, these inertial characteristics change with fuel consumption; however, the rate of change for these parameters is low because, by design, the center of gravity of the fuel tanks is located close to the aircraft cg. Nevertheless, rapid changes in the moments of inertia can be experienced due to different reasons, such as fuel slosh, dropping of wing stores for military aircraft, or non-nominal events, such as sudden shifts of cargos within the fuselage.
- The aircraft is symmetric.
- There is constant wind.

2.2.8 Euler angles and aircraft attitude

In flight dynamics the orientation of any reference frame relative to another can be given by three angles, Euler angles (ϕ, θ, ψ) .A function of these angles allow the mutual transformation from a fixed reference frame (coordinate system, $\mathrm{F_E}$)) to the local reference frame (fixed-body frame, $\mathrm{F_B}$), for small angles, each of the Euler angles has the following designation:

- Roll angle : $\phi \in [-\pi, \pi]$ (rad)
- Yaw angle : $\psi \in [0, 2\pi]$ (rad)
- Pitch angle : $\theta \in \left[-\frac{\pi}{2}, \frac{\pi}{2}\right]$ (rad)

The aircraft attitude is the angular orientation of the airframe fixed axes with respect to earth axes. Therefore attitude angles are a particular application of Euler angles. As shown in Figure 2.5 (ox_0, y_0, z_0) are reference axes and (ox_3, y_3, z_3) are aircraft fixed axes, referred

to the generalized body axes or wind axes. The attitude of the aircraft may be obtained considering the rotation about each axis and bringing (ox_3, y_3, z_3) into coincidence with (ox_0, y_0, z_0) . Thus, first rotate about ox_3 through the roll angle ϕ to (ox_2, y_2, z_2) . Second, rotate about oy_2 through the pitch angle θ to (ox_1, y_1, z_1) and third, rotate about oz_1 through the yaw angle ψ to (ox_0, y_0, z_0) . Clearly, with the respect of earth axes the attitude is considered, then (ox_0, y_0, z_0) and (ox_E, y_E, z_E) are coincident.

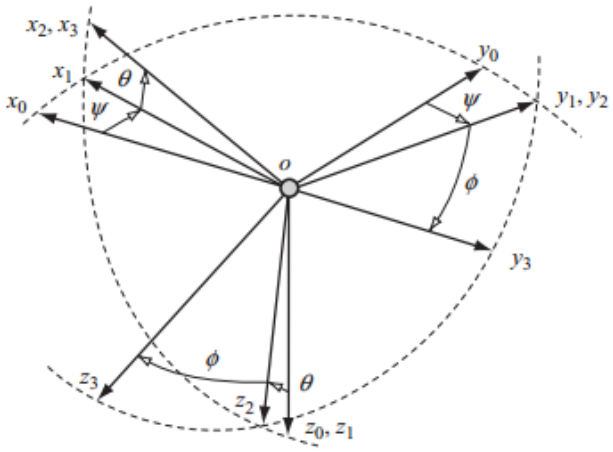

Figure 2.5: *The Euler angles* [6].

2.2.9 Controls notation

To control an aircraft, control surfaces are generally used. Examples are elevators, flaps and spoilers. When dealing with control surfaces, we can make a distinction between primary and secondary flight control surfaces. When primary control surfaces fail, the whole aircraft becomes uncontrollable, (examples are elevators, ailerons and rudders).However, when secondary control surfaces fail, the aircraft is just a bit harder to control. (Examples

are aps and trim tabs).The whole system that is necessary to control the aircraft is called the control system. When a control system provides direct feedback to the pilot, it is called a reversible system.

2.2.9.1 Aerodynamic controls

An aircraft typically has three aerodynamic controls, each capable of producing moments about one of the three basic axes as shown in Figure 2.6. The elevator consists of a trailing-edge flap on the horizontal tail. Elevator deflection is characterized by the deflection angle δ_η. Elevator deflection is defined as positive when the trailing edge rotates downward, so for a configuration in which the tail is aft of the vehicle center of mass.

The rudder consists of a trailing-edge flap on the vertical tail. Rudder deflection is characterized by the deflection angle δ_ζ. Rudder deflection is defined as positive when the trailing edge rotates to the left.

The ailerons consist of a pair of trailing-edge flaps, one on each wing, designed to deflect differentially. Aileron deflection is characterized by the deflection angle δ_ξ. Aileron deflection is defined as positive when the trailing edge of the aileron on the right wing rotates up (and, correspondingly, the trailing edge of the aileron on the left wing rotates down).

Aileron, elevator and rudder surface displacements are denoted ξ, η and ζ respectively as indicated in Figure 2.6.

By vehicle symmetry, the elevator produces only pitching moments, but there invariably is some cross-coupling of the rudder and aileron controls, means that rudder deflection usually produces some rolling moment and aileron deflection usually produces some yawing moment.

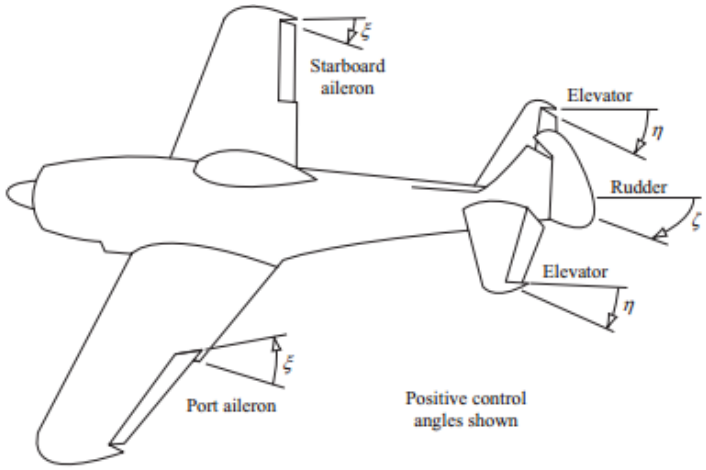

Figure 2.6: *Aerodynamic controls* [6].

2.2.9.2 Aerodynamic controls of F-16 model

The F-16 model allow for control over thrust, elevator, aileron and rudder. The thrust is measured in pounds and acts positively along the positive body x −axis. Positive thrust causes an increase in acceleration along the body x −axis. For the other control surfaces a positive deflection gives a decrease in the body rates. A positive aileron deflection gives a decrease in the roll rates , p, this requires that the right aileron deflect downward and the left aileron deflect upward. A positive elevator deflection results in a decrease in pitch rate , q , thus elevator is deflected downwards. Positive deflection of the rudder decreases the yaw rate , r, and can be described as a deflection to right. The positive orientation for each control surface is shown in Figure 2.7 the maximum values and units are listed in table 2.3. It is important to understand the motion of the airplane and the basic parts that make an airplane move, Figure 2.7 shows the basic three parts that moves the airplane.

Figure 2.7: *Control Surfaces of an F-16 Model* [7].

Table 2.3: *The control input units and maximum values* [7].

	UNITS			
Control	Input	Used by nplant	Min	Max.
Thrust	lbs.	Lbs.	1000	19000 lbs.
Elevator	deg.	deg.	-25	25 deg.
Aileron	deg.	deg.	-21.5	21.5 deg.
Rudder	deg.	deg.	-30	30 deg.
Leading Edge Flap	deg	deg	0	25 deg.

2.2.9.3 Engine control

Engine thrust is controlled by throttle lever displacement ε. It is usually in the forward push sense and results in a positive increase in thrust. For a turbojet engine the relationship between thrust and throttle lever angle is approximated by a simple first order lag transfer function:

$$\frac{\tau(s)}{\varepsilon(s)} = \frac{k_\tau}{(1 + sT_\tau)} \tag{2.6}$$

Where k_τ is a suitable gain constant and T_τ is the lag time constant which is typically of the order of 2–3 s.

2.3 The Nonlinear equations of motion of a rigid symmetric aircraft

The equations of motion for a rigid symmetric aircraft starts from the well-known Newton's second law of motion for each of the six degrees of freedom given by:

$$F = ma \tag{2.7}$$

For a rotational motion the mass and acceleration are evaluated to moment of inertia and angular acceleration respectively while the disturbing force becomes the disturbing moment or torque. Thus the derivation of the EOM requires that equation (2.7) be expressed in terms of the motion variables defined previously.

2.3.1 The components of inertial acceleration

In result from the application of disturbing force components to the aircraft, the inertial acceleration components are defined. Consider the motion referred to an orthogonal axis set $(oxyz)$ with the origin o coincident with the cg of the arbitrary .The body, and hence the axes, are assumed to be in motion with respect to an external reference frame such as earth (or inertial) axes.

The components of velocity and force along the axes ox, oy and oz are denoted (U, V, W) and (X, Y, Z) respectively as presented in Figure 2.8. The components of angular velocity and moment about the same axes are denoted (p, q, r) and (L, M, N) respectively. The point p is an arbitrarily chosen point within the body with coordinates (x, y, z). The local components of velocity and acceleration at p relative to the body axes are denoted

(u, v, w) and (ax, ay, az) respectively. The velocity components at p (x, y, z) relative to o are given by:

$$\begin{aligned} u &= \dot{x} - ry + qz \\ v &= \dot{y} - pz + rx \\ w &= \dot{z} - qx + py \end{aligned} \tag{2.8}$$

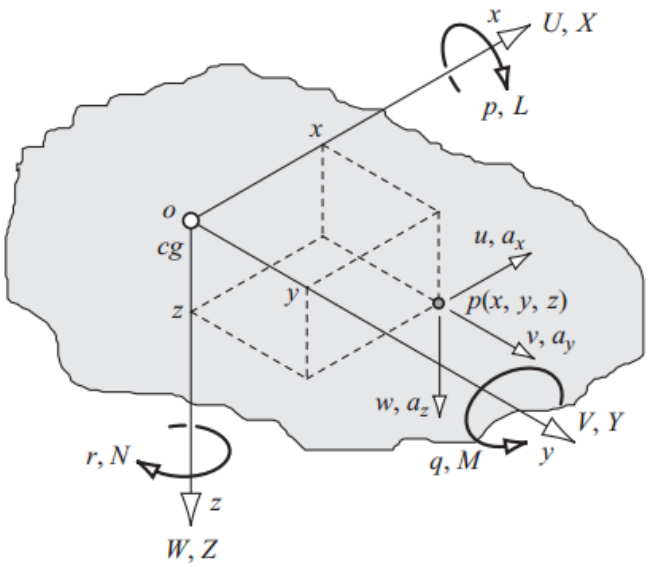

Figure 2.8: *Motion referred to generalized body axes* [6].

Now, since the generalized body shown in Figure 2.8 represents the aircraft which is assumed to be rigid then:

$$\dot{x} = \dot{y} = \dot{z} = 0 \tag{2.9}$$

and equations (2.8) reduce to:

$$\begin{aligned} u &= qz - ry \\ v &= rx - pz \\ w &= py - qx \end{aligned} \tag{2.10}$$

The corresponding components of acceleration at $p(x, y, z)$ relative to o are given by:

$$\begin{aligned} a_x &= \dot{u} - \mathrm{rv} + \mathrm{qw} \\ a_y &= \dot{v} - pw + ru \\ \mathrm{a}_z &= \dot{w} - \mathrm{qu} + \mathrm{pv} \end{aligned} \tag{2.11}$$

By superimposing the velocity components of the cg (U, V, W) on to the local velocity components (u, v, w) the inertial, velocity components (u', v', w') of the point $p(x, y, z)$ are obtained. Thus:

$$\begin{aligned} u' &= U + u = U - ry + qz \\ v' &= V + v = V - pz + rx \\ w' &= W + w = W - qx + py \end{aligned} \tag{2.12}$$

where the expressions for (u, v, w) are substituted from equations (2.10). Similarly, the components of inertial acceleration (a'_x, a'_y, a'_z) at the point $p(x, y, z)$ are obtained simply by substituting the expressions for (u', v', w') , equations (2.12), in place of (u, v, w) in equations (2.11). Whence:

$$\begin{aligned} a'_x &= \dot{u}' - rv' + qw' \\ a'_y &= \dot{v}' - pw' + ru' \\ a'_z &= \dot{w}' - qu' + pv' \end{aligned} \tag{2.13}$$

Differentiate equations (2.12) with respect to time and note that since a rigid body is assumed equation (2.9) applies then:

$$\begin{aligned} \dot{u}' &= \dot{U} - \dot{r}y + \dot{q}z \\ \dot{v}' &= \dot{V} - \dot{p}z + \dot{r}x \\ \dot{w}' &= \dot{W} - \dot{q}x + \dot{p}y \end{aligned} \tag{2.14}$$

Thus, by substituting from equations (2.12) and (2.14) into equations (2.13) the inertial acceleration components of the point $p(x, y, z)$ in the rigid body are obtained which, after some rearrangement, may be written:

$$\begin{aligned} a'_x &= \dot{U} - rV + qW - x(q^2 + r^2) + y(pq - \dot{r}) + z(pr + \dot{q}) \\ a'_y &= \dot{V} - pW + rU + x(pq + \dot{r}) - y(p^2 + r^2) + z(qr - \dot{p}) \\ a'_z &= \dot{W} - qU + pV + x(pr - \dot{q}) + y(qr + \dot{p}) - z(p^2 + q^2) \end{aligned} \tag{2.15}$$

2.3.2 The generalized force equations

Consider now an incremental mass δm at point $p(x, y, z)$ in the rigid body. Applying Newton's second law, equation (2.7) to the incremental mass the incremental components of force acting on the mass are given by $(\delta m a'_x, \delta m a'_y, \delta m a'_z)$. Thus the total force components (X, Y, Z) acting on the body are given by summing the force increments over the whole body, whence:

$$\begin{aligned} \sum \delta m a'_x &= X \\ \sum \delta m a'_y &= Y \\ \sum \delta m a'_z &= Z \end{aligned} \tag{2.16}$$

Substitute the expressions for the components of inertial acceleration (ax, ay, az) from equations (2.15) into equations (2.16) and note that since the origin of axes coincides with the cg:

$$\sum \delta m x = \sum \delta m y = \sum \delta m z = 0 \tag{2.17}$$

Therefore the resultant components of total force acting on the rigid body are given by:

$$\begin{aligned} m(\dot{U} - rV + qW) &= X \\ m\big(\dot{V} - pW + rU\big) &= Y \\ m(\dot{W} - qU + pV) &= Z \end{aligned} \tag{2.18}$$

where m is the total mass of the body.

2.3.3 The generalized moment equation

Consider now the moments produced by the forces acting on the incremental mass δm at point $p(x, y, z)$ in the rigid body. The moment equations are the realization of the rotational form of Newton's second law of motion. The total moments L, M, N about the ox, oy and oz axes respectively are given by summing the incremental moment components over the whole body:

$$\begin{aligned}\sum \delta m\left(ya'_z - za'_y\right) &= L\\ \sum \delta m\left(za'_x - xa'_z\right) &= M\\ \sum \delta m\left(xa'_y - ya'_x\right) &= N\end{aligned} \tag{2.19}$$

Equations (2.19) may therefore be rewritten and using the definition of the inertia that will be introduced as set out in Table 2.4.

$$\begin{aligned}&I_x\dot{p} - \left(I_y - I_z\right)qr + I_{xy}(pr - \dot{q}) - I_{xz}(pq + \dot{r}) + I_{yz}(r^2 - q^2) = L\\ &I_y\dot{q} + (I_x - I_z)pr + I_{yz}(pq - \dot{r}) + I_{xz}(p^2 - r^2) - I_{xy}(qr + \dot{p}) = M\\ &I_z\dot{r} - (I_x - I_y)pq - I_{yz}(pr + \dot{q}) + I_{xz}(qr - \dot{p}) + I_{xy}(q^2 - p^2) = N\end{aligned} \tag{2.20}$$

Table 2.4: *Moments and Products of Inertia* [6].

I_x=$\sum \delta m\,(y^2 + z^2)$	Moment of inertia about ox axis
I_y=$\sum \delta m\,(x^2 + z^2)$	Moment of inertia about oy axis
I_z=$\sum \delta m\,(x^2 + y^2)$	Moment of inertia about oz axis
I_{xy}=$\sum \delta mxy$	Product of inertia about ox and oy axes
I_{xz}= $\sum \delta mxz$	Product of inertia about ox and oz axes
I_{yz}=$\sum \delta myz$	Product of inertia about oy and oz axes

Equations (2.20) represent the moment equations of a generalized rigid body and describe the rotational motion about the orthogonal axes through its cg.

The moment equations may be simplified since it is assumed that the aircraft is symmetric about the oxz plane and that the mass is uniformly distributed. As a result the products of inertia $I_{xy} = I_{yz} = 0$.

Thus the moment equations simplify to the following:

$$\begin{aligned}I_x\dot{p} - (I_y - \ I_z)qr - I_{xz}(pq + \dot{r}) &= L\\ I_y\dot{q} + (I_x - I_z)pr + I_{xz}(p^2 - r^2) &= M\end{aligned} \tag{2.21}$$

$$I_z\dot{r} - (I_x - I_y)pq + I_{xz}(qr - \dot{p}) = N$$

The equations (2.21), describe rolling motion, pitching motion and yawing motion respectively.

2.3.4 Disturbance forces and moments

According to Bryan (1911), is to assume that the disturbing forces and moments are due to aerodynamic effects, gravitational effects, movement of aerodynamic controls, power effects and the effects of atmospheric disturbances. Thus bringing together equations (2.18) and (2.21) they may be written as follows:

$$\begin{aligned} m(\dot{U} - rV + qW) &= X_a + X_g + X_c + X_p + X_d \\ m(\dot{V} - pW + rU) &= Y_a + Y_g + Y_c + Y_p + Y_d \\ m(\dot{W} - qU + pV) &= Z_a + Z_g + Z_c + Z_p + Z_d \end{aligned} \tag{2.22}$$

$$\begin{aligned} I_x\dot{p} - (I_y - I_z)qr - I_{xz}(pq + \dot{r}) &= L_a + L_g + L_c + L_p + L_d \\ I_y\dot{q} + (I_x - I_z)pr + I_{xz}(p^2 - r^2) &= M_a + M_g + M_c + M_p + M_d \\ I_z\dot{r} - (I_x - I_y)pq + I_{xz}(qr - \dot{p}) &= N_a + N_g + N_c + N_p + N_d \end{aligned}$$

Now the equations developed in (2.22) describe the moments and forces, these equations are nonlinear and coupled nonlinear, however they can only be solved numerically and they must be linearized. Linearization is very simply accomplished by constraining the motion of the airplane to small perturbations about the trim condition.

2.4 The linearized equations of motion

The nonlinear equations are really complex to solve with numerical method, so we will linearize them which will give us the good understanding of aircraft dynamics and stability in

control. Initially we will be deriving the nonlinear equations respecting the steady-state conditions.

The small perturbation theory is based on a simple technique used for linearizing a set of differential equations, thus the velocity of the airplane is V_0, the components of linear

velocity are (U_e, V_e, W_e) and the angular velocity components are all zero. Since there is no sideslip $V_e = 0$. A stable undisturbed atmosphere is also assumed such that:

$$X_d = Y_d = Z_d = L_d = M_d = N_d = 0 \tag{2.23}$$

If now the airplane experiences a small perturbation about trim, the components of the linear disturbance velocities are (u, v, w) and the components of the angular disturbance velocities are (p, q, r) with respect to the undisturbed aeroplane axes $(oxyz)$.

Thus the total velocity components of the cg in the disturbed motion are given by:

$$\begin{aligned} U &= U_e + u \\ V &= V_e + v = v \\ W &= W_e + w \end{aligned} \tag{2.24}$$

Now, by definition (u, v, w) and (p, q, r) are small quantities such that terms involving products and squares of these terms are insignificantly small and may be ignored. Thus, substituting equations (2.23) and (2.24) into equations (2.22), note that (U_e, V_e, W_e) are steady and hence constant, and eliminating the insignificantly small terms, the linearized equations of motion are obtained:

$$\begin{aligned} m(\dot{u} + qW_e) &= X_a + X_g + X_c + X_p \\ m(\dot{v} - pW_e + rU_e) &= Y_a + Y_g + Y_c + Y_p \\ m(\dot{w} - qU_e) &= Z_a + Z_g + Z_c + Z_p \end{aligned} \tag{2.25}$$

$$\begin{aligned} I_x\dot{p} - I_{xz}\dot{r} &= L_a + L_g + L_c + L_p \\ I_y\dot{q} &= M_a + M_g + M_c + M_p \\ I_z\dot{r} - I_{xz}\dot{p} &= N_a + N_g + N_c + N_p \end{aligned}$$

2.4.1 Gravitational terms

The weight force mg acting on the airplane can be decomposed into three components. In case of any disturbance they will vary within the perturbations in attitude. Since the origin of the body axes is coincident with the cg then the weight moments are all zero. Therefore:

$$L_g = M_g = N_g = 0 \tag{2.26}$$

Since the aircraft flies horizontally in the initial symmetrical flight condition, the components of weight appear only in the plane of symmetry as shown in Figure 2.9. Thus in steady state the weight components resolved in aircraft axes are:

$$\begin{bmatrix} X_{g_e} \\ Y_{g_e} \\ Z_{g_e} \end{bmatrix} = \begin{bmatrix} -mg\ \sin\theta_e \\ 0 \\ mg\ \cos\theta_e \end{bmatrix} \tag{2.27}$$

Thus, the gravitational force components in the small perturbation equations of motion are given by:

$$\begin{aligned} X_g &= -mg\sin\theta_e - mg\theta\cos\theta_e \\ Y_g &= mg\,\psi\sin\theta_e + mg\phi\cos\theta_e \\ Z_g &= mg\cos\theta_e - mg\theta\sin\theta_e \end{aligned} \tag{2.28}$$

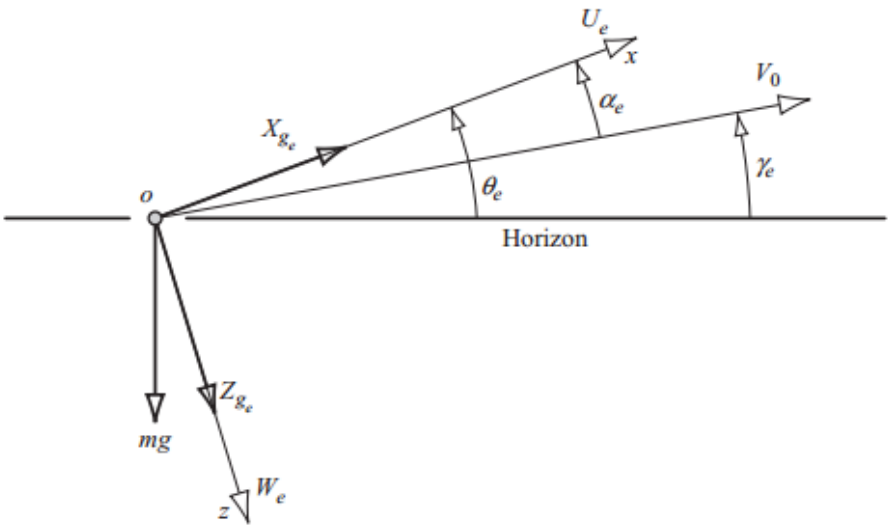

Figure 2.9: *Steady state weight components in the plane of symmetry* [6].

2.4.2 Aerodynamic terms

The aerodynamic force and moment terms in equations (2.22) depend only on the disturbed motion variables and their derivatives. Mathematically, this is expressed as a function comprising the sum of a number of Taylor series, each series involving a motion variable or a derivative of a motion variable. (u, v, w) are the motion variables and (p, q, r) the aerodynamic term X_a in the axial force equation. The simplified form of this equation is:

$$X_a = X_{a_e} + \mathring{X}_u u + \mathring{X}_v v + \mathring{X}_w w + \mathring{X}_p p + \mathring{X}_q q + \mathring{X}_r r + \mathring{X}_{\dot{w}} \dot{w} \tag{2.29}$$

Where:

X_{a_e} is a constant term .

($\mathring{X}_u$, $\mathring{X}_v$, $\mathring{X}_w$, $\mathring{X}_p$, $\mathring{X}_q$,$\mathring{X}_{\dot{w}}$) are aerodynamic stability derivatives .

(◦) denotes the derivatives to be dimensional.

2.4.3 Thrust terms

Thrust τ is the force which moves an aircraft through the air. Thrust is used to overcome the drag of an airplane. It is generated by the engines of the aircraft through some kind of propulsion system. It is generated most often through the reaction of accelerating a mass of gas. Since thrust is a force, it is a vector quantity having both a magnitude and a direction.

Thrust τ is controlled by throttle lever angle ε and the relationship between the two variables is given by equation (2.6). Thrust change is caused by the movement of the throttle lever which leads to a change in the force and moment. As an example the normal force due to thrust may be expressed:

$$Z_p = \mathring{Z}_\tau \tau \tag{2.30}$$

2.4.4 The equations of motion for small perturbations

To complete the development of the linearized equations of motion using the aerodynamic, gravitational, and thrust terms, the EOM may be written:

$$m(\dot{u} + qW_e) = X_{a_e} + \mathring{X}_u u + \mathring{X}_v v + \mathring{X}_w w + \mathring{X}_p p + \mathring{X}_q q + \mathring{X}_r r + \mathring{X}_{\dot{w}} \dot{w} - mg \sin\theta_e - mg\theta \cos\theta_e + \mathring{X}_\xi \xi + \mathring{X}_\eta \eta + \mathring{X}_\zeta \zeta + \mathring{X}_\tau \tau$$

$$m(\dot{v} - pW_e + rU_e) = Y_{a_e} + \mathring{Y}_u u + \mathring{Y}_v v + \mathring{Y}_w w + \mathring{Y}_p p + \mathring{Y}_q q + \mathring{Y}_r r + \mathring{Y}_{\dot{w}} \dot{w} + mg\psi \sin\theta_e + mg\phi \cos\theta_e + \mathring{Y}_\xi \xi + \mathring{Y}_\eta \eta + \mathring{Y}_\zeta \zeta + \mathring{Y}_\tau \tau$$

$$m(\dot{w} - qU_e) = Z_{a_e} + \mathring{Z}_u u + \mathring{Z}_v v + \mathring{Z}_w w + \mathring{Z}_p p + \mathring{Z}_q q + \mathring{Z}_r r + \mathring{Z}_{\dot{w}} \dot{w} + mg \cos\theta_e - mg\theta \sin\theta_e + \mathring{Z}_\xi \xi + \mathring{Z}_\eta \eta + \mathring{Z}_\zeta \zeta + \mathring{Z}_\tau \tau$$

$$I_x \dot{p} - I_{xz} \dot{r} = L_{a_e} + \mathring{L}_u u + \mathring{L}_v v + \mathring{L}_w w + \mathring{L}_p p + \mathring{L}_q q + \mathring{L}_r r + \mathring{L}_{\dot{w}} \dot{w} + \mathring{L}_\xi \xi + \mathring{L}_\eta \eta + \mathring{L}_\zeta \zeta + \mathring{L}_\tau \tau$$

$$I_y \dot{q} = M_{a_e} + \mathring{M}_u u + \mathring{M}_v v + \mathring{M}_w w + \mathring{M}_p p + \mathring{M}_q q + \mathring{M}_r r + \mathring{M}_{\dot{w}} \dot{w} + \mathring{M}_\xi \xi + \mathring{M}_\eta \eta + \mathring{M}_\zeta \zeta + \mathring{M}_\tau \tau$$

$$I_z \dot{r} - I_{xz} \dot{p} = N_{a_e} + \mathring{N}_u u + \mathring{N}_v v + \mathring{N}_w w + \mathring{N}_p p + \mathring{N}_q q + \mathring{N}_r r + \mathring{N}_{\dot{w}} \dot{w} + \mathring{N}_\xi \xi + \mathring{N}_\eta \eta + \mathring{N}_\zeta + \mathring{N}_\tau \tau \quad (2.31)$$

Now, by definition all the perturbation variables and their derivatives are assumed to be zero .Thus in the steady state equations (2.31) reduce to:

$$X_{a_e} = mg \sin\theta_e$$

$$Y_{a_e} = 0$$

$$Z_{a_e} = -mg \cos\theta_e \quad (2.32)$$

$$L_{a_e} = 0$$

$$M_{a_e} = 0$$

$$N_{a_e} = 0$$

The new rearrangement may be written as follows :

$$m\dot{u} - \mathring{X}_u u - \mathring{X}_v v - \mathring{X}_w w$$

$$-\mathring{X}_p p - (\mathring{X}_q - mW_e)q - \mathring{X}_r r + mg\theta\cos\theta_e = \mathring{X}_\xi \xi + \mathring{X}_\eta \eta + \mathring{X}_\zeta \zeta + \mathring{X}_\tau \tau$$

$$-\mathring{Y}_u u + m\dot{v} - \mathring{Y}_v v - \mathring{Y}_{\dot{w}}\dot{w} - \mathring{Y}_w w - \left(\mathring{Y}_p + mW_e\right)p$$

$$-\mathring{Y}_q q - (\mathring{Y}_r - mU_e)r - mg\phi\cos\theta_e - mg\,\psi\sin\theta_e = \mathring{Y}_\xi \xi + \mathring{Y}_\eta \eta + \mathring{Y}_\zeta \zeta + \mathring{Y}_\tau \tau$$

$$-\mathring{Z}_u u - \mathring{Z}_v v + (m - \mathring{Z}_{\dot{w}})\,\dot{w} - \mathring{Z}_w w$$

$$-\mathring{Z}_p p - (\mathring{Z}_q + mU_e)\,q - \mathring{Z}_r r + mg\theta\sin\theta_e = \mathring{Z}_\xi \xi + \mathring{Z}_\eta \eta + \mathring{Z}_\zeta \zeta + \mathring{Z}_\tau \tau$$

$$-\mathring{L}_u u - \mathring{L}_v v - \mathring{L}_{\dot{w}}\dot{w} - \mathring{L}_w w$$

$$+I_x\dot{p} - \mathring{L}_p p - \mathring{L}_q q - I_{xz}\dot{r} - \mathring{L}_r r = \mathring{L}_\xi \xi + \mathring{L}_\eta \eta + \mathring{L}_\zeta \zeta + \mathring{L}_\tau \tau$$

$$-\mathring{M}_u u - \mathring{M}_v v - \mathring{M}_{\dot{w}}\dot{w}$$

$$-\mathring{M}_w w - \mathring{M}_p p + I_y\dot{q} - \mathring{M}_q q - \mathring{M}_r r = \mathring{M}_\xi \xi + \mathring{M}_\eta \eta + \mathring{M}_\zeta \zeta + \mathring{M}_\tau \tau$$

$$-\mathring{N}_u u - \mathring{N}_v v - \mathring{N}_{\dot{w}}\dot{w} - \mathring{N}_w w$$

$$-I_{xz}\dot{p} - \mathring{N}_p p - \mathring{N}_q q + I_z\dot{r} - \mathring{N}_r r = \mathring{N}_\xi \xi + \mathring{N}_\eta \eta + \mathring{N}_\zeta + \mathring{N}_\tau \tau \qquad (2.33)$$

With the expanded general equations of motion (2.33) defined on the body axis reference frame , and with a defined steady-state , it is possible to begin the decoupling of these equations for lateral and longitudinal movement.

2.5 The decoupled equations of motion

2.5.1 The longitudinal equations of motion

The development of the longitudinal equations of motion which for the most general case are referred to the body axis , recognizing that the aerodynamic contributions to the EOM are determined with respect to the disturbance. The motion is described by the axial force X, the normal force Z and the pitching moment M equations only. Therefore the lateral motion variables v, p and r and their derivatives are all zero whence:

$$\mathring{X}_v = \mathring{X}_p = \mathring{X}_r = \mathring{Z}_v = \mathring{Z}_p = \mathring{Z}_r = \mathring{M}_v = \mathring{M}_p = \mathring{M}_r = 0 \tag{2.34}$$

Similarly, since aileron or rudder deflections do not usually cause motion in the longitudinal plane of symmetry the coupling aerodynamic control derivatives may also be taken as zero thus:

$$\mathring{X}_\xi = \mathring{X}_\zeta = \mathring{Z}_\xi = \mathring{Z}_\zeta = \mathring{M}_\xi = \mathring{M}_\zeta = 0 \tag{2.35}$$

The longitudinal equations are given:

$$\begin{aligned} m\dot{u} - \mathring{X}_u u - \mathring{X}_{\dot{w}}\dot{w} - \mathring{X}_w w - (\mathring{X}_q - mW_e)q + mg\theta\cos\theta_e &= \mathring{X}_\eta\eta + \mathring{X}_\tau\tau \\ -\mathring{Z}_u u + (m - \mathring{Z}_{\dot{w}})\dot{w} - \mathring{Z}_w w - (\mathring{Z}_q + mU_e)q + mg\theta\sin\theta_e &= \mathring{Z}_\eta\eta + \mathring{Z}_\tau\tau \\ -\mathring{M}_u u - \mathring{M}_{\dot{w}}\dot{w} - \mathring{M}_w w + I_y\dot{q} - \mathring{M}_q q &= \mathring{M}_\eta\eta + \mathring{M}_\tau\tau \end{aligned} \tag{2.36}$$

Equations (2.36) are the most general form of the dimensional decoupled equations of longitudinal symmetric motion. If it is assumed that the aeroplane is in level flight and the reference axes are wind or stability axes then:

$$\theta_e = W_e = 0 \tag{2.37}$$

and the equations simplify further to:

$$\begin{aligned} m\dot{u} - \mathring{X}_u u - \mathring{X}_{\dot{w}}\dot{w} - \mathring{X}_w w - \mathring{X}_q q + mg\theta &= \mathring{X}_\eta\eta + \mathring{X}_\tau\tau \\ -\mathring{Z}_u u + (m - \mathring{Z}_{\dot{w}})\dot{w} - \mathring{Z}_w w - (\mathring{Z}_q + mU_e)q &= \mathring{Z}_\eta\eta + \mathring{Z}_\tau\tau \\ -\mathring{M}_u u - \mathring{M}_{\dot{w}}\dot{w} - \mathring{M}_w w + I_y\dot{q} - \mathring{M}_q q &= \mathring{M}_\eta\eta + \mathring{M}_\tau\tau \end{aligned} \tag{2.38}$$

2.5.2 The lateral–directional equations of motion

Decoupled lateral–directional motion involves roll, yaw and sideslip only. The motion is therefore described by the side force Y, the rolling moment Land the yawing moment N equations. As no longitudinal motion is involved the longitudinal motion variables u, w and q and their derivatives are all zero. Whence:

$$\mathring{\mathrm{Y}}_{\mathrm{u}} = \mathring{\mathrm{Y}}_{\dot{\mathrm{w}}} = \mathring{\mathrm{Y}}_{\mathrm{w}} = \mathring{\mathrm{Y}}_{\mathrm{q}} = \mathring{\mathrm{L}}_{\mathrm{u}} = \mathring{\mathrm{L}}_{\dot{\mathrm{w}}} = \mathring{\mathrm{L}}_{\mathrm{w}} = \mathring{\mathrm{L}}_{\mathrm{q}} = \mathring{\mathrm{N}}_{\mathrm{u}} = \mathring{\mathrm{N}}_{\dot{\mathrm{w}}} = \mathring{\mathrm{N}}_{\mathrm{w}} = \mathring{\mathrm{N}}_{\mathrm{q}} = 0 \qquad (2.39)$$

Since the airframe is symmetric, elevator deflection and thrust variation do not usually cause lateral–directional motion and the coupling aerodynamic control derivatives may also be taken as zero thus:

$$\mathring{\mathrm{Y}}_{\eta} = \mathring{\mathrm{Y}}_{\tau} = \mathring{\mathrm{L}}_{\eta} = \mathring{\mathrm{L}}_{\tau} = \mathring{\mathrm{N}}_{\eta} = \mathring{\mathrm{N}}_{\tau} = 0 \qquad (2.40)$$

The lateral equations are given by:

$$\begin{pmatrix} m\dot{v} - \mathring{\mathrm{Y}}_{v}v - (\mathring{\mathrm{Y}}_{p} + mW_{e})p - (\mathring{\mathrm{Y}}_{r} - mU_{e})r \\ -mg\phi\cos\theta_{e} - mg\,\psi\sin\theta_{e} \end{pmatrix} = \mathring{\mathrm{Y}}_{\xi}\xi + \mathring{\mathrm{Y}}_{\zeta}\zeta$$

$$\begin{aligned} -\mathring{\mathrm{L}}_{v}v + I_{x}\dot{p} - \mathring{\mathrm{L}}_{p}p - I_{xz}\dot{r} - \mathring{\mathrm{L}}_{r}r &= \mathring{\mathrm{L}}_{\xi}\xi + \mathring{\mathrm{L}}_{\zeta}\zeta \\ -\mathring{\mathrm{N}}_{v}v - I_{xz}\dot{p} - \mathring{\mathrm{N}}_{p}p + I_{z}\dot{r} - \mathring{\mathrm{N}}_{r}r &= \mathring{\mathrm{N}}_{\xi}\xi + \mathring{\mathrm{N}}_{\zeta}\zeta \end{aligned} \qquad (2.41)$$

If it is assumed that the airplane is in level flight and the reference axes are wind or stability axes then, as before,

$$\theta_{e} = W_{e} = 0 \qquad (2.42)$$

and the equations simplify further to:

$$\begin{aligned} m\dot{v} - \mathring{\mathrm{Y}}_{v}v - p\mathring{\mathrm{Y}}_{p} - \left(\mathring{\mathrm{Y}}_{r} - mU_{e}\right)r - mg\phi &= \mathring{\mathrm{Y}}_{\xi}\xi + \mathring{\mathrm{Y}}_{\zeta}\zeta \\ -\mathring{\mathrm{L}}_{v}v + I_{x}\dot{p} - \mathring{\mathrm{L}}_{p}p - I_{xz}\dot{r} - \mathring{\mathrm{L}}_{r}r &= \mathring{\mathrm{L}}_{\xi}\xi + \mathring{\mathrm{L}}_{\zeta}\zeta \\ -\mathring{\mathrm{N}}_{v}v - I_{xz}\dot{p} - \mathring{\mathrm{N}}_{p}p + I_{z}\dot{r} - \mathring{\mathrm{N}}_{r}r &= \mathring{\mathrm{N}}_{\xi}\xi + \mathring{\mathrm{N}}_{\zeta}\zeta \end{aligned} \qquad (2.43)$$

2.6 The equations of motion in state space form

As systems and equations becomes more complex, solving them is more difficult .Today the numerical methods give rise , this is more true if the system has multiple inputs and outputs. We will introduce the state space method which is largely used and alleviates this problem. The state space representation of the system replaces an n^{th} order differential equation with a single first order matrix differential equation. However, it is first necessary to arrange the EOM in a suitable format, the equation of motion, or state equation, of the linear time invariant (LTI) multi-variable system is written:

$$\dot{\mathbf{X}}(\mathbf{t}) = \mathbf{A}\mathbf{x}(t) + \mathbf{B}\mathbf{u}(t) \tag{2.44}$$

Where :

$\mathbf{x}(t)$ is the column vector of n state variables called the state vector.

$\mathbf{u}(t)$ is the column vector of m input variables called the input vector.

$\mathbf{A}$ is the $(n \times n)$ state matrix.

$\mathbf{B}$ is the $(n \times m)$ input matrix.

Now for many systems some of the state variables may be inaccessible or their values may not be determined directly. Thus a second equation is required to determine the system output variables. The output equation is written in the general form:

$$\mathbf{y}(t) = \mathbf{C}\mathbf{x}(t) + \mathbf{D}\mathbf{u}(t) \tag{2.45}$$

Where :

$\mathbf{y}(t)$ is the column vector of r output variables called the output vector.

$\mathbf{C}$ is the $(r \times n)$ output matrix.

$\mathbf{D}$ is the $(r \times m)$ direct matrix.

and, typically, $r \leq n$, for a LTI system the matrices $\mathbf{C}$ and $\mathbf{D}$ have constant elements. Together equations (2.44) and (2.45) provide a complete description of the system. For most aeroplane problems it is convenient to choose the output variables to be the state variables. Thus:

$$\mathbf{y}(t) = \mathbf{x}(t) \text{ and } r = n$$

and consequently

$\mathbf{C} = \mathbf{I}$, the $(n \times n)$ identity matrix

$\mathbf{D} = \mathbf{0}$, the $(n \times m)$ zero matrix

As a result the output equation simplifies to:

$$\mathbf{y}(t) = \mathbf{I}\mathbf{x}(t) \equiv \mathbf{x}(t) \tag{2.53}$$

The longitudinal equation of motion in the state space format may be written as follows:

$$\mathbf{M}\dot{\mathbf{x}}(t) = \mathbf{A}'\mathbf{x}(t) + \mathbf{B}'\mathbf{u}(t) \tag{2.54}$$

Where :

$$\mathbf{x}^T(t) = [u \quad w \quad q \quad \theta \ ] \qquad \mathbf{u}^T(t) = [\eta \quad \tau]$$

$$\mathbf{M} = \begin{bmatrix} m & -\mathring{\mathrm{X}}_{\dot{w}} & 0 & 0 \\ 0 & \left(m - \mathring{\mathrm{Z}}_{\dot{w}}\right) & 0 & 0 \\ 0 & -\mathring{\mathrm{M}}_{\dot{w}} & I_y & 0 \\ 0 & 0 & 0 & 1 \end{bmatrix}$$

$$\mathbf{A}' = \begin{bmatrix} \mathring{\mathrm{X}}_u & \mathring{\mathrm{X}}_w & (\mathring{\mathrm{X}}_q - mW_e) & -mg\cos\theta_e \\ \mathring{\mathrm{Z}}_u & \mathring{\mathrm{Z}}_w & (\mathring{\mathrm{Z}}_q + mU_e) & -mg\sin\theta_e \\ \mathring{\mathrm{M}}_u & \mathring{\mathrm{M}}_w & \mathring{\mathrm{M}}_q & 0 \\ 0 & 0 & 1 & 0 \end{bmatrix} \qquad \mathbf{B}' = \begin{bmatrix} \mathring{\mathrm{X}}_\eta & \mathring{\mathrm{X}}_\tau \\ \mathring{\mathrm{Z}}_\eta & \mathring{\mathrm{Z}}_\tau \\ \mathring{\mathrm{M}}_\eta & \mathring{\mathrm{M}}_\tau \\ 0 & 0 \end{bmatrix}$$

The longitudinal state equation is derived by pre-multiplying equation (2.56) by the inverse of the mass matrix $\mathbf{M}$ whence :

$$\dot{\mathbf{x}}(t) = \mathbf{A}\mathbf{x}(t) + \mathbf{B}\mathbf{u}(t) \tag{2.55}$$

Where:

$$\mathbf{A} = \mathbf{M}^{-1}\ \mathbf{A}' = \begin{bmatrix} x_u & x_w & x_q & x_\theta \\ z_u & z_w & z_q & z_\theta \\ m_u & m_w & m_q & m_\theta \\ 0 & 0 & 1 & 0 \end{bmatrix} \qquad \mathbf{B} = \mathbf{M}^{-1}\ \mathbf{B}' = \begin{bmatrix} x_\eta & x_\tau \\ z_\eta & z_\tau \\ z_\eta & m_\tau \\ 0 & 0 \end{bmatrix}$$

Thus the longitudinal state equation may be written out in full:

$$\begin{bmatrix} \dot{u} \\ \dot{w} \\ \dot{q} \\ \dot{\theta} \end{bmatrix} = \begin{bmatrix} x_u & x_w & x_q & x_\theta \\ z_u & z_w & z_q & z_\theta \\ m_u & m_w & m_q & m_\theta \\ 0 & 0 & 1 & 0 \end{bmatrix} \begin{bmatrix} u \\ w \\ q \\ \theta \end{bmatrix} + \begin{bmatrix} x_\eta & x_\tau \\ z_\eta & z_\tau \\ z_\eta & m_\tau \\ 0 & 0 \end{bmatrix} \begin{bmatrix} \eta \\ \tau \end{bmatrix} \tag{2.56}$$

and the output equation is:

$$\mathbf{y}(t) = \mathbf{I}\mathbf{x}(t) = \begin{bmatrix} 1 & 0 & 0 & 0 \\ 0 & 1 & 0 & 0 \\ 0 & 0 & 1 & 0 \\ 0 & 0 & 0 & 1 \end{bmatrix} \begin{bmatrix} u \\ w \\ q \\ \theta \end{bmatrix} \tag{2.57}$$

Clearly the longitudinal small perturbation motion of the airplane is completely described by the four state variables u, w, q and θ.

2.7 The equations of motion in American normalized form

The preferred North American form of the equations of motion expresses the axial equations of motion in units of linear acceleration, rather than force, and the angular equations of motion in terms of angular acceleration, rather than moment. This is easily achieved by normalizing the force and moment equations, by dividing by mass or moment of inertia as appropriate. Re-stating the linear equations of motion (2.25):

$$\begin{aligned} m(\dot{u} + qW_e) &= X \\ m(\dot{v} - pW_e + rU_e) &= Y \\ m(\dot{w} - qU_e) &= Z \\ I_x\dot{p} - I_{xz}\dot{r} &= L \\ I_y\dot{q} &= M \\ I_z\dot{r} - I_{xz}\dot{p} &= N \end{aligned} \tag{2.58}$$

The normalized form of the decoupled longitudinal equations of motion from equations (2.58) are written:

$$\begin{aligned} \dot{u} + qW_e &= \frac{X}{m} \\ \dot{w} - qU_e &= \frac{Z}{m} \\ \dot{q} &= \frac{M}{I_y} \end{aligned} \tag{2.59}$$

and the normalized form of the decoupled lateral–directional equations of motion may also be extracted from equations (2.58):

$$\begin{aligned} \dot{v} - pW_e + rU_e &= \frac{Y}{m} \\ \dot{p} - \frac{I_{xz}}{I_x}\dot{r} &= \frac{L}{I_x} \\ \dot{r} - \frac{I_{xz}}{I_z}\dot{p} &= \frac{N}{I_z} \end{aligned} \tag{2.60}$$

Now the decoupled longitudinal force and moment expressions may be expressed in terms of American normalized derivatives as follows:

$$\begin{aligned} \dot{u} &= \mathrm{X}_u u + \mathrm{X}_{\dot{w}}\dot{w} + \mathrm{X}_w w + (\mathrm{X}_q - mW_e)q - g\theta\cos\theta_e + \mathrm{X}_{\delta e}\delta_e + \mathrm{X}_{\delta th}\delta_{th} \\ \dot{w} &= \mathrm{Z}_u u + \mathrm{Z}_{\dot{w}}\dot{w} + \mathrm{Z}_w w + (\mathrm{Z}_q + U_e)q - g\theta\, sin\theta_e + \mathrm{Z}_{\delta e}\delta_e + \mathrm{Z}_{\delta th}\delta_{th} \\ \dot{q} &= \mathrm{M}_u u + \mathrm{M}_{\dot{w}}\dot{w} + \mathrm{M}_w w + \mathrm{M}_q q + \mathrm{M}_{\delta e}\delta_e + \mathrm{M}_{\delta th}\delta_{th} \end{aligned} \tag{2.61}$$

and the control inputs are stated in American notation, elevator angle $\boldsymbol{\delta_e \equiv \eta}$ and thrust $\boldsymbol{\delta_{th} \equiv \tau}$.

In a similar way, the decoupled lateral–directional force and moment expressions may Be given by:

$$\begin{aligned} \dot{v} &= \mathrm{Y}_v v + \left(\mathrm{Y}_p + W_e\right)p + (\mathrm{Y}_r - U_e)r + \mathrm{Y}_{\delta a}\delta_a + \mathrm{Y}_{\delta r}\delta_r + g\phi\cos\theta_e + g\psi\, sin\theta_e \\ \dot{p} &= \mathrm{L'}_v v + \mathrm{L'}_p p + \mathrm{L'}_r r + \mathrm{L'}_{\delta a}\delta_a + \mathrm{L'}_{\delta r}\delta_r \\ \dot{r} &= \mathrm{N'}_v v + \mathrm{N'}_p p + \mathrm{N'}_r r + \mathrm{N'}_{\delta a}\delta_a + \mathrm{N'}_{\delta r}\delta_r \end{aligned} \tag{2.62}$$

2.8 Summary

In this chapter we have described how the aerodynamic forces and moments acting on an aircraft are created, how they are modeled mathematically. Next, the equations of motions have been characterized for two specific flight conditions: steady-state flight conditions and perturbed flight conditions under the small perturbation assumptions. In particular, the small perturbation equations of motion are important for setting up the mathematical framework for a simplified solution because of the assumption of neglecting the nonlinear terms associated with the products of small perturbation terms.

It has been shown that the equations of motion can be linearized around a steady-state condition and that they can then be separated into two decoupled sets, one of these sets describes the longitudinal motion of an aircraft, and the other describes the lateral-directional motion. The linear equations have been expressed in terms of the aerodynamic derivatives, and the significance of these derivatives has been explained. We also introduced the EOM in the state space representation that we will be using in our simulation.

All of the chapters following this one will make use of the mathematical models presented in this chapter in some form and thus demonstrate the importance of modeling in the design of aircraft control systems.

Chapter 3: Aircraft stability and control analysis

Chapter 3: Aircraft stability and control analysis

3.1 Introduction

Stability and control analysis is an important discipline to consider when designing an aircraft, the efficiency of the control surfaces is really important remaining the aircraft safe and stable during the flight. The definition of the stability of an aircraft motion got many standards, it is essential to begin with the notion of *"equilibrium flight"* which refers to a steady motion of flight.

Stability is a property of the state of equilibrium and tendency to return to its equilibrium point after a disturbance applied on it and it can be an input of the pilot or atmospheric phenomena such as: wind guts, wind gradients, turbulence. In order to that an airplane can remain stable during its phase of flight, it is necessary that the result of forces and moments in its cg are equal to zero.

An aircraft followed by a small perturbations is divergent and said to be dynamically unstable, it becomes stable if it returns to it equilibrium flight path. In this chapter two types of stability are presented for an airplane, static and dynamic. These two concepts are divided into longitudinal, lateral and directional modes.

3.2 What is stability and control?

To achieve the best performance in flight, an aircraft must have sufficient stability to maintain a uniform flightpath and a proper response to the movement of the pilot controls surfaces. When an aircraft is said to be controllable it means that it responds easily to movement of the controls, moving the control surfaces changes the airflow over the aircraft's surface causing changes in the balance of the forces acting to keep it flying straight and level.

Three nomenclatures are used in the stability and control topic: stability, controllability, maneuverability. Understanding of those terminologies is more critical to develop more complex systems without considering the type, stability can be described by the tendency of an airplane to return to a trimmed position after disturbance in an air stream. Controllability is the response in a steady flight on the pilot control input. Maneuverability is the characteristic of an aircraft to be directed along a desired flightpath and to withstand the stresses imposed.

Controllability is the capacity to respond to the pilot's commands and maneuverability is the quality of the aircraft that can easily controlled in the given space region. If something is very stable it is more difficult to change the altitude of that, and in the contrary if it's unstable it is easier to change its altitude.

As a conclusion stability and controllability have an inverse relationship as stability can be increased by expensing the controllability. So that the military aircrafts are more controllable and less stable which make it more difficult to handle by pilots , thus artificial stability methods such as computerized controlling are used. On the contrary commercial aircrafts are more stable and less controllable to ensure the comfortability.

3.3 Linear and non-linear stability systems

The study of the stability analysis has taken an important place for engineers, it is important to ensure a good stability and control in order to achieve good flight performances. Now the stability for a linear system is simply the classical theory of linearization : we assume that the perturbations arbitrarily small and in the equations and boundary conditions of the problem, we neglect terms non-linear in the perturbations quantities as compared to the linear ones, hence the disturbance inputs must be small to consider the system is linear. However this is not often the case for example fighter aircrafts such as F-16 , big perturbations inputs are applied due to the rotational and difficult combat movements in the air with high altitude and supersonic speed which lead to a non-linearity response systems. The non-linear problems of stability require special mathematical techniques, today understanding the non-linearity behavior is developing to enquiry stability criteria for a more complex and high performances fighter aircrafts.

3.4 Static and dynamic stability

3.4.1 static stability

Static stability is the initial tendency of an object to return to its original position after being disturbed, an example is shown in Figure 3.1.

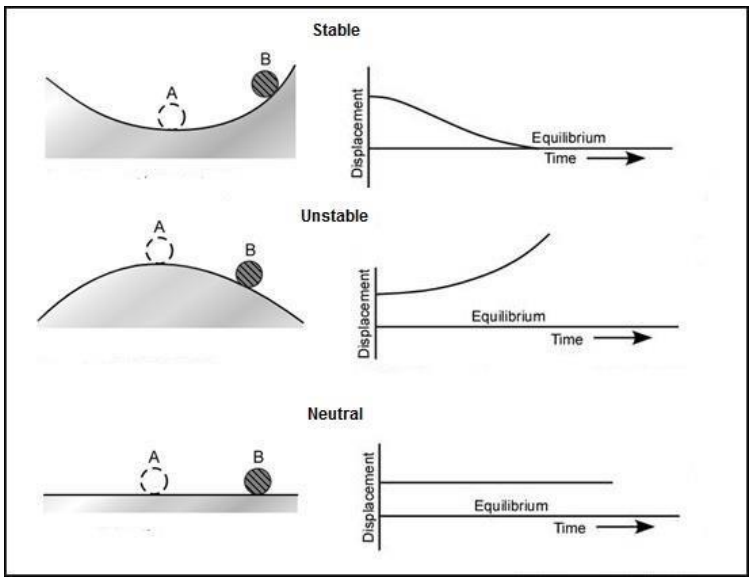

Figure 3.1: *stable, unstable, neutral systems behaviors* [8].

When the controls are changed and release, the ball initially moves back to the original position is the positive static stability. When it stays where it is after changing the controls, that shows neutral stability and when it tends to move further away from the original position that means negative stability.

3.4.2 Dynamic stability

After presenting the static stability of an aircraft, it is necessary to look at it dynamic stability. While static stability deals with the tendency of a displaced body to return to equilibrium, dynamic stability deals with the resulting motion with time as a result dynamic stability is the main part of study of stability, it allows seeing if there is resistance to movement and if there is a loss of energy (positive damping). In the case of energy loss the system is considered dynamically stable, the airplane, however, may pass through level flight and remain oscillation. If the oscillations lessen over time, the airplane is still classified as having positive dynamic stability. If the oscillations increase over time, the airplane is classified as having negative dynamic stability. If the oscillations remain the same over time, the airplane is classified as having neutral dynamic stability.

Figure 3.2 shows the concept of dynamic stability. In view A, the displacement from equilibrium goes through three oscillations and then returns to equilibrium. In view B, the displacement from equilibrium is increasing after two oscillations, and will not return to equilibrium. In view C, the displacement from equilibrium is staying the same with each oscillation.

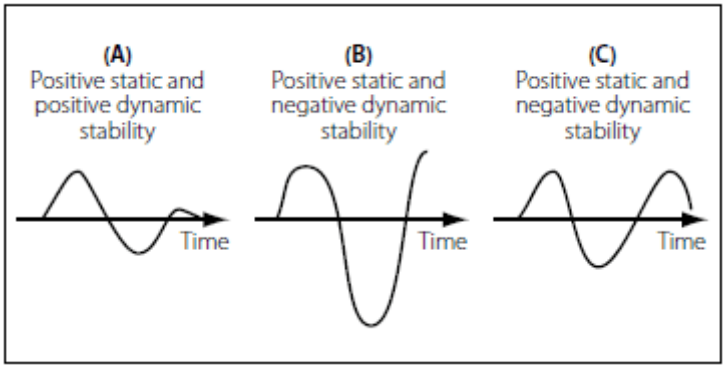

Figure 3.2: *Dynamic systems behaviors* [8].

3.5 Aerodynamic properties of airfoils

Airfoil is a shaped surface, such as an airplane wing, tail or propeller blade that produces lift and drag when moved through the air. An airfoil produces a lifting force that acts at right angles to the airstream and dragging force that acts in the same direction as the airstream. Its shape will determine the behavior of lift, drag and moments coefficients.

3.5.1 Lift coefficient (C_L)

The lift coefficient relates the angle of attack (*AOA)* to the lift force. If the lift force is known at a specific airspeed the lift coefficient can be calculated from:

$$C_L = \frac{2L}{\rho v^2 S} \tag{3.1}$$

3.5.2 Drag coefficient (C_D)

Drag coefficient is due to friction, pressure, and induced drag. The friction component is associated to the boundary layer development; its magnitude depends on the characteristics

of the fluid and the Reynolds number. The pressure component is due to the pressure difference between the leading and trailing edge of the profile. The induced drag is produced by the eddies that are generated at the tip of the blade. The drag coefficient is calculated as:

$$C_D = \frac{2D}{\rho v^2 S} \tag{3.2}$$

3.5.3 Moment coefficient (C_m)

The moment coefficient is obtained by the same way of the drag and lift coefficients but instead of a force, a moment is the result of the aerodynamic equation. During the stability analysis the pitch moment coefficient (C_m) is used but in some steps it will be necessary to use the yaw moment coefficient (C_n).

3.6 The F-16 aircraft stability

The design of flight control systems has evolved from purely mechanical to active over the past two decades. The advent of high-performance airplanes in the mid-1950's that were required to operate over larger performance envelopes necessitated the development of three-axis electronic stability augmentation systems. The functions of the F-16 flight control system are very similar to those of most other new high performance aircraft, the basic functions of the flight control system that are common are air data scheduled gains, stability augmentation (dynamic) , interconnects between roll and yaw axis and command augmentation. The unique features and functions of the flight control system are static longitudinal stability augmentation (RSS), minimum displacement side-stick controller (SSC), total Fly-By-Wire implementation (FBW) and angle-of-attack and normal acceleration limiting.

The basic RSS concept can be stated in a very simple way:

1. Balance the airplane for optimum performance.

2. Rely on the flight control system to provide the desired level of static stability as well as dynamic characteristics.

Illustrations of the differences between a conventionally-balanced airplane and an airplane with relaxed static stability are given in Figures 3.3. In the subsonic flight regime the conventionally balanced airplane is shown to have its wing-body lift acting forward of the center of gravity and the total lift acting aft of the center of gravity, Since in a stable system the moment produced by the wing-body lift as a function of angle of attack must be less than that produced by the tail, the tail must be deflected in a direction to reduce the total tail lift in order to trim the system. Therefore, the total trimmed lift available at a given angle of attack is reduced for a conventionally-balanced aircraft. The RSS-balanced aircraft has both the wing-body and the total lift acting forward of the center of gravity. In this case the moment produced by the wing-body lift as a function of angle of attack is greater than that produced by the tail and the tail must be deflected in a direction to increase the total tail lift in order to trim the system. Therefore, the total trimmed lift available at a given angle of attack is increased for an RSS configuration. Note that the benefits are most pronounced at the higher lift coefficients, which is an extremely important region for the YF-16. A secondary benefit of the RSS balance is a somewhat reduced weight because of reduced tail loads [5, 9].

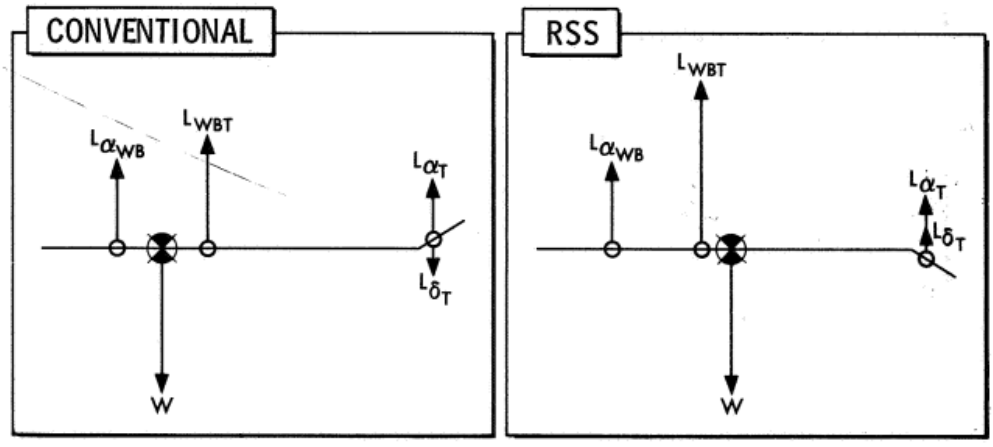

Figure 3.3: *Subsonic balance comparison* [9].

3.7 Static stability and control

3.7.1 Longitudinal Static stability

The pitch behavior of the aircraft is defined by the longitudinal stability. A stable state significates that in case of small variations in the AOA(α) , this will produce small variations in the pitch moment that will bring the aircraft back to equilibrium conditions , this is possible only if the (C_m) decreases with the AOA passing through a state of equilibrium ($C_m = 0$) as shown in Figure 3.4. Otherwise (positive slope) the aircraft will constantly move away from it equilibrium position.

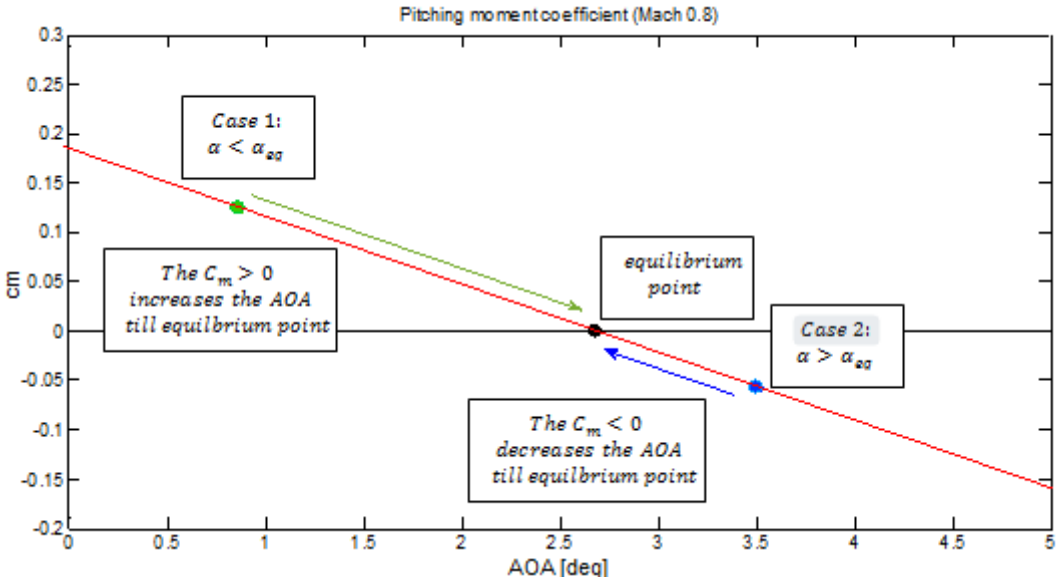

Figure 3.4: *pitching moment in terms of AOA.*

Thus the longitudinal static stability is verified compared to the coefficient of the pitch moment derivative in terms of the variation of the AOA (C_{m_α}). This coefficient gives the first static stability condition given by the equation 3.3:

$$C_{m_\alpha} = \frac{\partial C_m}{\partial \alpha} < 0 \qquad (3.3)$$

The criterion used by the various regulations to guarantee longitudinal static stability is the static margin (SM) presented in equation (3.4). A typical transport aircraft has a

positive static margin of approximately 5-10% of the MAC. The negative static margin (0 to -15%) is also used in fighters like the F-16 and F-22, this concept is known as "*relaxed static stability*" and uses a control system to deflect the elevator, providing an artificial stability which is explained in the previous section of this chapter.

$$SM = \frac{(x_{ac} - x_{cg})}{MAC} \tag{3.4}$$

Now we are going to represent the static margin (SM) in terms of C_{m_α}. Firs we must express the C_m with equation (3.5) that shows the approximation of the pitching moment coefficient with:

C_m : Pitch moment coefficient.

C_{m_0}: Pitch moment coefficient at zero AOA generated by the wing.

$x_{cg} - x_{ac}$: The distance between the cg and the aerodynamic center and MAC mean aerodynamic chord.

$$C_m = C_{m_0} + C_L \frac{(x_{cg} - x_{ac})}{MAC} \tag{3.5}$$

We must therefore now define C_{m_α}:

$$C_{m_\alpha} = \frac{\partial C_m}{\partial \alpha} = \frac{\partial C_{m_0}}{\partial \alpha} + \frac{\partial C_L}{\partial \alpha}\frac{(x_{cg} - x_{ac})}{MAC} + \frac{C_L}{MAC}\frac{\partial x_{cg}}{\partial \alpha} - \frac{C_L}{MAC}\frac{\partial x_{ac}}{\partial \alpha} \tag{3.6}$$

C_{m_0} and x_{cg} are constant values ,so they don't depend on the AOA . While x_{ac} varies in depending to the AOA but these variations are neglected.

$$C_{m_\alpha} = 0 + C_{L_\alpha}\frac{(x_{cg} - x_{ac})}{MAC} - 0 = C_{L_\alpha}\frac{(x_{cg} - x_{ac})}{MAC} \tag{3.7}$$

The equation (3.7) becomes:

$$C_{m_\alpha} = C_{L_\alpha} SM \tag{3.8}$$

Thus C_{m_α} must be $(C_{m_\alpha} < 0)$ to ensure the longitudinal static stability, also that C_{L_α} is always positive up to the stall angle of attack.

3.7.2 longitudinal control

The elevator stabilizes the aircraft longitudinally. Its efficiency is an important factor for the control of the plane. The variation of the moment is presented by $C_{m\delta_e}$ generated by the tail when the elevator is deflected by an angle δ. The larger is the value of $C_{m\delta_e}$ the more effective is the generation of pitching moment for the stabilization. The value of $C_{m\delta_e}$ is $1.02\, rad^{-1}$, there are no specific ranges for this value. The representation of the characteristics of longitudinal control is therefore:

$$C_m = C_{m\delta_e}.\delta_e + C_{m_\alpha}.\alpha + C_{m_0} \tag{3.9}$$

Where:

C_{m0} is the moment coefficient for $\delta = 0$ = 0 and $\alpha = 0$.

C_{m_α} is the derivative of moment coefficient with respect to the angle of attack.

$C_{m\delta_e}$ is the derivative moment coefficient with respect to the elevator deflection.

δ_e is the deflection of the elevator.

3.7.3 Lateral Static stability

Previously the pitch behavior is defined by the longitudinal stability, now the roll behavior is defined by lateral stability. Thus the lateral static stability is verified with respect to the derivative of rolling moment coefficient C_l in terms of the variation of the sideslip angle β which should be negative to ensure the lateral stability. Equation (3.10) represents this

condition, it is also possible to verify that the derivative of the roll moment coefficient with respect to the variation of the roll angle ϕ is also negative.

$$C_{l_\beta} = \frac{\partial C_l}{\partial \beta} < 0 \tag{3.10}$$

3.7.4 Lateral control

The control surfaces of the roll are ailerons and they are located at the wings ,when the pilot gives a roll command the ailerons deflects to opposite directions modifying the lift distribution at the wing and making the aircraft roll.

A simple way to calculate the roll power control for an aileron is to solve an integral to compute all the moment it can generate. The roll control power $C_{l_{\delta a}}$can be calculated as follows:

$$C_{l_{\delta a}} = \frac{2C_{l_{aw}}\tau_a}{Sb}\int_{y_2}^{y_1} c\ ydy \tag{3.11}$$

Where:

c is the chord of the aileron.

y is the aileron span.

y_1 and y_2 are the beginning and the end of the aileron.

S is the wing area.

b is the wing span.

τ_a is the aileron control surface effectiveness parameter.

3.7.5 Directional Static stability

Finally the aircraft's yawing behavior is defined by directional stability. It is a stability along the z-axis and concerns the ability of the airplane to return to it equilibrium conditions after undergoing a yaw disturbanceψ. The directional static stability is verified with respect to the derivative of yawing moment coefficient C_n in terms of the variation of the sideslip angle β. This must be positive in order to ensure the directional static stability, this condition is represented in equation (3.12).

$$C_{n_\beta} = \frac{\partial C_n}{\partial \beta} > 0 \tag{3.12}$$

3.7.6 Directional control

The control surfaces of the yaw is the rudder, it is a movable surface that is mounted on the trailing edge of the vertical stabilizer or fin. The rudder control effectiveness is the rate of change of yawing moment with rudder deflection angle:

$$\frac{\partial C_{l_v}}{\partial \delta_r} = C_{l_v} \tau_r \tag{3.13}$$

Where:

C_{l_v} is the lift coefficient for vertical tail .

τ_r is the rudder control surface effectiveness parameter.

2.1 Dynamic stability and control

To be able to analyze the temporal responses of dynamic stability, first we have to study the aircraft movement which is described by a set of non-linear equations, they are generally linearized using small displacements with small angle variations. The linearized equations of motion for a mechanical system “Mass-Spring-Damper” are presented in the equation (3.14) with:

$\mathbf{M}$: Mass matrix.

$\mathbf{C}$: Structural damping matrix.

$\mathbf{K}$: Stiffness matrix.

$\mathbf{x}$: Nodal displacement vector.

$\mathbf{f}$: Vector of the aerodynamic forces applied to the system

$$\boldsymbol{M\ddot{x} + C\dot{x} + Kx = f}(t) \tag{3.14}$$

Using an incompressible aerodynamic linear model, it is possible to rewrite the vector $\mathbf{f}$ according to the nodal displacement vector $\mathbf{x}$ as well as the dynamic pressure of the free flowq_∞:

$$\boldsymbol{f} = \boldsymbol{q}_\infty * \boldsymbol{A} * \boldsymbol{x} \tag{3.15}$$

In equation (3.15) the matrix $\mathbf{A}$ represents the matrix of the aerodynamic coefficients of the system. The eigenvalues of the matrix $\mathbf{A}$ define the dynamic stability. In order to find the eigenvalues, we have first to solve the equation (3.16) as well for the longitudinal and lateral movements. Each of the movements is defined by its own matrix $\mathbf{A}$**.**

$$\boldsymbol{det}|\boldsymbol{\lambda I} - \boldsymbol{A}| = 0 \tag{3.16}$$

The matrix $\mathbf{I}$, which is an identity matrix, is in this case a 4 × 4 matrix. By solving equation (3.16) for the two movements, we obtain characteristic polynomials depending only on the different eigenvalues. Equation (3.17) corresponds to both longitudinal movement and lateral movement. In this equation, the a_i represent the coefficients.

$$\lambda^4 + \boldsymbol{a_1}\lambda^3 + \boldsymbol{a_2}\lambda^2 + \boldsymbol{a_3}\lambda + \boldsymbol{a_4} = 0 \tag{3.17}$$

The airplane is considered dynamically stable if all the eigenvalues λ_i have a negative real part. If only one of the eigenvalues has a positive real part, then the airplane will be dynamically unstable. In general, equation (3.17) is factored in order to show the different modes of movement. Longitudinal motion has two modes: Short Period and Phugoid, see equation (3.18). While the lateral movement has three modes: Roll, Spiral and Dutch-Roll, see equation (3.19). These different modes will be explained in detail in the next sections.

$$\left(\lambda^2 + 2\zeta_{sp}\omega_{sp}\lambda + {\omega^2}_{sp}\right)\left(\lambda^2 + 2 * \zeta_{ph}\omega_{ph}\lambda + {\omega^2}_{ph}\right) = 0 \tag{3.18}$$

$$\left(\lambda + c_{spiral}\right)(\lambda + c_{roll})(\lambda^2 + 2\zeta_{DR}\omega_{DR}\lambda + {\omega^2}_{DR}) = 0 \tag{3.19}$$

In the previous equations, ζ and ω respectively represent the damping rate and the natural frequency not damped. For Roll and Spiral modes, since the eigenvalue contains only a real part, the stability calculations are based on the calculation of the roll damping time equation (3.20) and the time to reduce to halve the amplitude equation (3.21).

$$T_{2roll} = \frac{1}{c_{roll}} \tag{3.20}$$

$$T_{\frac{1}{2}spiral} = \frac{\ln 2}{c_{spiral}} \tag{3.21}$$

Before talking in more detail about the stability conditions of the different modes, it is necessary to present each of these modes in order to see what its influence on the behavior of the aircraft. First, we will present the longitudinal modes then the lateral modes.

3.7.7 Longitudinal modes

3.7.7.1 Short Period

The short period is characterized by a fast and strongly damped oscillatory mode. In this mode the altitude and the flight direction remains constant while the angle of attack know some variations.

An oscillation is created due to the derivative of the pitch moment coefficient with respect to the variation of the AOA, which provides longitudinal static stability which tends to return the aircraft to its initial position. The Figure 3.5 illustrates this mode:

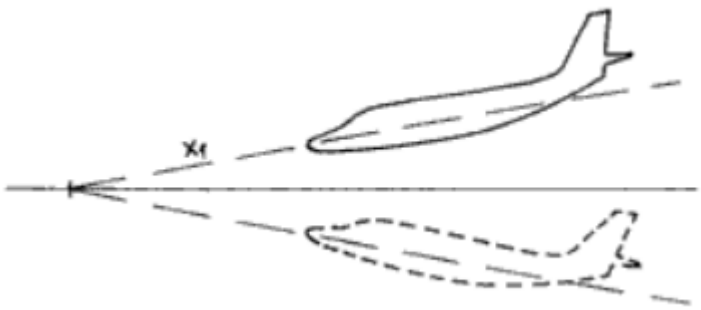

Figure 3.5: *Movement associated to the Short Period mode* [8].

3.7.7.2 Phugoid

The phugoid is a constant angle of attack but varying pitch angle exchange of airspeed and altitude. It can be excited by an elevator pulse (a short, sharp deflection followed by a return to the centered position) resulting in a pitch increase with no change in trim from cruise condition. As speed decays, the nose will drop below the horizon, speed will increase and the nose will climb above the horizon Figure 3.6. Periods can vary from under 30 seconds for light aircraft to minute for larger aircraft.

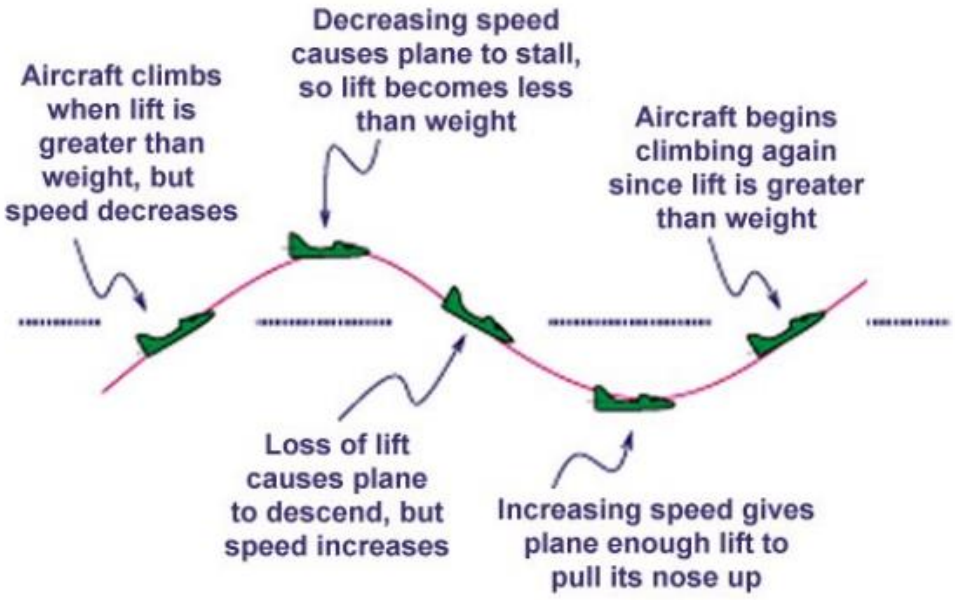

Figure 3.6: *Schematic representation of Phugoid effect* [8].

3.7.7.3 CAP

The control anticipation parameter (CAP) is not a mode but it is an important criterion for verifying longitudinal stability. CAP is based on the pilot's ability perceiving and anticipating pitch and vertical acceleration. It is a function of the natural frequency of the Short Period mode in terms of acceleration sensitivity $n_{z\alpha}$ as shown in equation (3.22).

$$CAP = \frac{{\omega^2}_{sp}}{n_{z\alpha}} \tag{3.22}$$

The acceleration sensitivity is defined as follows:

$$n_{z\alpha} = -\frac{U_0}{gZ_w} \quad (3.23)$$

Where:

$$Z_w = \frac{-\rho.S.U_0.(C_{L\alpha} + C_D)}{2.m} \quad (3.24)$$

3.7.8 Lateral modes

3.7.8.1 Dutch Roll

The Dutch roll is a coupled dynamic lateral and directional mode of motion .It is characterized by a slight damping and a low frequency oscillation. Frequency similar to longitudinal short period mode, not as well damped (fin less effective than horizontal tail).

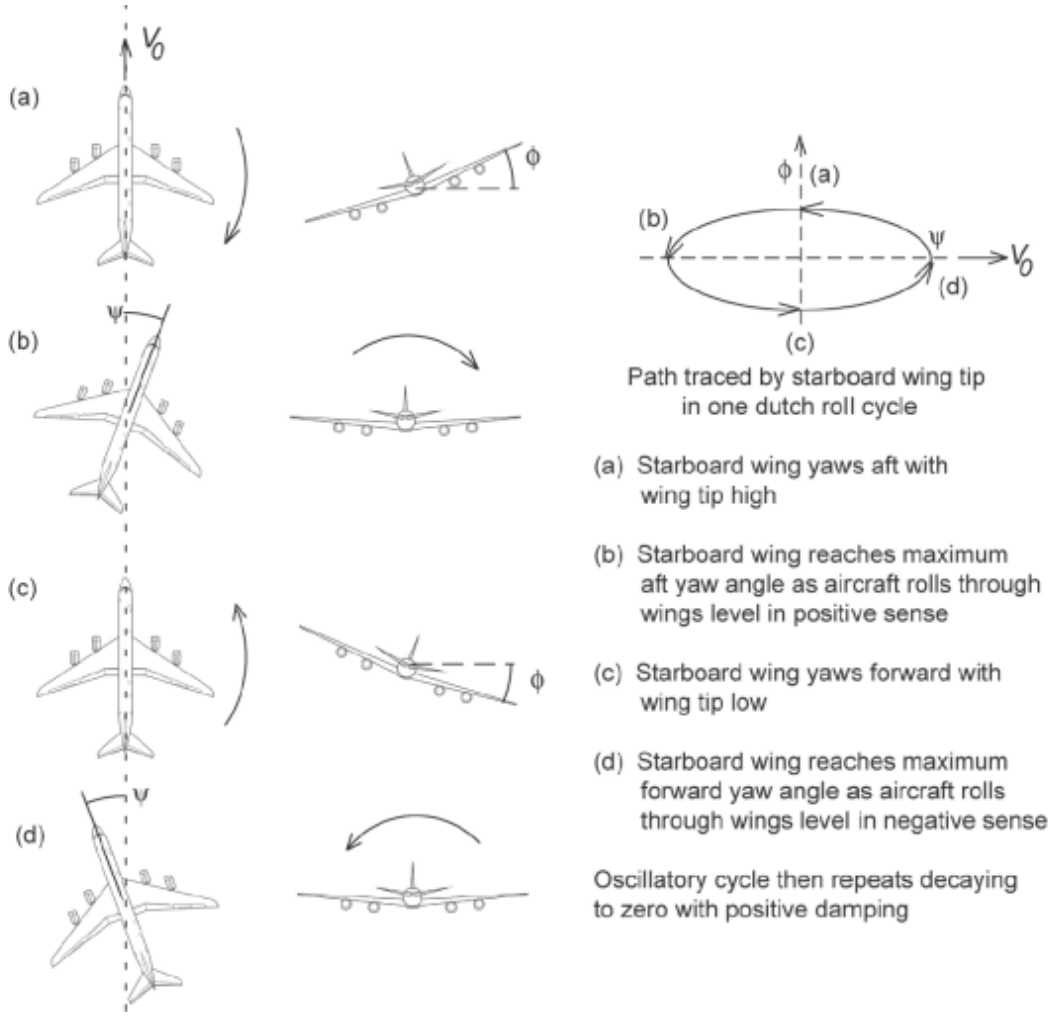

Figure 3.7: *Schematic representation of Dutch Roll effect* [8].

The heading and sideslip angles in a Dutch roll are out of phase with each other with the heading and sideslip motions being consistent with those in a relatively flat yawing oscillation, implying that rolling component is relatively less significant. However, the bank angle cannot be totally ignored and it leads the sideslip and lags behind the yaw, indicating that the sideslip follows the roll motion, which follows the yaw motion as shown in Figure 3.7 above.

3.7.8.2 Roll

Roll mode is a non-oscillating mode that has a high damping factor. It occurs after the appearance of lateral perturbation which may be due to an action to the stick or lateral wings. During this mode there is a roll angle variation ϕ, even they exist the variations of sideslip and yaw angles are neglected as they are very small in the calculation of Roll mode, Figure 3.8 illustrates this phenomena.

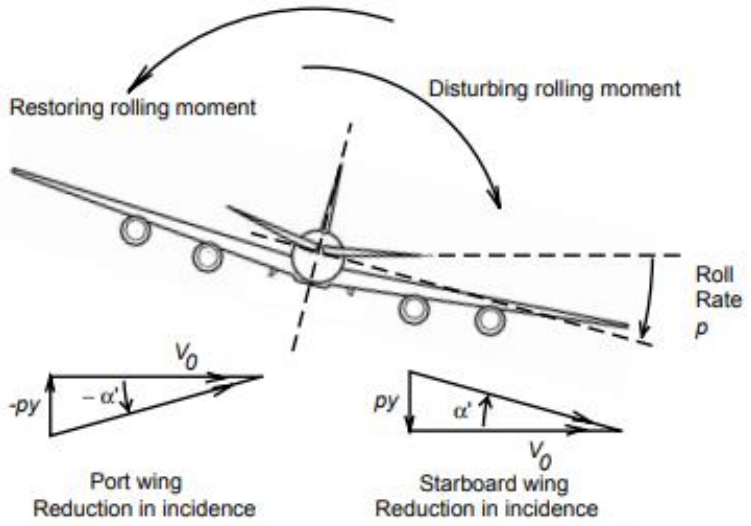

Figure 3.8: *Movement associated to the Roll mode* [8].

3.7.8.3 Spiral

Spiral mode is like Roll mode a non-oscillating mode. It's a mode that converges or diverges very slowly and often unstable, which makes it the least important mode in the stability calculations. It is characterized by the variation of the roll and yaw angles when the aircraft is inclined. It is usually excited by a disturbance in sideslip, which typically follows a disturbance in roll and causes a wing to drop. Assume that the aircraft is initially in trimmed wings level flight and that a disturbance causes a small positive roll angle ϕ to develop. Left unchecked, this result in a small positive sideslip velocity v as indicated at (a) in Figure 3.9. The sideslip puts the fin at incidence β, which produces lift and in turn, generates a yawing moment to turn the aircraft into the direction of the sideslip. The yawing motion produces differential lift across the wing span, which in turn results in a rolling moment, causing the starboard wing to drop further there by exacerbating the situation. This developing divergence is indicated at (b) and (c). Simultaneously, the dihedral effect of the wing generates a negative restoring rolling moment due to sideslip that acts to return the wing to a level attitude; the fin lift force also generates some additional restoring rolling moment when it acts at a point above the roll axis *ox*, which is usual.

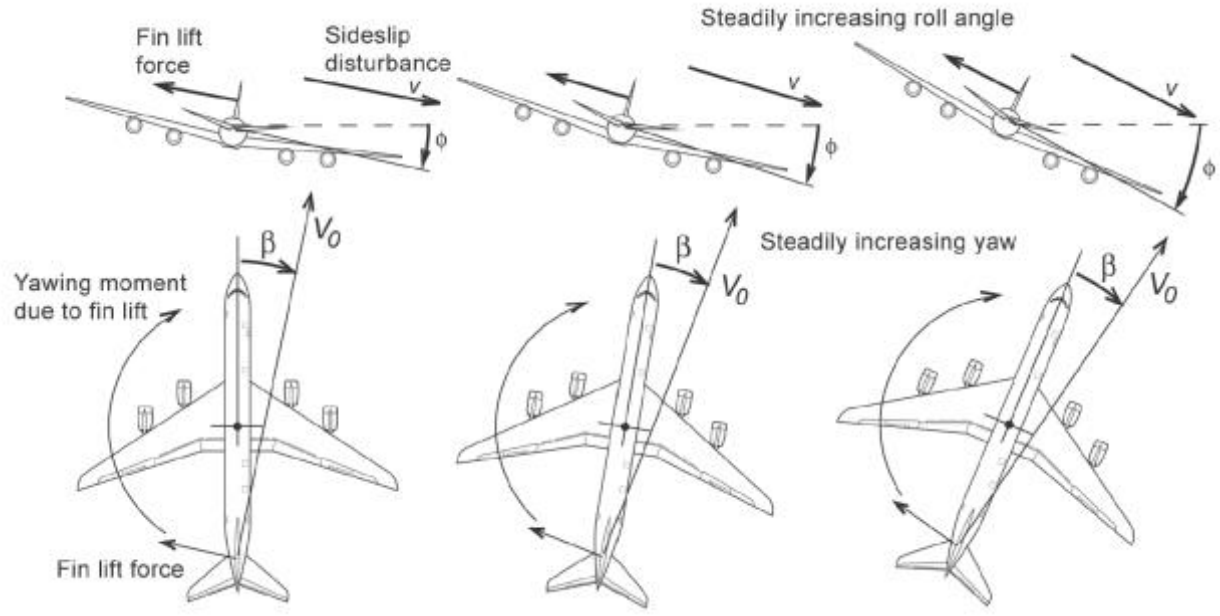

Figure 3.9: *Schematic representing the Spiral mode effect* [8].

3.8 Military flying qualities requirements

In the aircraft design it is necessary to know what levels of stability and control are desirable and performance criteria are available, so that the pilot can evaluates the aircraft in different ways depending on the type of aircraft and phase of flight, also he can keep the aircraft safe and controllable. However, in order to standardize all of these recommendations, both national and international authorities, such as the JAR or the FAA, have published a list of specifications that deal with flight qualities.

A survey and a large bibliography covering twenty-five years of handling qualities research has been given by Ashkenas (1984). The "background information and user guides" for the military flying qualities specifications MIL-F-8785B and MIL-F-8785C (Chalk et al., 1969; Moorhouse and Woodcock, 1982) also provide much useful information. The military specification defines airplane classes, flight phases, and flying qualities levels, so that different modes can be specified for the various combinations. The airplane classes and the flight phases are defined in Table 3.1, Table3.2 respectively; the flying qualities levels are linked to the Cooper-Harper ratings as shown in Table 3.3 [3].

Table 3.1: *Airplane classes* [3].

Class I	Small, light airplanes.
Class II	Medium weight, low-to-medium-maneuverability airplanes.
Class III	Large, heavy, low-to-medium-maneuverability airplanes.
Class IV	High-maneuverability airplanes.

Table 3.2: *Flight phases* [3].

Categories	Flight phases
Category A	Nonterminal flight phases generally requiring rapid maneuvering.
Category B	Nonterminal flight phases normally accomplished using gradual maneuvers without precision tracking, although accurate flight-path control may be required.
Category C	Terminal flight phases normally accomplished using gradual maneuvers and usually requiring accurate flight-path control.

Table 3.3: *Flying qualities* [3].

Levels	Flying qualities
Level 1	Flying qualities adequate for the mission flight phase.
Level 2	Flying qualities adequate to accomplish the mission flight phase, but some increase in pilot workload or degradation in mission effectiveness exists.
Level 3	Flying qualities such that the airplane can be controlled safely, but pilot workload is excessive, or mission effectiveness is inadequate, or both.

3.8.1 Nelson stability matrix

3.8.2 Longitudinal stability matrix

In order to construct the stability matrix A, we must first define the state vector x.in this section two state vectors are presented. The calculation of derivatives is summarized in Appendix A.

The first vector is:

$$\vec{x} = \begin{pmatrix} u \\ w \\ q \\ \theta \end{pmatrix} \tag{3.25}$$

From this state vector, it is possible to obtain the stability matrix given by equation (3.26). This matrix has been constructed in such a way as to minimize approximations. Table 3.4 describes in detail the different coefficients of this matrix.

$$\mathbf{A} = \begin{bmatrix} X_u & X_w & X_q & -g\cos(\alpha) \\ \mathrm{Z_u} & \mathrm{Z_w} & U_0 + Z_q & -g\sin(\alpha) \\ \widetilde{M}_u & \widetilde{M}_w & \widetilde{M}_q & -M_{\dot{w}}\sin(\alpha) \\ 0 & 0 & 1 & 0 \end{bmatrix} \tag{3.26}$$

Table 3.4: *Definition of the different coefficients of longitudinal matrix A* [8].

Variables	Equations
X	$X_u = \frac{\rho S u}{2m}(-2C_D\cos(\alpha) + 2C_L\sin(\alpha) - C_{D_u}\cos(\alpha) + C_D(\sin(\alpha)^2) - C_L\cos(\alpha)\sin(\alpha) + C_{L_u}\sin(\alpha))$
	$X_w = \frac{\rho S U_0}{2m}(C_{L_\alpha}\sin(\alpha) + C_L\cos(\alpha) - C_{D_\alpha}\cos(\alpha) - C_D\sin(\alpha))$
	$X_q = \frac{\rho S U_0 \bar{c}}{4m} C_{x_q}$
Z	$Z_u = -\frac{\rho S u}{2m}(2C_L(\cos(\alpha)^2) + C_D cos(\alpha) sin(\alpha) + C_{L_u} cos(\alpha) + C_L(\sin(\alpha)^2))$
	$Z_w = -\frac{\rho S U_0}{2m}(C_{L_\alpha}\cos(\alpha) - C_L\sin(\alpha) + C_{D_\alpha}\sin(\alpha) + C_D\cos(\alpha))$
	$Z_q = -\frac{\rho S U_0 \bar{c}}{4m} C_{z_q}$
$\widetilde{M}$	$\widetilde{M}_u = \frac{\rho S U_0 \bar{c}}{2I_{yy}}\left(C_{m_u} + 2C_m cos(\alpha)\right) + M_{\dot{w}} Z_u \;\; with \;\; M_{\dot{w}} = \frac{\rho S \bar{c}^2}{4I_{yy}} C_{m_{\dot{\alpha}}}$
	$\widetilde{M}_w = \frac{\rho S U_0 \bar{c}}{2I_{yy}} C_{m_\alpha} + M_{\dot{w}} Z_u$
	$\widetilde{M}_q = \frac{\rho S U_0 \bar{c}^2}{4I_{yy}} C_{m_q} + M_{\dot{w}} U_0$

3.8.3 Lateral stability matrix

The state vector is defined as:

$$\vec{x} = \begin{pmatrix} \beta \\ p \\ r \\ \psi \end{pmatrix} \tag{3.27}$$

It is also possible to meet this state vector with the speed v instead of the sideslip angle β. However, it is easier to find the derivatives of the different coefficients with respect to the sideslip angle than the speed v. The link between these two variables is given by the

approximation $\beta = \tan\left(\frac{v}{U_0}\right) \approx \frac{v}{U_0}$. From this state vector, it is possible to obtain the stability matrix presented in equation (3.28), Table 3.5 describes in detail the different coefficients of this matrix.

$$\mathbf{A} = \begin{bmatrix} \frac{Y_\beta}{U_0} & \frac{Y_p}{U_0} & \frac{Y_r}{U_0} - 1 & g\frac{cos(\alpha)}{U_0} \\ L'_\beta & L'_p & L'_r & 0 \\ N'_\beta & N'_P & N'_r & 0 \\ 0 & 1 & \sin(\alpha) & 0 \end{bmatrix} \tag{3.28}$$

Table 3.5: Definition of the different coefficients of lateral matrix A [8].

Variables	v	p	r
Y	$Y_v = \frac{\rho S U_0}{2m} C_{y_\beta}$	$Y_p = \frac{\rho S U_0}{4m} C_{y_p}$	$Y_r = \frac{\rho S U_0 b}{4m} C_{y_r}$
L	$L_v = -\frac{\rho S U_0 b}{2I_{xx}} C_{l_\beta}$	$L_p = \frac{\rho S U_0 b^2}{4I_{xx}} C_{l_p}$	$L_r = \frac{\rho S U_0 b^2}{4I_{xx}} C_{l_r}$
N	$N_v = -\frac{\rho S U_0 b}{2I_{zz}} C_{n_\beta}$	$N_p = \frac{\rho S U_0 b^2}{4I_{zz}} C_{n_p}$	$N_r = \frac{\rho S U_0 b^2}{4I_{zz}} C_{n_r}$
L'_i	$L'_i = L_i + \frac{I_{xz}}{I_{zz}} N_i$		
N'_i	$N'_i = N_i + \frac{I_{xz}}{I_{zz}} L_i$		

3.9 Summary

In this chapter we have presented the importance of the aircraft's stability analyses in control systems design. We have introduced the static stability and control for longitudinal, lateral and direction motions as well as the lateral and longitudinal dynamic stability and control has been discussed with a clear description of Short Period, Ducth Roll, Roll, Spiral dynamic modes.

The important points to recognize from this chapter are: A stable aircraft is an aircraft that can be established in an equilibrium flight condition where it will remain showing no tendency to diverge. It must be made statically stable, either through inherent aerodynamic characteristics or by artificial means through the use of an automatic control system as our F-16 aircraft's model that demand high stability and equilibrium because of the complex maneuvers. Flying Qualities have a critical bearing on the safety of flight and on the ease of controlling an aircraft in both steady and maneuvering flights. An aircraft with poor flying qualities can result in undesirable response characteristics potentially leading to catastrophic loss of vehicle and life.

Chapter 4: Controller design

Chapter 4: Controller design

4.1 Introduction

The design of an automatic flight control generally begins with selecting the appropriate desired functions of the autopilots. The next step involves choosing an appropriate control structure. Many controllers exists from a simplest to a more complex controller structure, adaptive or self-tuning, internal model or even a sophisticated non-linear control structure. The choice depends on the flying requirements, safety, stability margins, robustness and handling qualities that were introduced in chapter 3. The final stage of control design provides choosing an appropriate architecture of a modern controller implemented digitally dedicated for civil or military aircrafts.

In the previous chapters, we have succeeded obtaining the mathematical linear and non-linear model, which can be used to determine control derivatives and stability that are utilized in control surfaces and designing flight control systems and simulation.

This chapter will cover the design and evaluation of the different controllers: LQR, PID, Fuzzy logic, used to design controller of the F-16 model, as well as some mixed controllers technology will be introduced. Each of these techniques has its proponents and each one has its advantages and disadvantages. Our strategy in developing modern control system is explained in details showing examples how it is used in aircraft controls, we now discuss some controllers' background.

4.2 Background

4.2.1 Linear Quadratic Regulator (LQR)

Linear quadratic regulator or LQR is commonly used technique to find the state feedback gain for a closed loop system. This is the optimal regulator, by which the open-loop poles can be relocated to get a stable system with optimal control and minimum cost for given weighting matrices of the cost function. On the other hand, by using the optimal regulator technique, that freedom of choice is lost for both discrete-time and continuous-time systems, because, in order to get a positive definite Riccati equation solution, there are some areas where the poles cannot be assigned [12].

Consider the state feedback controller is given by:

$$u(t) = Kx(t) \tag{4.1}$$

That stabilized the closed loop system and minimizes

$$J := \int_0^\infty x(t)^T\, Qx(t) + u(t)^T Ru(t)dt \tag{4.2}$$

Where x and u are the state and control of the LTI system

$$\dot{x}(t) = Ax(t) + Bu(t) \quad , \qquad x(0) = x_0 \tag{4.3}$$

Assumption:

a) $Q \geq 0$, $R > 0$;

b) (A, B) stabilizable ;

A first step toward a solution,

The closed loop cost is:

$$J := \int_0^\infty x(t)^T\, (Q + K^T RK)x(t)dt \tag{4.4}$$

And the closed loop system (Figure 4.1) is:

$$\dot{x}(t) = (A + BK)x\,, \qquad x(0) = x_0 \tag{4.5}$$

But for a given gain K and x_0

$$x(t) = e^{(A+BK)t}x_0 \tag{4.6}$$

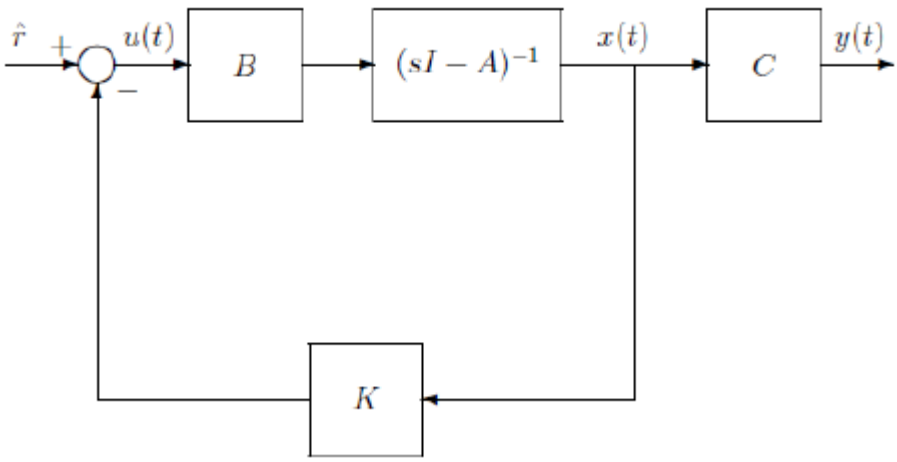

Figure 4.1: *The closed loop LQR system* [12].

Hence:

$$\boldsymbol{J = \int_0^{\infty} x_0{}^T e^{(A+BK)T_t} (Q + K^T R K) e^{(A+BK)t} x_0 dt} \tag{4.7}$$

$$\boldsymbol{= x_0{}^T \left(\int_0^{\infty} e^{(A+BK)T_t} (Q + K^T R K) e^{(A+BK)t} dt \right) x_0}$$

This means that J can be computed as:

$$J = x_0{}^T X \, x_0 \tag{4.8}$$

Where X is the solution to the Lyapunov equation

$$\boldsymbol{(A + BK)^T X + X(A + BK) + Q + K^T RK = 0} \tag{4.9}$$

Before proceeding we need to learn how to solve the above Lyapunov equation in X and K. This is not always possible. In this case, because $R \succ 0$, we can complete the squares, rewriting the above equation in the form

$$\boldsymbol{A^T X + XA - XB\, R^{-1}\, B^T\, X + Q + (XBR^{-1} + K^T)\, R(R^{-1}B^T\, X + K) = 0} \quad (4.10)$$

Note that K is confined to the term

$$(XBR^{-1} + K^T)R(R^{-1}B^TX + K) \geq 0 \quad (4.11)$$

In addition, that for:

$$k = -R^{-1}B^TX \quad (4.12)$$

We have:

$$Q + (XBR^{-1} + K^T)R(R^{-1}B^TX + K) = Q \quad (4.13)$$

This reduces the above equation to:

$$A^TX + XA - XBR^{-1}B^TX + Q = 0 \quad (4.14)$$

This is an Algebraic Riccati Equation (ARE) in X.

As we learn more about AREs we shall prove that the above choice of K and X is so that

1- $A + BK$ is Hurwitz (asymptotically stable);

2- X is "minimum" in a certain sense;

3- The associated J is minimized.

4.2.2 Proportional Integral Derivative (PID)

PID controllers are the most widely used type of controller for industrial applications. They are structurally simple and exhibit robust performance over a wide range of operating

conditions. In the absence of the complete knowledge of the process, these types of controllers are the most efficient of choices. The three main parameters involved are Proportional (P), Integral (I) and Derivative (D) in which the proportional term is for providing an overall control action proportional to the error signal through the constant gain factor, the integral term is to reduce steady-state errors through low-frequency compensation by an integrator, The derivative term improves transient response through high-frequency compensation by a differentiator.

In this section, we will be discussing the PID structures, presenting his three parts and the PID controller parameters; also, we described few tuning methods used in control design [14].

4.2.2.1 PID structure:

The general form for of the PID controller output $u(t)$ is given by equation (4.15) and presented in a schematic in Figure 4.2:

$$u(t) = K_p e(t) + K_i \int_0^t e(\tau)d\tau + K_d \frac{de(t)}{dt} \qquad (4.15)$$

Where:

K_p : Proportional gain.

K_I : Integral gain.

K_D : Derivative gain.

$e(t)$: Is the error ($e(t) = r(t) - y(t)$).

t : Is the present time.

τ: Is the variable of integration (takes value from 0 to the present time$t$).

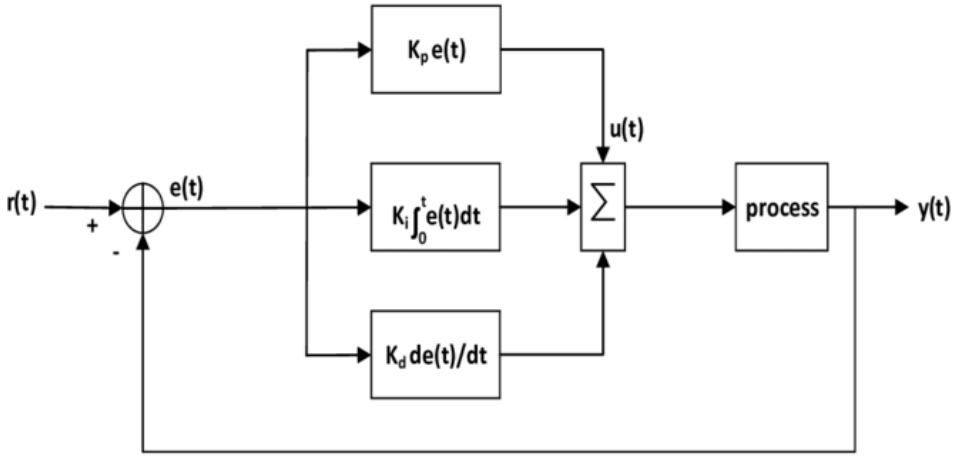

Figure 4.2: *Block diagram of PID controller system* [14].

There are four types of controllers that belong to the family of PID controllers: the proportional (P) controller, the proportional plus integral (PI) controller, the proportional plus derivative (PD) controller and the proportional plus integral plus derivative (PID) controller.

- **The proportional part:**

The proportional part (P-part) of the control signal is proportional to the control error,

$$u_p(t) = Ke_p(t) + u_0, \qquad e_p(t) = br(t) - y(t) \tag{4.16}$$

Such that it reacts to present deviations from the set point. The proportional gain, K, is the parameter normally associated with the P-part. A P-controller alone cannot guarantee zero static control errors, the control signal becomes zero for $e_p(t) = 0$. The bias term u_0 is used to reduce this effect in controllers that lack an integral part. The magnitude of the static error depends on K. The speed and noise sensitivity of the closed-loop system will typically increase with an increasing K at the same time as the robustness decreases. The P-part is sensitive to noise since K is multiplied directly with the measurements $y(t)$ unless filtered first. Abrupt changes in the set point can be smoothed out in the control signal by choosing a set-point weight $0 \leq b < 1$.

- **Integral part:**

The integral part (I-part) integrates past values of the control error,

$$u_i(t) = \frac{K}{T_i}\int_0^t e(\tau)d\tau = k_i\int_0^t e(\tau)d\tau, \qquad e_i(t) = r(t) - y(t) \tag{4.17}$$

and will thus remove static control errors due to step load disturbances and set-point changes. It introduces the integral time T_i , but also depends on the proportional gain K unless the fraction $\frac{K}{T_i}$ is replaced by an independent parameter k_i called the integral gain. Reducing T_i normally leads to a faster, although less robust, closed-loop system. The summation of past control errors makes the I-part insensitive to noise.

- **Derivative part:**

The derivative part (D-part) of the PID controller,

$$u_d(t) = KT_d\frac{de_d(t)}{dt} = k_d\frac{de_d(t)}{dt}, \qquad e_d(t) = cr(t) - y(t) \tag{4.18}$$

Predicts future behavior of the controlled variable. It introduces the derivative time T_d, but also depends on K unless KT_d is replaced by the derivative gain k_d. Closed-loop robustness will typically increase with an increasing T_d at the same time as the performance decreases. This is a consequence of the damping properties of the D-part. The system as a whole can still obtain better performance, since the proportional and integral gains can be increased to balance robustness. It is thus important to use a low-pass filter together with the D-part. The set-point weight c is normally set to zero to avoid large transients in the control signal.

4.2.2.2 PID design methods

In this section, we will be distinguishing PID design based on tuning methods. Tuning methods are a set of formulas from which one can determine the controller parameters and they typically depend on the parameters of some specific process model.

- **Ziegler-Nichols Method**

Two classical methods for determining the parameters of PID controllers were presented by Ziegler and Nicholas in 1942. They are still widely used, either in their

original form or in some modification, this method remains a popular technique for tuning controllers.

1- Closed-loop tuning method: This method has given simple formulas for the parameters of the controller in terms of the ultimate K_u gain and the ultimate period T_u, This basic test requires that the response of the system be recorded, preferably by a plotter or computer, once certain process response values are found, they can be plugged into the Ziegler-Nichols equation with specific multiplier constants for the gains of a controller with either P, PI or PID actions. The PID parameters obtained from this method are presented in Table 4.1.

Table 4.1: *PID control parameters obtained from Closed-loop Ziegler-Nichols method* [15].

Controller	K	T_i	T_d	T_p
P	$0.5K_u$			T_u
PI	$0.4K_u$	$0.8T_u$		$1.4T_u$
PID	$0.6K_u$	$0.5T_u$	$0.125T_u$	$0.85T_u$

2- Open-loop tuning method: The Ziegler-Nichols open-loop method is also referred to as a process reaction method, because it tests the open-loop reaction of the process to a change in the control variable output. The parameters determined from this method are given in Table 4.2.

Table 4.2: *PID control parameters obtained from Open loop Ziegler-Nichols method* [15].

Controller	K_c	T_i	T_d
P	K_0		
PI	$0.9K_0$	$3.3\tau_{dead}$	
PID	$1.2K_0$	$2\tau_{dead}$	$0.5\tau_{dead}$

Where:

τ_{dead} is the transportation lag or dead time and K_0 is given by the equation (4.19):

$$K_0 = \frac{X_0}{M_u}\frac{\tau}{\tau_{dead}} \tag{4.19}$$

$X_0$is the step change in the input and M_u the ultimate value that the response reaches at steady-state.

- **Cohen-Coon Method**

The Cohen-Coon tuning rules are suited to a wider variety of processes than the Ziegler-Nichols tuning rules. The Ziegler-Nichols rules work well only on processes where the dead time is less than half the length of the time constant. The Cohen-Coon tuning rules work well on processes where the dead time is less than two times the length of the time constant. In addition, it provides one of the few sets of tuning rules that has rules for PD controllers.

Like the Ziegler-Nichols tuning rules, the Cohen-Coon rules aim for a quarter-amplitude damping response. Although quarter-amplitude damping-type of tuning provides very fast disturbance rejection, it tends to be very oscillatory and frequently interacts with similarly tuned loops. Quarter-amplitude damping-type tuning also leaves the loop vulnerable to going unstable if the process gain or dead time doubles in value. These settings are shown in Table 4.3.

Table 4.3: *Standard recommended equations to optimize Cohen Coon predictions* [15].

Controller	K_c	T_i	T_d
P	$\left(\frac{P}{NL}\right) * \left(1 + \left(\frac{R}{3}\right)\right)$		
PI	$\left(\frac{P}{NL}\right) * \left(0.9 + \left(\frac{R}{12}\right)\right)$	$L * \frac{(30 + 3R)}{(9 + 20R)}$	
PID	$\left(\frac{P}{NL}\right) * \left(1.33 + \left(\frac{R}{4}\right)\right)$	$L * \frac{(30 + 3R)}{(9 + 20R)}$	$\frac{4L}{11 + 2R}$

Where the variables P, N, and L are defined below in Table 4.4.

Table 4.4: *PID control parameters obtained from Ziegler-Nichols method* [15].

P	Percent change of input
N	Percent change of output/τ
L	τ_{dead}
R	$\frac{\tau_{dead}}{\tau}$

Remark: $\frac{P}{NL}$ can be replaced with K_0.

It exist other PID tuning methods that are used:

- ***Analytical methods:*** At these methods, the PID parameters are calculated with analytical or algebraic relations based in a plant model representation and in some design specification.
- ***Heuristic methods:*** These methods are evolved from practical experience in manual tuning and are coded with artificial intelligence techniques, like expert systems, fuzzy logic and neural networks.
- ***Frequency response methods:*** the frequency response characteristics of the controlled process are used to tune the PID controller. Frequently these are offline and academic methods, where the main concern of design is stability robustness since plant transfer function have unstructured uncertainty.
- ***Optimization methods:*** these methods utilize an offline numerical optimization method for a single composite objective or use computerized heuristics or, yet, an evolutionary algorithm for multiple design objectives. According to the characteristics of the problem, an exhaustive search for the best solution may be applied. Some kind of enhanced searching method may be used also. These are often time-domain methods and mostly applied offline. This is the tuning method used at the development of this work.
- ***Automatic tuning methods:*** these methods are based in automated online tuning, where the parameters are adjusted in real-time through one or a combination of the previous methods. System identification may be used to obtain the process dynamics over the use of the input-output data analysis and real time modelling in MATLAB using PID objects or in Simulink using PID Controller blocks.

4.2.3 Fuzzy Logic Controller (FLC)

Fuzzy logic controllers (FLCs) are used in control system design for processes that do not admit a mathematical model or where the data is imprecise. FLCs are fuzzy expert systems that can model the human operator of a process. They are based on a linguistic description of the process variables.

A fuzzy logic controller is a fuzzy expert system that is a generalization of the expert systems widely used in artificial intelligence (AI). An intelligent control system combines the techniques from the fields of artificial intelligence (AI), with those of control engineering to design autonomous systems that can sense, reason, and plan, learn and act in an intelligent manner applications. The main difference between fuzzy expert systems and AI expert systems is in the way they handle uncertainty. In an AI expert system, uncertainty is handled using a probabilistic approach. A fuzzy expert system attempts to handle uncertainty in the way humans do, using linguistic variables and fuzzy sets. The knowledge of the human operator is embedded in the fuzzy rule base. The inference engine and the defuzzifier approximate the response of the human operator to a given set of inputs. Initially fuzzy logic controllers were applications characterized by slow time applied in process control constants and lacking the mathematical models of the process, but reasonably controlled by a human [18].

4.2.3.1 Structure of Fuzzy Logic Controller

Basically, fuzzy controller comprises of four main components, fuzzification interface, knowledge base, inference mechanism and defuzzification interface. Figure 4 shows components of fuzzy logic controller.

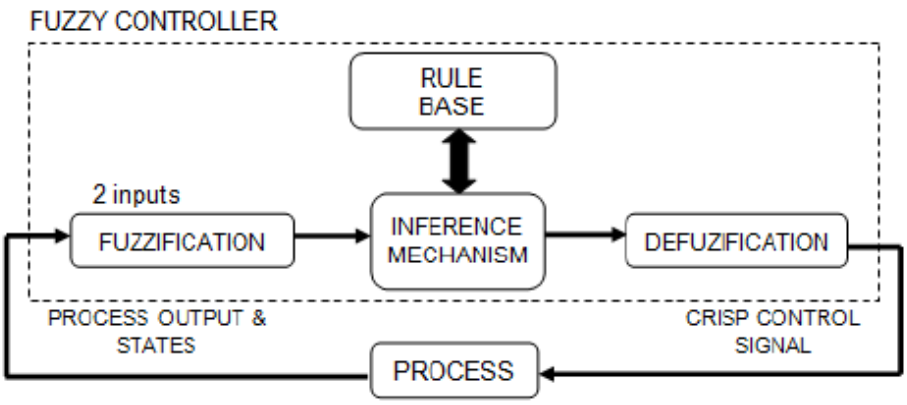

Figure 4.3: *Components of Fuzzy Logic Controller* [18].

In order to understand the concept of the fuzzy logic controller (FLC) controller, we will be describing it components as follows:

- **Fuzzy:** A qualitative value rooted in conceptual ideas and abstract constructs used to approximate a crisp value.
- **Crisp:** A quantitative value rooted in mathematical ideas carrying specific values represented by real or complex numbers.
- **Rule-base:** A set of IF-THEN rules used by the interface system to infer input values to output values as part of the inference system.
- **Membership Function:** A distribution function, which maps linguistic values to crisp values.
- **Universe-of-Discourse:** The set of values over which an input or output is valid. This includes real or complex numbers, a finite set of integers, a closed-infinite set, or any other group of values.

-**Linguistic Values and Variables:** The concept of linguistic variables plays a fundamental role in modelling fuzzy systems. It provides a good means of describing the behavior of complex systems by representing uncertain variables in terms of propositions that humans use. These propositions expressed in natural language are then converted into fuzzy meaning (fuzzy sets or fuzzy numbers). An example of a linguistic variable might be controlling the desired pitch angle θ_d based on the Automatic Landing System data which is shown in Figure 4.4. The linguistic variable, pitch angle, is defined as a base variable on a specified universe of real numbers, it is abstract terms used to describe the value of an input or output. These constitute the descriptive terms of a fuzzy logic system; they are linguistic variables.

A linguistic value is the numerical value associated with a linguistic variable. It is expressed as seven linguistic values: Negative small, Zero, Positive small, Negative big, Positive big, Negative, Positive. These linguistic values are represented by specific fuzzy numbers defined on the base variable universe.

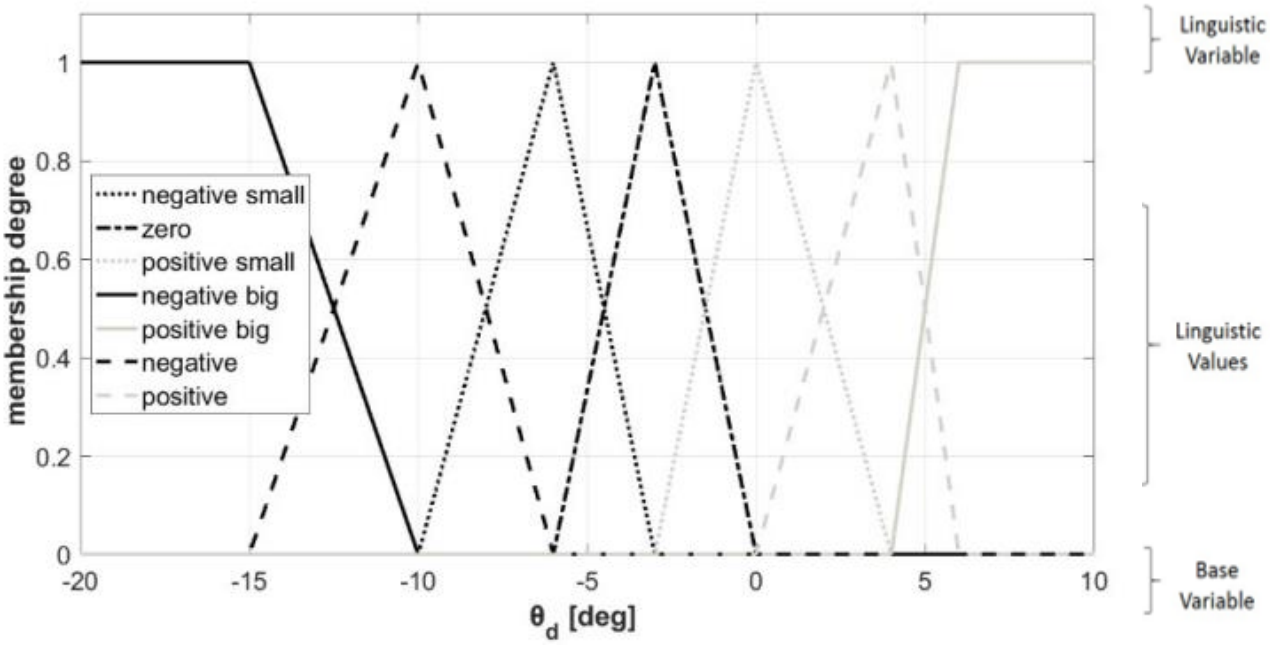

Figure 4.4: *Illustration of linguistic variable of the desired pitch angle* [20].

- **Fuzzification:** It is a process of converting data of the input variable into a fuzzy format in order to incorporate the necessary uncertainty into the input variable. That is, to determine a fuzzy set representing all membership degrees of the linguistic values corresponding to the input variable data. The input to the fuzzification process can be a crisp or fuzzy value but the output.

- **Defuzzification**: Unlike fuzzification, defuzzification is a process of converting fuzzy output value into a single crisp value as needed in many real-world application. Many methods have been proposed in literature to perform defuzzification. Among the commonly used defuzzification methods are: Weighted Average method, Centroid method, and Mean-Max method.

  The formula presented in equation (4.20) describes the defuzzification process mathematically where $y_{crisp}$the crisp output is, μ_i is a specific inference rule, and y_i is the output singleton associated with the given rule.

$$y_{crisp} = \frac{\sum_i^n 1\mu_i \, y_i}{\sum_i^n 1\mu_i} \tag{4.20}$$

- **Inference system:** Fuzzy inference system is classified into three types on the basis of the consequent of the fuzzy rules that are required for the inference procedure:
  - Mamdani fuzzy inference system : It was initially developed by using a set of linguistic variables. The fuzzy rules in such control system are obtained from experienced human operator .The fuzzy rules in Mamdani fuzzy inference system are of the form:

    If x is small then y is small.

    If x is small then y is medium.

    Here antecedent and consequent of the rules are linguistic variables and both are fuzzy. Mamdani fuzzy inference system generates output in fuzzy form so there is a need to convert this fuzzy output into crisp form. For this purpose different defuzzification techniques are used to defuzzify fuzzy output into crisp .
  - Takagi Sugeno Kang fuzzy inference system: It was proposed by Takagi, Sugeno and Kang for developing systematic approach that can generate fuzzy rules from given input output data set .A typical fuzzy rule in this model is of the form:

    If x is A and y is B then $z = f(x, y)$.

    Where antecedent of the rule is in fuzzy form and consequent of rule is represented by a function in x and y fuzzy input. $z = f(x, y)$ is a crisp function. $f(x, y)$ is a polynomial in x and y. If $f(x, y)$ is a first order polynomial then the inference system is called as first order Sugeno fuzzy model. If f is constant then the inference system is zero order Sugeno fuzzy model which is a special case of Mamdani fuzzy model, then its order changes with the polynomial.
  - Tsukamoto fuzzy inference system: In this interface, the consequent of fuzzy if-then rule is represented by a fuzzy set with monotonically membership function. So the output of each rule is defined as a crisp value. However, Tsukamoto fuzzy inference system is not used often in applications because this system is not much transparent in comparison to Mamdani fuzzy model and Takagi Sugeno fuzzy model. The rules in this inference system are represented as:

If x is small then y is $c1$.

If x is medium then y is $c2$.

Here the consequent of the rules are fuzzy sets such that the output of Tsukamoto fuzzy inference system is crisp even if the input is fuzzy [20].

4.2.4 Mixed controllers

The controller design always depends on the plant's mathematical model, whether it is based on linear system theory or non-linear design methods like feedback linearization. The classical controllers has been largely used, but for a complex non-linear system with uncertainty and big effect of disturbance a novel control design is presented systematically to synthesize a robust nonlinear feedback controller. A robust and fast-response control system plays an important role in designing and developing a high-performance aircraft.

In our study, we will be introducing some modern intelligent controllers design methodology to examine their overall performance primarily based on time response specification for controlling movement of aircraft. This new technology consists of combining the different controllers and tuning methods using specific structures such as: PID, FLC, LQR and H. Moreover, this intelligent controller can be developed using algorithms such as some specific algorithms are used can be optimized using various optimization techniques such as Genetic Algorithm, Artificial intelligence. Some mixed controllers design is reviewed in which we will be used in implementations.

4.2.4.1 PID-Fuzzy controller design

Fuzzy PI type control is known to be more practical than fuzzy PD type, since it is difficult for the fuzzy PD to remove the steady state error. The fuzzy PI type control is however known to give poor performance in the transient response for higher order process due to the internal integration operation. To improve the performance of the fuzzy PI type and fuzzy PD type at the same time we want to design a Fuzzy controller that process the fine characteristics of the PID controller only by using the error and the rate of change of error as its inputs

The structures of PID-Fuzzy controllers which have been developed for the aircraft pitch and roll control model, it is developing to control the rigid body motion of the system. The

common structure of PID-type fuzzy controller that has two inputs and rules base is depicted in Figure 4.5, as can be seen, the output from controller, u_c is fed by integrator output, u_1 and gain u_2 [21].

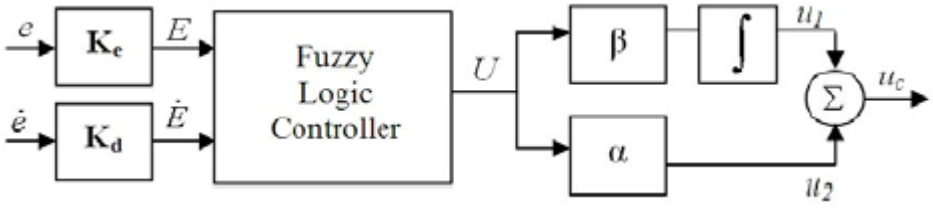

Figure 4.5: *PID-type fuzzy logic controller* [21].

The output of PID-type fuzzy controller is given by equation (4.21):

$$\begin{aligned} u_c &= \alpha U + \beta \int U dt \\ &= \alpha(A + PK_e e + DK_d \dot{e}\ ) + \beta \int (A + PK_e e + DK_d \dot{e}\ ) dt \\ &= \alpha A + \beta A t + (\alpha K_e P + \beta K_d D) e + \beta K_e P \int e\, dt + \alpha K_d D \dot{e} \end{aligned} \qquad (4.21)$$

Where:

Proportional: $\alpha K_e P + \beta K_d D$.

Integral: $\beta K_e P$.

Derivative: $\alpha K_d D$.

4.2.4.2 Genetic algorithm based PID controller

The novelty of this mixed controller is achieved by the development of a new methodology based on creating to find a PID controller that gives the smallest overshoot, fastest rise time or quickest settling time. However, in order to combine all of these objectives it was decided to design an objective function that will minimize the error of the controlled system instead. Each element in the population is passed into the objective function one at a time, which is obtained by optimizing all the five parameters by using an evolutionary algorithm optimization technique known as a genetic algorithm which is a very powerful search tool and carrying heuristic characteristics.

4.2.4.3 Preliminary and background of Genetic Algorithm (GA)

Genetic algorithm (GA) uses the principles of evolution, natural selection and genetics from natural biological systems in a computer algorithm to simulate evolution. Essentially, the genetic algorithm is an optimization technique that performs a parallel, stochastic, but directed search to evolve the fittest population. John Holland formally introduced this method in the United States in the 1970 at the University of Michigan, the continuing performance improvements of computational systems have made them attractive for some types of optimization.

Biological evolution is an appealing source of inspiration for addressing optimization problems. Evolution is a method of searching among an enormous number of possibilities for "solutions." In biology the enormous set of possibilities is the set of possible genetic sequences, and the desired "solutions" are highly favorable organisms—organisms, which are able to survive and reproduce in their environments.

The idea, in all the system based on Genetic algorithm as shown in Figure 4.6, was to evolve a population of candidate solutions to a given problem, using operators inspired by natural genetic variation and natural selection, such that most important step in applying genetic algorithm is the selection of the fitness function. The fitness criteria continually change as creatures evolve, so evolution is searching a constantly changing set of possibilities and searching for solutions in the face of changing conditions is precisely what is required for adaptive computer programs.

In this way, GA has been shown to be capable of locating high performance areas for designing innovative solutions to complex problems [23].

The most challenging part of creating a GA is writing the objective function. However, in order to combine all of these objectives it was decided to design an objective function that will minimize the error of the controlled system instead. Each chromosome in the population is passed into the objective function one at a time. The chromosome is then evaluated and assigned a number to represent its fitness, the bigger its number the better its fitness. The genetic algorithm uses the chromosomes fitness value to create a new population consisting of the fittest members.

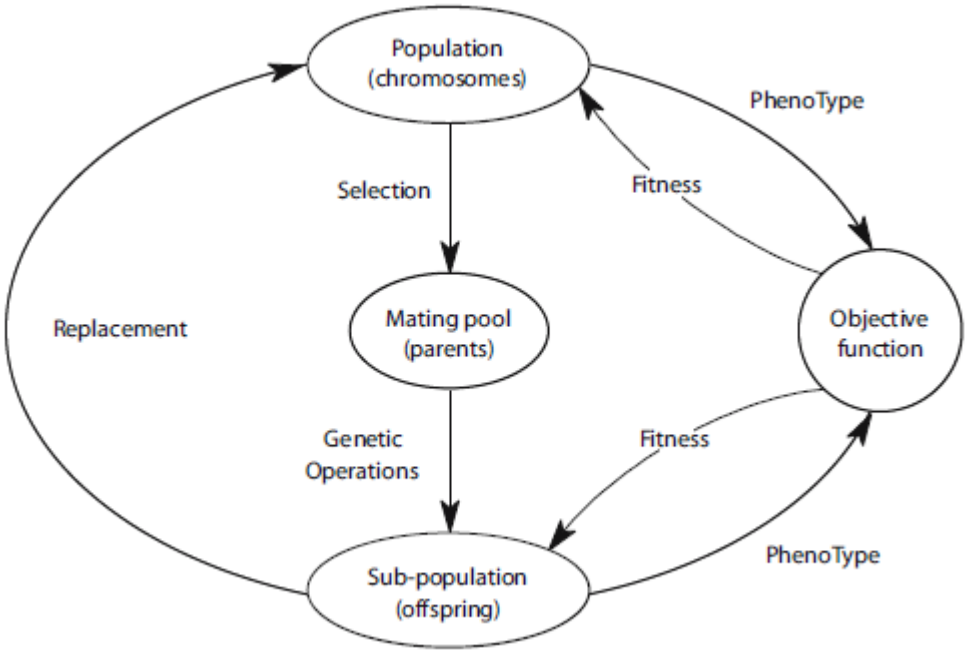

Figure 4.6: *The genetic cycle* [17].

4.2.4.4 Principles of GA-PID controller

Genetic algorithm is a robust optimization technique based on natural selection. The basic objective of GA is to optimize fitness function. In genetic algorithms, the term chromosome typically refers to a candidate solution to a problem. In our work, GA works directly on real parameters. Decimal type GA are equivalent to the traditionally used binary-type GA's in optimization. Decimal-type GA's for computer-based numerical simulation lead to high computational efficiency, smaller computer requirements with no reduction of precision and greater freedom in selecting genetic operator. GA has been successfully implemented in the area of industrial electronics, for instance, parameter and system identification, control robotics, pattern recognition, planning and scheduling. For its use in control engineering, GA can be applied to a number of control methodologies for the improvement of the overall system performance [24].

4.2.4.5 Structure and design of GA-PID controller

The structure of a control system with GA-PID as a controller is shown in the Figure 4.7 below. It consists of a conventional PID controller with its parameter optimized by genetic algorithm. The initial population of size N is generated randomly to start the optimization process; the next generation can be obtained through the genetic operators. The genetic operators are the most important features of GA and are described below:

- **Genetic operator**: The decision to make during implantation of genetic algorithm is the choice of genetic operators that are to be used. The basic genetic operators are:
  1- Reproduction: By using the values of the performance fitness functions, select the best $N/2$ individuals of the current generation to be the parents for producing the next generation. This means that only genetically good individuals are selected to become parents.
  2- Crossover : Two parents are randomly selected to exchange the genetic information with each other and two new individuals are generated so as to keep the population size at constant value N. Cross over operation can be mathematically described as follows :
  If parents are (w_{n1}, k_{f1}) and (w_{n2}, k_{f2})), then
  Child-1: $w_n = r * w_{n1} + (1-r) * w_{n2}$
  $k_f = r * k_{f1} + (1-r) * k_{f2}$
  Child-2: $w_n = (1-r) * w_{n1} + r * w_{n2}$
  $k_f = (1-r) * k_{f1} + r * k_{f2}$ (4.21)

  Where $r \in (0,1)$ is a random number.
  Here the crossover operator works with real decimal pairs instead of any coded strings.
  3- Mutation: It plays a secondary role in genetic algorithms. It is needed because, occasionally, chromosomes may lose some potentially useful genetic material. Mutation takes place with a certain probability; thus genetic content of a particular individual gets changed and a new generation is produced. Mutation is important in nature as it brings a change in genetic content of the individuals in order to enable them to adapt to a different environment. In the same way, in artificial systems the mutation will direct the search algorithm to a new search space so that a global minima can be found. In our simulations, mutation rate is set to be 0.1. After mutation,

we get a modified mating pool $M(k)$. To form the next generation for the population, we let:

$$P(k+1) = M(k) \tag{4.22}$$

Where $M(k)$ is the one that was formed by selection and modified by crossover and mutation. Then the above steps repeat, successive generations are produced, and the evolution is modelled.

- **Fitness function:** A fitness function takes a chromosome as an input and returns a number that is a measure of the chromosome's performance on the problem to be solved. Fitness function plays the same role in GA as the environment plays in natural evolution. The interaction of an individual with its environment provides a measure of fitness to reproduce. Similarly, the interaction of a chromosome with a fitness function provides a measure of fitness that the GA uses while carrying out reproduction. Genetic algorithm is a maximization routine; the fitness function must be a non-negative figure of merit. In this particular situation, our main aim is to minimize error and reduce the rise time and overshoot. Hence, the fitness function, in this case, is a function of error and rise time.

$$J = \int_0^\infty \left(w_1|e(t)| + w_2 u^2(t)\right)dt + w_3\, t_r \tag{4.23}$$

Where w_1, w_2, w_3 are the weight coefficients. $U(t)$ is the output of the controller, $e(t)$ is the error.

The square term of control output is added to overcome the large energy of the controller. The fitness function is presented by:

$$f = \frac{1}{J + 10^{-8}} \tag{4.24}$$

The term 10^{-8} is added in the denominator of fitness function to avoid it from becoming zero.

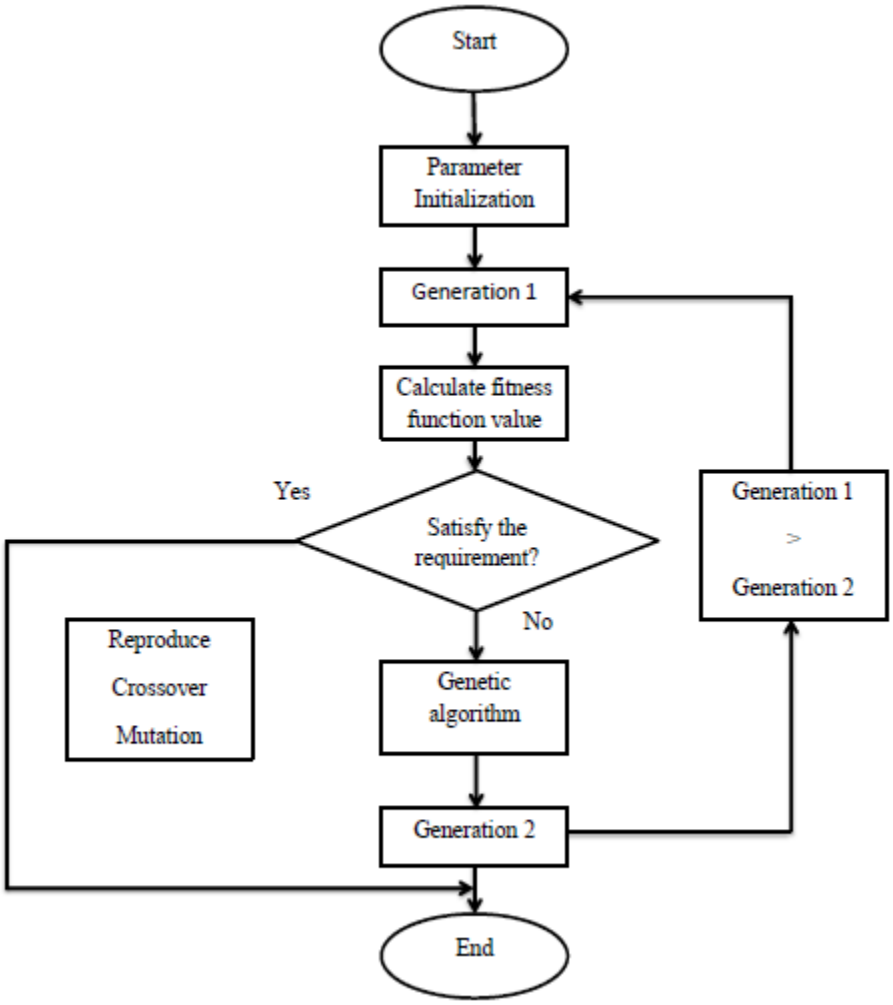

Figure 4.7: *Diagram for auto-tuning GA-PID controller* [24].

4.2.4.6 LMI based H_2/H_∞ regional pole constraints

In many real-world applications, the designed system needs to meet multiple performance requirements. This makes multi-objective synthesis highly desirable in practice, and the Linear Matrix Inequalities LMI theory is a relatively new field of research for analysis and design of control systems. It offers powerful tools to attack such problems, many control problems can be expressed in the form of LMI and solved with recently developed efficient convex optimization techniques. Mixed H_2/H_∞ is a robust controller with combined constraints on pole locations and they serve an LMI based method to find the optimal output or state feedback control in which, H_∞ controller is good at performance and robustness, H_2 controller is good at minimizing the consumed energy for control effort.

Therefore, the study on output feedback control is more practical. Moreover this controller indicates the relationship between robust stability and nominal performance by specifying the H_2/H_∞ constraints and criterion, which makes it possible to adequately capture multiple design specifications, it could also allow for direct placement of closed-loop poles, which is related to the time response and transient behavior of the closed-loop dynamics, in this section we will be presenting the mixed H_2/H_∞ controller design but before that we will be viewing some useful definitions.

4.2.4.7 Basics of Linear Matrix Inequality

- **Introduction of Linear Matrix Inequality**

A wide variety of problems in control theory and system can be reduced to a handful of standard convex and quasi-convex optimization problems that involve linear matrix inequalities (LMIs), they are mathematical tools that have various applications in control theory, especially in the robust control area [25].

The general form of LMI is given by:

$$F(x) = M_0 + \sum_{i=1}^{l} x_i M_i > 0 \qquad (4.25)$$

Where: M is positive (negative) if $x^T Mx > (<)\ 0$, $\forall x \neq 0$. Also M is called positive (negative) semi-definite if $x^T Mx \geq (\leq)\ 0$, $\forall x$.

x_i are real scalar variables, $\boldsymbol{X} = [x_1, \dots, x_l]^T$, and M_0 and M_i are constant symmetric matrices of dimension $n \times n$.

For control system design, it is more preferable to formulate the LMI as follows:

$$F(X_1, \dots, X_k) = M_0 + \sum_{i=1}^{k} G_i X_i H_i > 0 \qquad (4.26)$$

Where: X_i are matrix variables to be found, G_i and H_i are known matrices .

- **LMI formulation of poles placement**

For purposes of pole placement, it is important to define regions in a linear matrix inequality, Firstly a convex region for poles is defined using performance properties and

desired characteristics of the closed loop system. The clustering regions for pole are on the left half-plane and using transient response characteristic of a second order system with poles shown in equation (4.30):

$$\lambda = -\zeta\omega_n \pm j\omega_d \tag{4.27}$$

With:

ω_n is the undamped natural frequency, ζ is the damping ratio and ω_d is the damped frequency.

One can put on the specific bounds on these characteristics to ensure a satisfactory transient response. Regions of pole clustering include an α-stability regions on the left half plan such that $Re(s) \leq -\alpha$ vertical strips, disks, conic sectors or any convex geometry. Another interest in region is $s(\alpha, r, \theta)$ of complex numbers $x + jy$ such that:

$$x < -\alpha < 0\,, \qquad |x + jy| < r\,, \qquad \tan(\theta)\,.\,x < -|y| \tag{4.28}$$

The region of equation (4.28) is given in Figure 4.8. If all of the closed loops are in the shaded region, one can guarantee that a minimum decay rate is, a minimum damping ratio is $\zeta = \cos(\theta)$ and a maximum undamped natural frequency is $\omega_d = r.\sin(\theta)$. It is known that these values bound the maximum percent overshoot, the frequency of the oscillatory modes in transient response, the delay time, the rise time and the settling time. After convex region is defined (α, r, θ) , the mixed H_2/H_∞ problem can be easily formulated in LMI form, then the obtained problem can be solved extended Lyapunov theorem. The main improvement according to preceding methods, it eliminates Riccati based approaches and proposes a simpler algorithm for computer programs.

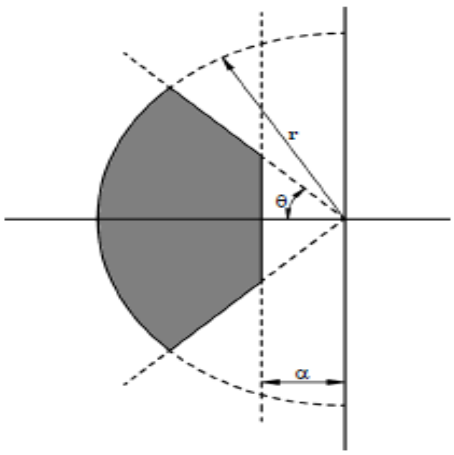

Figure 4.5: *Region (α,r,ϑ)* [25].

4.2.4.8 H_2/H_∞ Controller design

Treating difficult mathematical problems, especially for differential equations and matrix type inequalities provides robust controller synthesis with numerical solutions. The mixed H_2/H_∞ controller output feedback model is presented in Figure 4.9, where $P$and $K$are the linear time-invariant (LTI) plant and output feedback controller, respectively. The u, y, and w are the control signal, measured output signal, and external disturbance signal, respectively. The output channel Z_∞ is associated with the H_∞ performance, while the channel Z_2 is associated with the H_2 performance [26].

The state space representations of the variables shown in Figure 4.10 are:

$$\begin{aligned} \dot{x} &= Ax + Bw + B_u u \\ Z_\infty &= C_\infty x + D_\infty w + D_{\infty u} u \\ Z_2 &= C_2 x + D_2 w + D_{2u} u \\ y &= C_y x + D_y w + D_{yu} u \end{aligned} \tag{4.29}$$

Moreover, the picking P, K matrices for the generalized system and controller respectively in equations (4.33) and (4.34):

$$P = \begin{pmatrix} [A] & [B \quad B_u] \\ \begin{bmatrix} C_\infty \\ C_2 \\ C_y \end{bmatrix} & \begin{bmatrix} D_\infty & D_{\infty u} \\ D_2 & D_{2u} \\ D_y & D_{yu} \end{bmatrix} \end{pmatrix} \tag{4.30}$$

$$K = \begin{pmatrix} A_f & B_f \\ C_f & D_f \end{pmatrix} \tag{4.31}$$

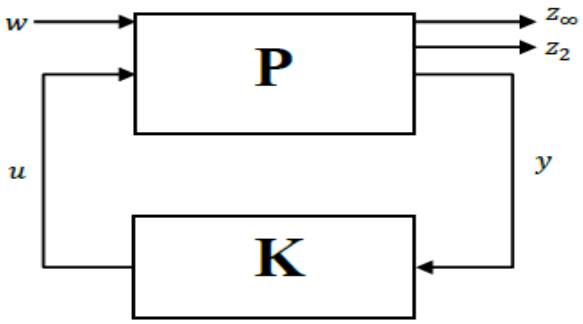

Figure 4.9: *Generalized plant for mixed* $\boldsymbol{H_2/H_\infty}$ [27].

The closed loop state space equations are given below:

$$\begin{aligned} \dot{x}_{cl} &= A_{cl}x_{cl} + B_{cl}w \\ Z_\infty &= C_{cl\infty}x_{cl} + D_{cl\infty}w \\ Z_2 &= C_{cl2}x_{cl} + D_{cl2}w \end{aligned} \tag{4.32}$$

T_∞ and T_2 are the closed-loop transfer functions from w to Z_∞ and Z_2 respectively. The problem definition of the mixed H_2/H_∞ is to find an output feedback controller such that it internally stabilizes the plant P.

The approach used in this study is the method proposed by Math works Corporation in MATLAB software, this software tool uses linear matrix inequalities (LMI). Therefore, for an output feedback mixed H_2/H_∞ controller case in LMI technique, the solution is formulated as two parts that have and performance bounds that will be defined next and these two problems are given as inequalities. Then, these two inequalities generate a convex optimization problem and the solution can be obtained via simultaneous solution of two distinct constraints.

- **H_∞ Performance:**

  The closed loop root mean square (RMS) gain for T_∞ does not exceed γ if and only if there exist as symmetric matrix x_∞ such that:

$$\begin{bmatrix} A_{cl}x_\infty + x_\infty {A^T}_{cl} & B_{cl} & x_\infty {C^T}_{cl\infty} \\ {B^T}_{cl\infty} & -I & {D^T}_{cl\infty} \\ {C^T}_{cl\infty}x_\infty & D_{cl\infty} & -\gamma^2 I \end{bmatrix} < 0 \qquad (4.33)$$

  With $x_\infty > 0$

- **H_2 Performance:**

  The closed loop H_2 norm of T_2 where $\left(\|T_2\|_2^2 = trace\,(C_{cl2}Q{C^T}_{cl2})\right)$ does not exceed v if and only if $D_{cl2} = 0$ there exist two symmetric matrices $x_2 > 0$ and Q such that:

$$\begin{bmatrix} A_{cl}x_2 + x_2{A^T}_{cl} & B_{cl2} \\ {B^T}_{cl2} & -I \end{bmatrix} < 0 \qquad (4.34)$$

4.3 Methodology

In this section, we will be presenting the methodology for designing controllers for our plant model F-16. To achieve this design an understanding of fundamental principles and analytical mathematical developments was introduced in the previous sections that helped

us in our controllers design architecture and simulation using MATLAB/Simulink software. However the technics used are explained in details starting with F-16 linear and non-linear aircraft modeling and furthermore, For the purpose of our work we have concentrated our analysis on controller design for the two inputs: pitch rate and velocity, by adjusting two control inputs, the elevator and the thrust.

4.3.1 F-16 modeling and linearization

The equations governing the motion of an aircraft are a very complicated set of six non-linear coupled differential equations. However, under certain assumptions, they can be decoupled and linearized into longitudinal and lateral equations. In this section, we will be presenting the non-linear and linear models mentioning all the state space representations and the transfer functions values of linear ones, indeed the lateral and longitudinal in which the measuring of the decoupled dynamic equations will be easy through specifying the state variables.

4.3.1.1 Non-linear F16 model

The non-linear F16 model is a 6-DOF model based the equations-of-motion.Model dynamics are solved via a fourth order Runge-Kutta or Jacobin method.

Having all the parameters of the non-linear F-16 model properly identified, a Simulink block diagram was built, as shown in Figure 4.10. This model generates 16 outputs.

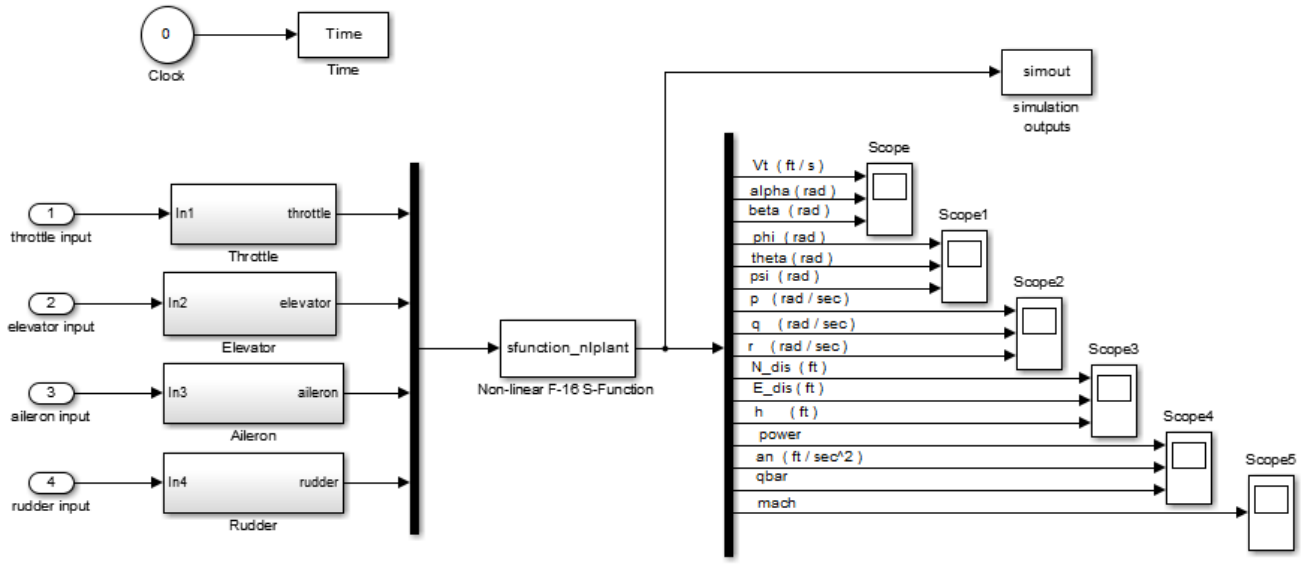

Figure 4.6: *Simulink model of the non-linear F-16 aircraft.*

4.3.1.2 Linear F-16 model

The state space representation of our F-16 linear model is presented in equation (4.36), which represents a model linearized under certain trim conditions using Jacobi methods.

4.3.1.3 Longitudinal F-16 dynamics model

The longitudinal dynamic matrix form is:

$$x = [v \quad \alpha \quad q \quad \theta]^T \quad u = [\delta_e] \quad y = [v \quad \alpha \quad q \quad \theta]^T \tag{4.35}$$

Thus the longitudinal state space representation is:

$$A = \begin{bmatrix} 0 & 0 & 0 & 1 \\ -32.1 & -0.013 & -2.66 & -1.18 \\ 0 & 0 & -0.67 & 0.93 \\ 0 & 0 & -0.57 & -0.87 \end{bmatrix} \qquad B = \begin{bmatrix} 0 \\ 0.0387 \\ -0.0014 \\ -0.1188 \end{bmatrix}$$

$$C = \begin{bmatrix} 57.2958 & 0 & 0 & 0 \\ 0 & 1 & 0 & 0 \\ 0 & 0 & 57.2958 & 0 \\ 0 & 0 & 0 & 57.2958 \end{bmatrix} \quad D = \begin{bmatrix} 0 \\ 0 \\ 0 \\ 0 \end{bmatrix} \tag{4.36}$$

In order to extract the longitudinal state variables from equations (4.37), we will convert them to the equivalent transfer functions form in MATLAB using the command “ss2tf”. The state variables are summarized in Table 4.5.

Given input of elevator pitch angle (δ_e), the transfer functions of the longitudinal state variables of the F-16 linear model are:

$$H_{sys1}(s) = v = \frac{-6.8067s^2 - 4.6033s - 0.0587}{s^4 + 1.553s^3 + 1.133s^2 + 0.0145s} \tag{4.37}$$

$$H_{sys2}(s) = \alpha = \frac{2.2173s^3 + 11.6600s^2 + 243.3159s + 144.9249}{s^4 + 1.553s^3 + 1.1330s^2 + 0.0145s} \tag{4.38}$$

$$H_{sys3}(s) = q = \frac{-0.0802s^3 - 6.4011s^2 - 0.0832s}{s^4 + 1.553s^3 + 1.133s^2 + 0.0145s} \tag{4.39}$$

$$H_{sys4}(s) = \theta = \frac{-6.8067s^3 - 4.6033s^2 - 0.0587s}{s^4 + 1.553s^3 + 1.133s^2 + 0.0145s} \tag{4.40}$$

Table 4.5: *Longitudinal state variables.*

	Longitudinal
Rates	α: Angle of attack (AOA) q: Pitch rate v: Velocity
Positions	θ: Pitch angle
Controls	δ_e: elevator deflection

4.3.1.4 Lateral F-16 dynamics model

The lateral dynamic matrix form is:

$$x^T(t) = [\beta \quad p \quad r \quad \phi]^T \quad u^T(t) = [\delta_a \quad \delta_r] \quad y = [\beta \quad p \quad r \quad \phi]^T \tag{4.41}$$

Thus the lateral state space representation is:

$$A = \begin{bmatrix} 0 & 0 & 1 & 0.078 \\ 0.064 & -0.202 & 0.078 & -0.99 \\ 0 & -22.92 & -2.25 & 0.54 \\ 0 & 6.00 & -0.04 & -0.31 \end{bmatrix} \qquad B = \begin{bmatrix} 0 & 0 \\ 0.0002 & 0.0005 \\ -0.4623 & 0.0569 \\ -0.0244 & -0.0469 \end{bmatrix}$$

$$C = \begin{bmatrix} 57.29 & 0 & 0 & 0 \\ 0 & 57.29 & 0 & 0 \\ 0 & 0 & 57.29 & 0 \\ 0 & 0 & 0 & 57.29 \end{bmatrix} \qquad D = \begin{bmatrix} 0 & 0 \\ 0 & 0 \\ 0 & 0 \\ 0 & 0 \end{bmatrix} \tag{4.42}$$

Given inputs of aileron roll angle (δ_a) and rudder yaw angle (δ_r) the transfer functions of the lateral state variables of the F-16 linear model are:

$$H'_{sys1}(s) = \beta = \frac{3.0502s^2 - 0.9491s - 42.1252}{s^4 + 2.762s^3 + 8.964s^2 + 0.0145s} \tag{4.43}$$

$$H'_{sys2}(s) = p = \frac{0.0286s^3 + 2.9876s^2 + 6.2956s - 0.059}{s^4 + 2.762s^3 + 8.964s^2 + 0.0145s} \tag{4.44}$$

$$H'_{sys3}(s) = r = \frac{3.2598s^3 - 0.4385s^2 - 41.8044s + 0.2098}{s^4 + 2.762s^3 + 8.964s^2 + 0.0145s} \tag{4.45}$$

$$H'_{sys4}(s) = \phi = \frac{-2.6869s^3 - 6.5468s^2 - 4.1125s - 2.6896}{s^4 + 2.762s^3 + 8.964s^2 + 0.0145s} \tag{4.46}$$

The lateral state variables are summarized in Table 4.6 below:

Table 4.6: *Lateral state variables.*

	Lateral
Rates	β: Side slip angle p: Roll rate r: Yaw rate
Positions	ϕ: Roll angle
Controls	δ_a: Aileron deflection δ_r: Rudder deflection

After specification of the transfer functions of lateral and longitudinal dynamic models, we can begin to analyze and simulate the outputs for the open-loop response of the linear F-16 model with MATLAB in which the results will be discussed in the next chapter.

4.3.1.5 Stability analysis of F-16 model

1- F-16 longitudinal stability analysis

One of the first things we want to do is to analyze whether the open-loop system of the F-16 longitudinal linear model (without any control) is stable. To know whether the aircraft is stable or no we use the eigenvalues of the system matrix A (equal to the poles of the transfer function) to determine stability. The eigenvalues of the A matrix are the values of S that are solutions of $\det(sI - A) = 0$.

Using the MATLAB function 'eig(A)', below is the MATLAB script code that will calculate the poles of matrix A:

The code script to analyze the longitudinal stability is:

```
%F-16 Stability Analysis
%F-16 Longitudinal Model
clear all
clc
A_long = [0 0 0 1; -32.1 -0.013 -2.66 -1.18; 0 0 -0.67 0.93; 0
0 -0.57 -0.87];
B_long = [0; 0.0387;-0.0014;-0.1188];
C_long =[57.2958 0 0 0; 0 1 0 0;0 0 57.2958 0; 0 0 0 57.2958
];
D_long = [0;0;0;0];
poles = eig(A_long)
```

This will give the following results:

```
poles =
 -0.0130 + 0.0000i
  0.0000 + 0.0000i
 -0.7700 + 0.7212i
 -0.7700 - 0.7212i
```

From this results, it can be seen that one of the poles is in the right-half plane (i.e. has positive real part), which means that the longitudinal F-16 linear model system is unstable.

2- F-16 lateral stability analysis

The code script to analyze the lateral stability is:

```
%F-16 Stability Analysis
%F-16 Lateral Model
clear all
clc
A_lat = [0 0 1 0.078; 0.064 -0.202 0.078 -0.99; 0 -22.92 -2.25
0.54; 0 6.00 -0.04 -0.31];
B_lat = [0 0; 0.0002 0.0005 ; -0.4623 0.0569; -0.0244 -
0.0469];
C_lat =[57.29 0 0 0; 0 57.29 0 0;0 0 57.29 0; 0 0 0 57.29 ];
D_lat = [0 0;0 0;0 0;0 0];
poles = eig(A_lat)
```

This will give the following results:

```
poles =
-0.3176 + 2.7366i
 -0.3176 - 2.7366i
 -0.0109 + 0.0000i
  -2.1158 + 0.0000i
```

We can conclude from this results that all the real part poles are negative, which means that the F-16 lateral model system is stable.

4.2.2 Design process of LQR and PID controllers

Aircraft pitch is governed by the longitudinal dynamics and aircraft roll is governed by the lateral dynamics. In this section, we will be designing Proportional-Integral-Derivative (PID) and Linear Quadratic Regulator (LQR) controllers that control the pitch and roll of the F-16 aircraft. The performance of the LQR will then be compared with that of PID controller.

We will simulate the linearized aircraft model with the state-feedback controller. We will specifically use the linearized state-space model obtained in equations (4.36) and (4.42) of longitudinal and lateral dynamics respectively using Simulink aerospace block diagram.

4.2.2.1 PID controller for pitch control

In basic PID controller measures the error signal value which gives the difference between reference signal and output of the system .The PID controller regulates the pitch control input in order to reduce the error signal. The parameters of PID controller consists of three variables known as the Proportional, the Integral and Derivative (K_p , K_i and K_d). For the PID controller Simulink design is shown in Figure 4.11, the system was set at initial conditions [δ_e= 25 deg] and the output data will be exported to MATLAB workspace for plotting graph. The requirement of these gains components achieved by proper tuning of the PID using the 'MATLAB PID Tuner application' for pitch control of an aircraft and they are shown in Table 4.7.

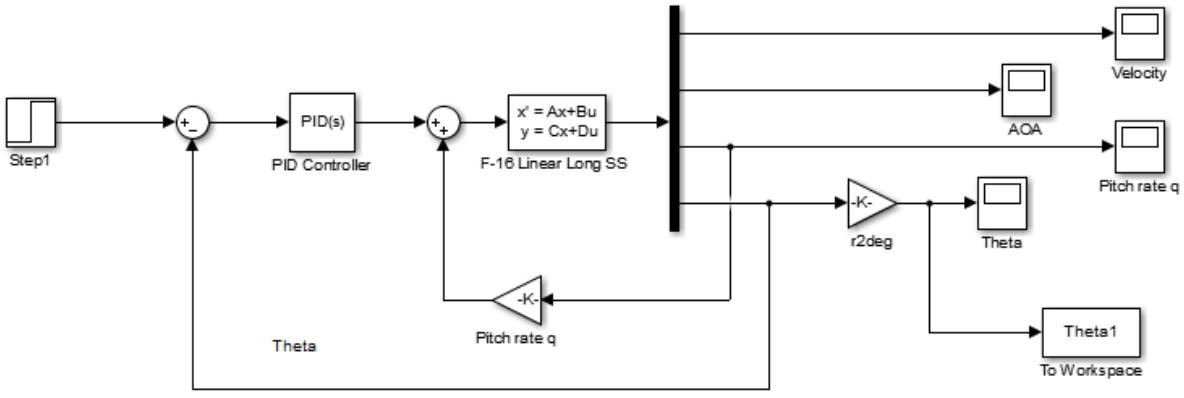

Figure 4.7: *Simulink model of PID pitch control.*

Table 4.7: *PID tuning parameters for pitch angle autopilot.*

PID parameters	Values
K_p	6.3
K_i	4.9
K_d	1.4

4.2.2.2 LQR controller for pitch control

In the state space form, the obtained LQR controller is expressed as $= -Kx$. For this solution, an LQR controller was first derived using the MATLAB "lqr" command then created in Simulink and finally the data of pitch angle will be exported to MATLAB workspace for plotting the output graph. The cost weighting matrices Q and R were selected as unit matrices and the LQR was realized. Simulink blocks for the designed LQR pitch controller with full state feedback is shown in Figure 4.12.

Where:

$$\mathrm{Q} = \mathrm{xC^{T}C}, \quad \mathrm{R} = 1$$

The value of x for LQR controller is chosen $x = 500$ which gives the best possible result. The MATLAB script code for calculating the gain matrix K and the value of gain (reference point) $Nbar$ is:

```
clc
clear all
%Lineat F-16 Model
%LQR pitch controller design
A_long = [0 0 0 1; -32.1 -0.013 -2.66 -1.18; 0 0 -0.67 0.93; 0
0 -0.57 -0.87];
B_long = [0; 0.0387;-0.0014;-0.1188];
C_long =[57.2958 0 0 0; 0 1 0 0;0 0 57.2958 0; 0 0 0 57.2958
];
D_long = [0;0;0;0];
%LQR gain K
x = 500;
Q = x*(C_long')*C_long;
R = 1;
[K] =lqr(A_long,B_long,Q,R)
%Calculating Nbar
Acl=A_long-B_long*K;
Nbar=inv(C_long*inv(Acl)*B_long)
```

This will give the following results:

```
K=1.0e+03 *

 -1.8682   0.0216  -0.2583  -1.2778

Nbar = -0.6800
```

The following Simulink model for LQR pitch controller is:

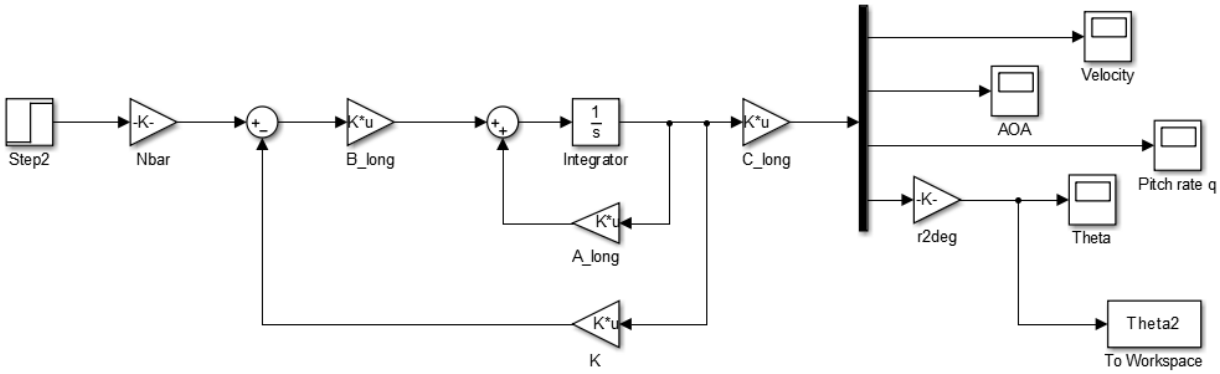

Figure 4.8: *Simulink model of LQR pitch control.*

4.2.3 Fuzzy logic / PID controllers design

4.2.3.1 FLC/ PID controllers design for pitch

In this section, we will be designing the FLC/PID controllers for comparative analysis purposes for the longitudinal control system.

We will be focusing Fuzzy Logic Controller (FLC) design, in which the methodology is described in detail using MATLAB/Simulink. The concept of (FLC) is a problem-solving control system methodology that will act as a feedback controller which is programmed to accept noisy, FLC's approach to control problems mimics how a person would make decisions, only much faster. The fuzzy controller is composed of four elements, these are fuzzification, rule base, inference mechanism and defuzzification.

A diagram which shows the designing steps of a fuzzy control system is given in Figure 4.13 and the Simulink model of FLC controller using the state space matrices of the longitudinal system is shown in Figure 4.14.

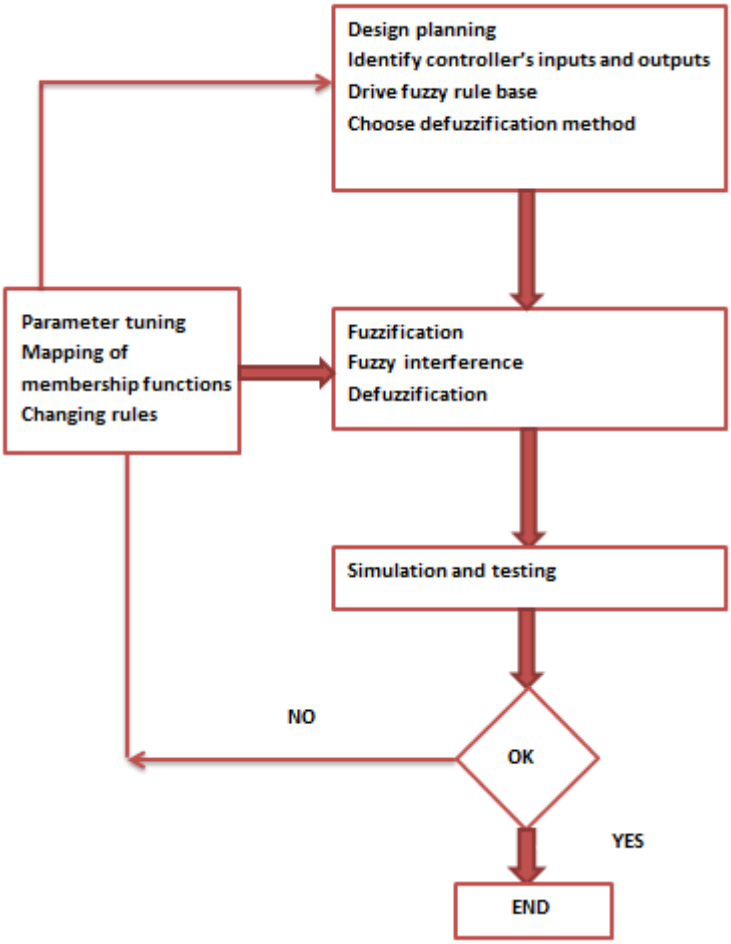

Figure 4.9: *Diagram of Fuzzy logic controller.*

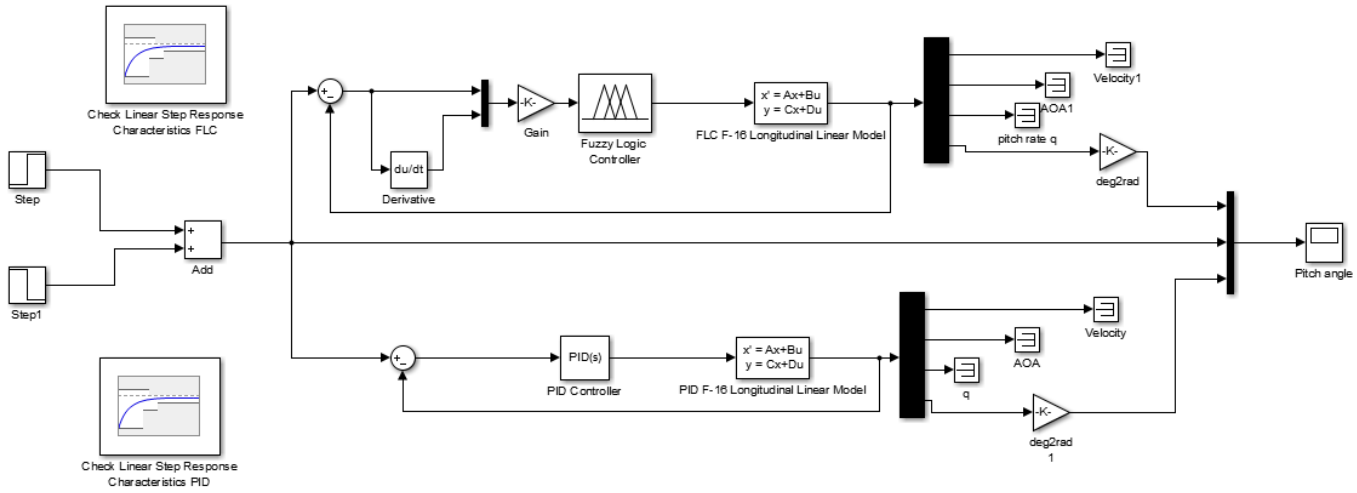

Figure 4.10: *Simulink model of Fuzzy logic and PID controllers for pitch.*

Remarks:

- The PID tuning parameters for pitch angle autopilot are the same values introduced before in Table 4.7.

- We used the simulation Data Inspector for a combined plotting of both PID/FLC and reference Scope data.

- The check linear step response characteristics is used to extract the PID/FLC simulation performance characteristics that will be shown in details in the next chapter.

4.2.3.2 Fuzzy Logic parameters structure

Now to formulate the FLC structure parameters we need to follow these construction steps of FLC:

1) Construction of the FLC designer application:

We use the command 'fuzzy' in MATLBA workspace to open the FLC designer application we will be getting this:

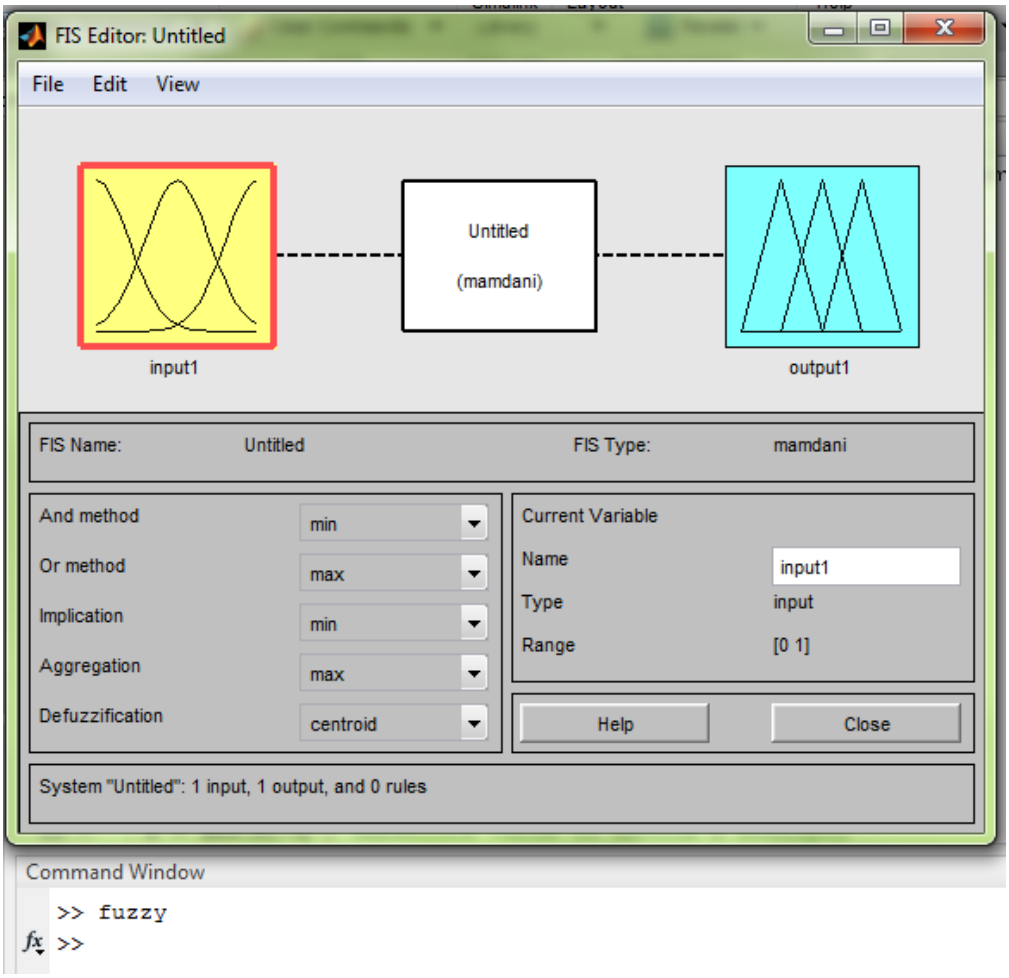

Figure 4.11: *FLC designer Application.*

FLC can be designed to add or remove input or output, fuzzy membership function, and IF-Then rules and select fuzzy inference functions using the Fuzzy Logic designer application of the system shown in Figure 4.15.

2) Construction membership function:

The membership functions should be chosen such that they cover the whole universe of discourse. Now the algorithm is implemented with two inputs (error and change in error) and one output (control). A Mamdani-type fuzzy inference approach is utilized. The setup is as shown in Figure 4.16.

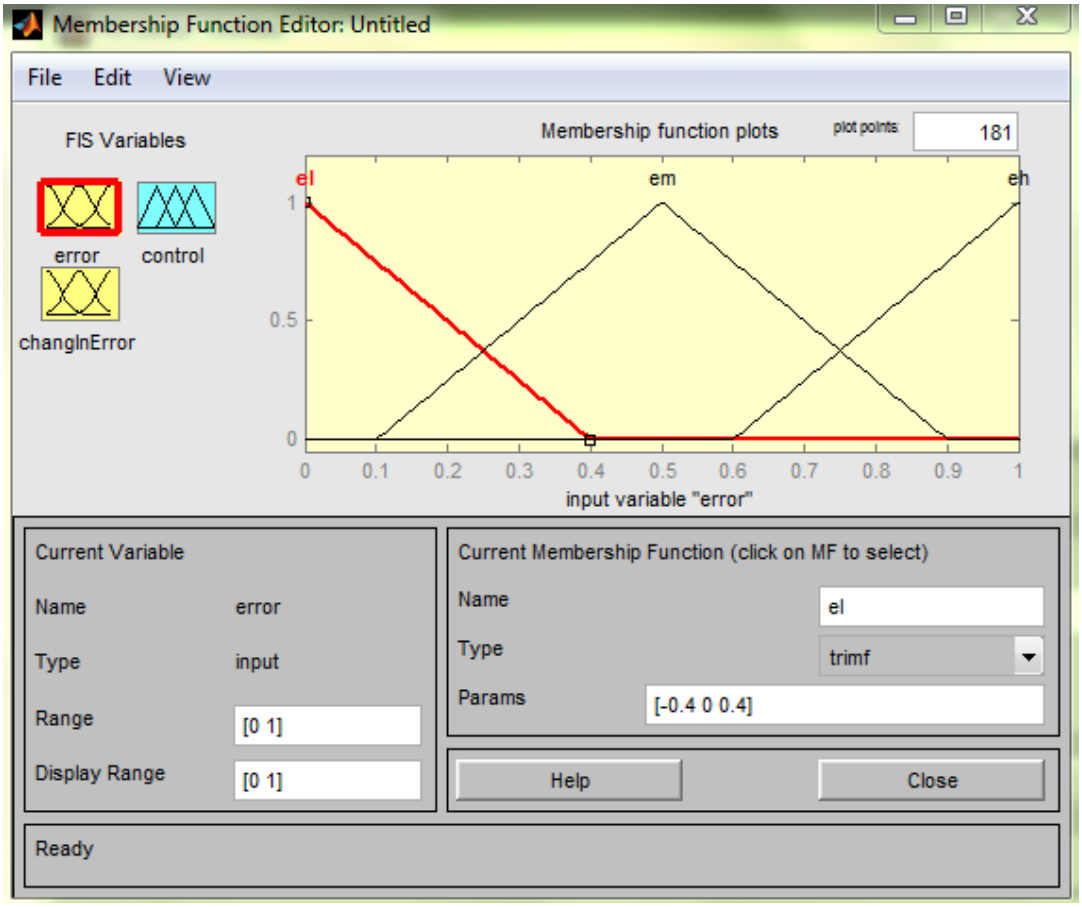

Figure 4.12: *Membership functions of the input to the fuzzy logic controller.*

3) Construction of rules and rule viewer :

Fuzzy 'If-Then' rules are shown and in Figure 4.17 and Figure 4.18 shows the rules viewer .There are total 9 rules output variables, in which (el=low error , eh= high error, em= medium error) and (ecl= low error control, ecm= medium error control, ech= high error control).

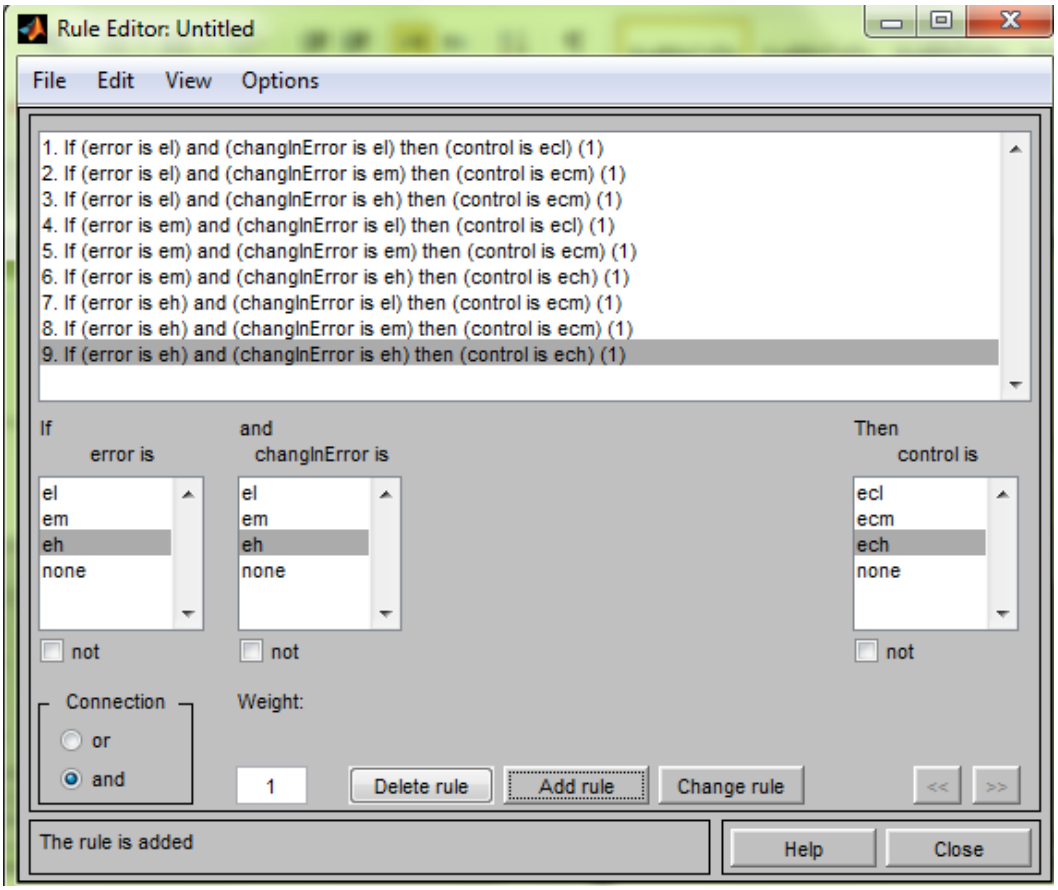

Figure 4.13: *'If-Then' FLC rules.*

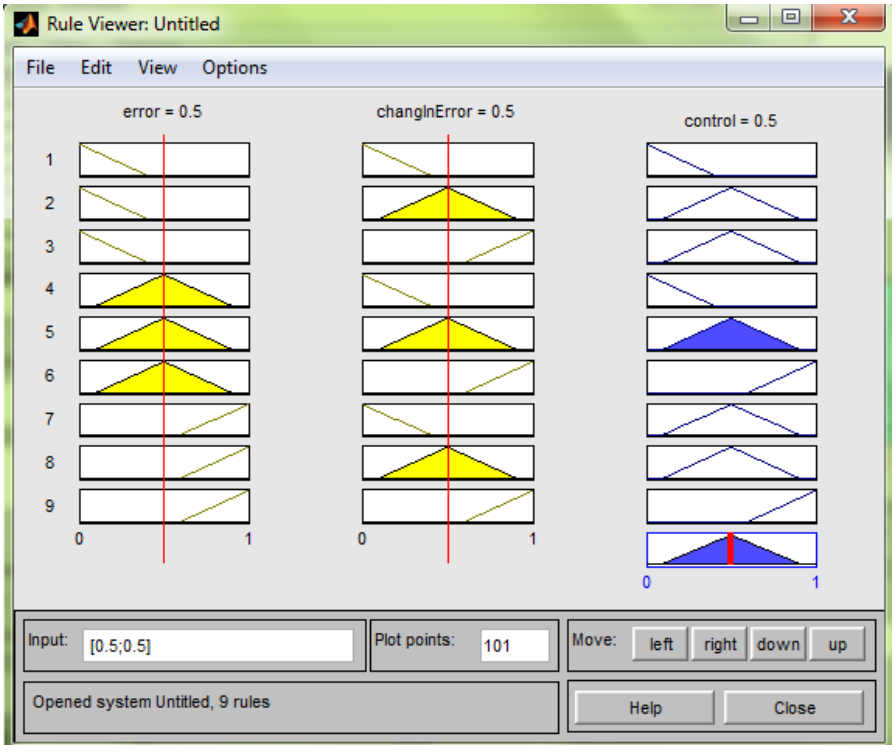

Figure 4.18: *'If-Then' FLC rules viewer.*

To see the entire output surface of our system, that is the entire span of the output set based on the entire span of the input set, we need to open up the Surface Viewer as shown in Figure 4.19 This is the last of the five basic GUI tools in the Fuzzy Logic Toolbox.

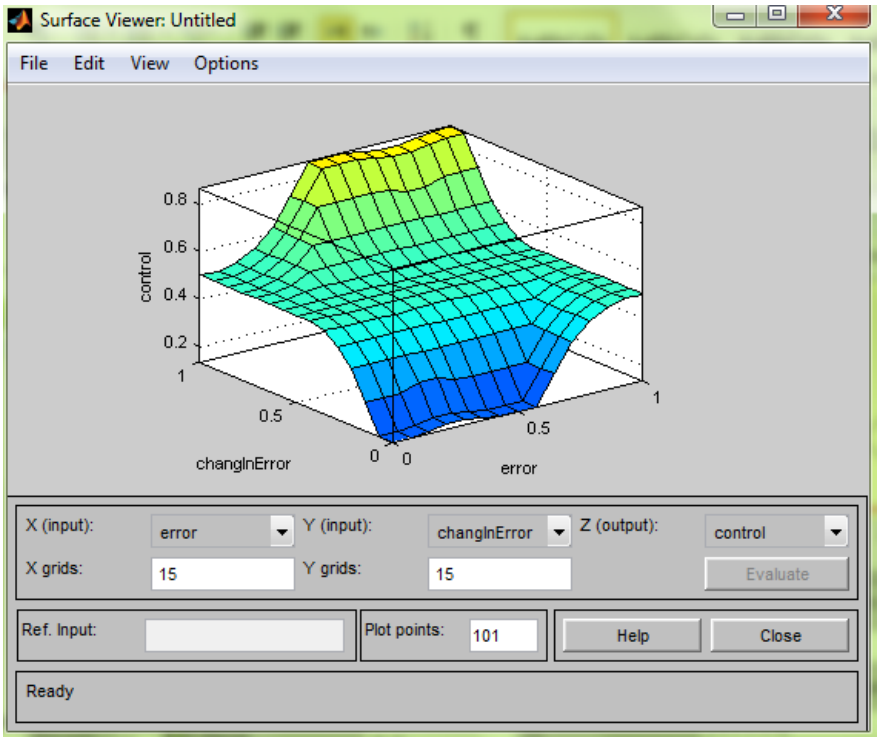

Figure 4.19: *FLC surface viewer.*

4.2.4 Self-tuning fuzzy PID controller

Self-tuning fuzzy PID subsystem block for pitch control consists of Fuzzy pid system and PID system for comparison and conventional PID block. The values of K_p, K_i, K_d are introduced previously in Table 4.7. While, the complete Simulink block for whole system including the Fuzzy PID and PID controllers are shown in Figure 4.20.

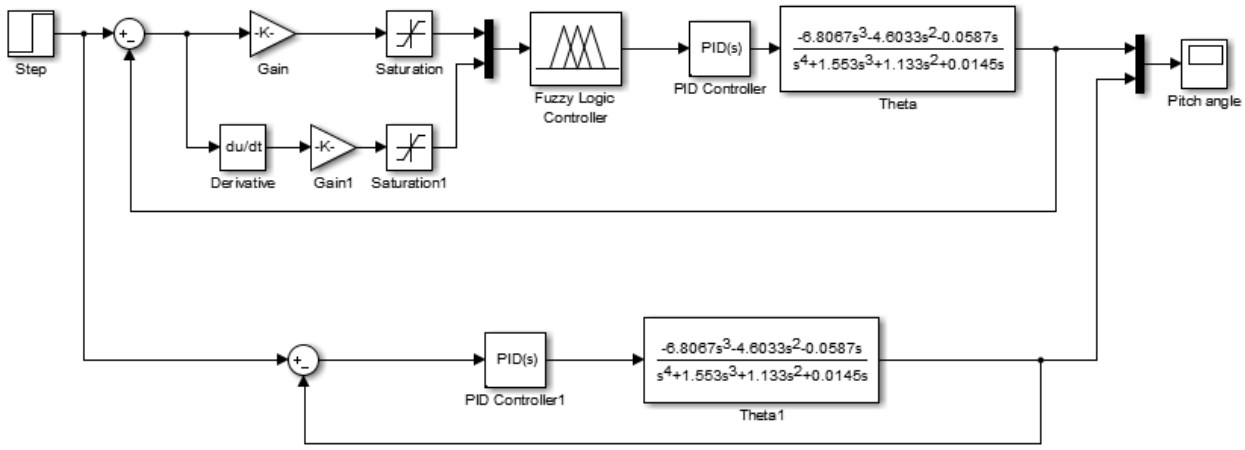

Figure 4.14: *Simulink model of Fuzzy PID and conventional PID pitch control.*

4.2.5 PID optimization using Genetic Algorithm (GA)

Genetic algorithms are substantially different to the more traditional search and optimization techniques. The objective is to use the (GA) as a solver to optimize the PID parameters (K_p, K_i, K_d), for that we are going to use the MATLAB optimization application, we will be seeing how to use the optimization tool to evaluate the performance of PID controller. First, we will generate the PID controller for linear F-16 plant model using MATLAB code script (Appendix B), the optimization process needs an objective function or cost function. In most of the case cost function defined to minimize the values of the parameter, to minimize the cost of the system. The Figure 4.21 presents the optimization tool application:

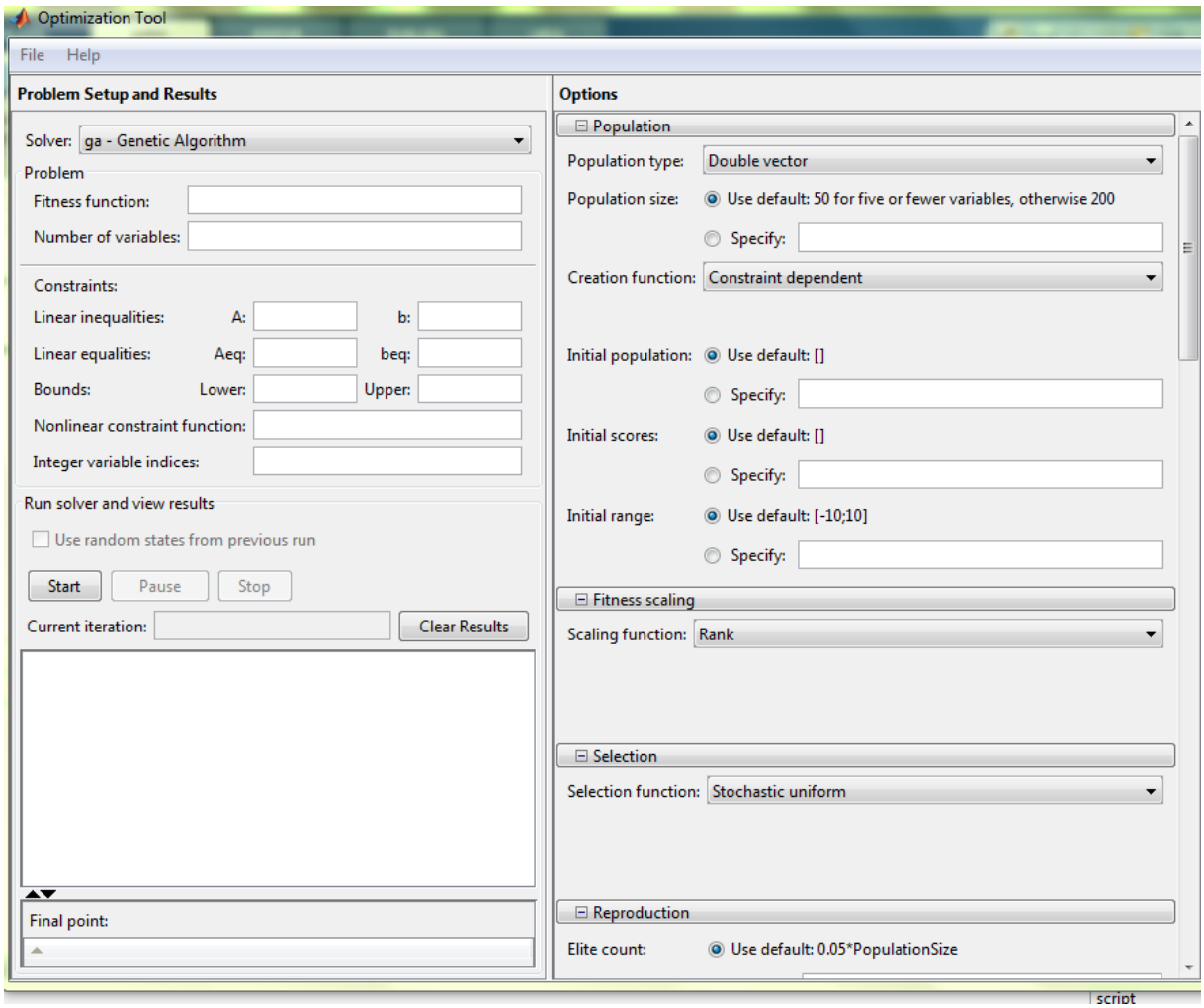

Figure 4.15: *Optimization tool application.*

The Genetic Algorithm has to be initialized before the algorithm can proceed. The Initialization of the population size, variable bounds and the evaluation function are required. These are the initial inputs that are required in order for the Genetic Algorithm process to start. The different (GA) initializing parameters are explained as:

- **Population Size:** The first stage of writing a Genetic Algorithm is to create a population. This command defines the population size of the (GA). Generally the bigger the population size the better is the final approximation.
- **Variable Bounds:** Since this project is using genetic algorithms to optimize the gains of a PID controller there are going to be three strings assigned to each member of the population, these members will be comprised of a P, I and a D string that will be evaluated throughout the course of the (GA) processes.

• **Bounds:** The variables bound are for the genetic algorithm to search within a specified area. These bounds may be different from the ones used to initialize the population and they define the entire search space for the genetic algorithm.

By selecting the parameters and specifying (GA) options, we get:

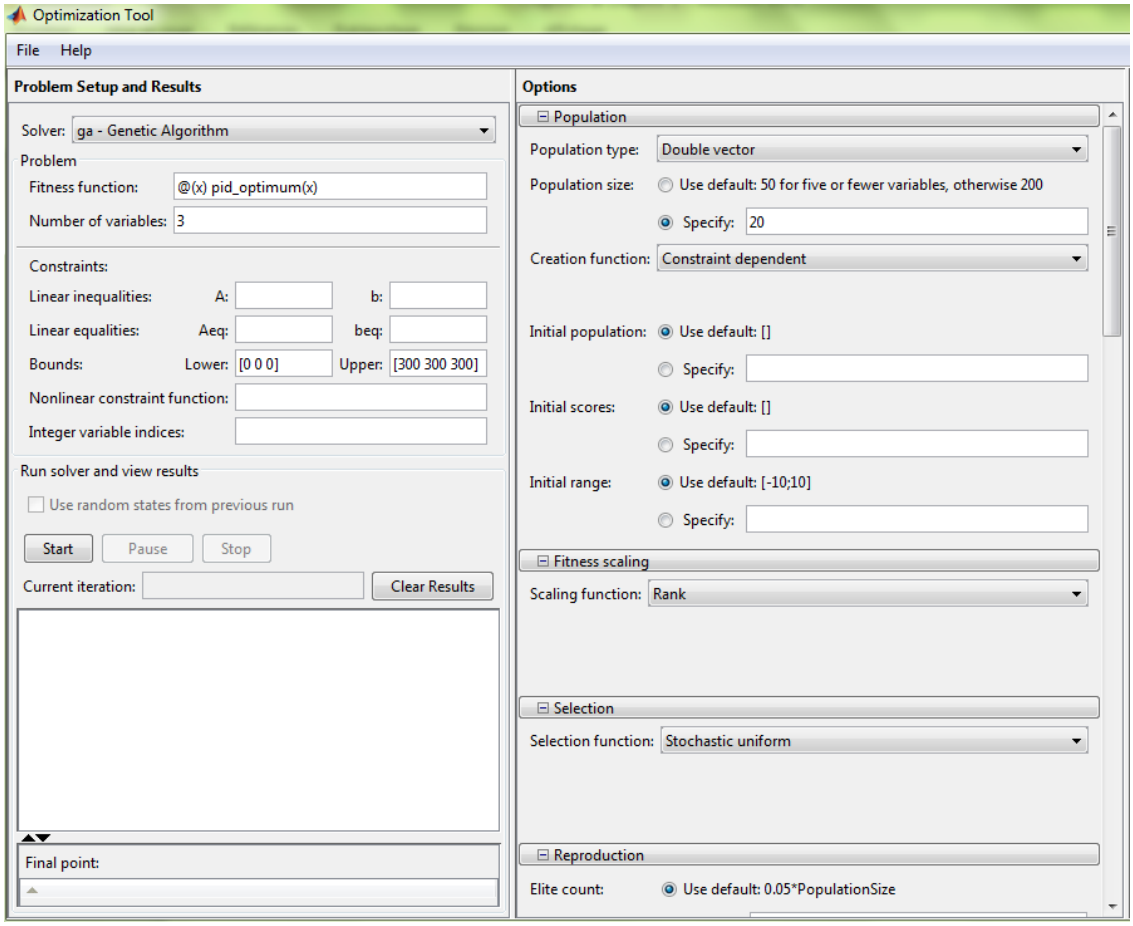

Figure 4.16: *GA initialization parameters.*

4.3.2 Mixed H_2/H_∞ controller design

The mixed controller is generated by using the MATLAB function 'h2hinfsyn' which returns guaranteed H_∞ and H_2 performances. This function 'h2hinfsyn' employs LMI techniques to compute an output-feedback control law $u = K(s) * y$. The LTI plant P has partitioned state-space form as described before in equation (4.30).

Now let's descript the code used for generating this mixed robust controller:

1)- To define the partitioned state space plant model P we will use the MATLAB function '$P = pck(A\_long, B\_long, C\_long, D\_long)$'.

2)- To Compute a controller for P using the LMI region to restrict the closed-loop pole locations , we Apply an H_2 norm constraint to one signal $(\mathrm{Nz2} = 1)$ and give the $\mathrm{H}_2$and H_∞ norms equal weight

3)- Calculate the poles of the closed loop system and Confirm that the poles of the closed-loop system have Re(s) < –1.

4)- Nmeas — Number of measurement signals positive integer

Ncon — Number of control signals positive integer

Nz2 — Number of signals subject to *H2* constraint positive integers

Wz — Weights for *H*∞ and *H*2 performance

After setting all the parameters we now can Compute the new controller and confirm the locations of the closed-loop poles.

4.4 Summary

A variety of control systems have been proposed for the F-16 fighter aircraft autopilot systems from classical controllers to a novel mixed controllers providing the state-space representations of F-16 modeling.

We started from mathematical comprehension and modeling to design procedures methodology based on MATLAB/Simulink, all of the developments have been illustrated with applications to aircraft, in which they were explained and illustrated. The obtained controllers design will be implemented and discussed in details in the next chapter.

Chapter 5: Simulation results and implementations

Chapter 5: Simulation results and implementation

5.1 Introduction

Simulation is an important part of this project, the F16 Fighting Falcon model was chosen for the simulation environment. It was performed using linear models, trimmed at different operation points, and a full six degree-of-freedom (6-DOF) non-linear model and as well as the decoupled (EOM) for both longitudinal and lateral models.

The simulation environment was created using MATLAB/Simulink. Each model was simulated with both classical controllers (LQR, PID, FLC) and mixed controllers (Self-tuning fuzzy PID, GA-PID, H_2/H_∞). The diagrams used in implementations were presented in chapter 4 and the MATLAB codes are in Appendix B.

5.2 Discussions and simulation results

5.2.1 Simulation of F-16 model

5.2.1.1 Non-linear simulation

The Non-linear simulation was implemented using Simulink in addition to a MATLAB coding shown in Appendix B. The results for the non-linear study are shown in the figures 5.1 and 5.2 below, where the Figure 5.1 shows the variation of the thrust or elevator as a function of time for an altitude of 1500 ft and a velocity of 152.4 m/s, in a similar manner Figure 5.2 shows for the same conditions of velocity and altitude but this time it shows the rudder and aileron. It is noted that these two figures are plotted for a 5 degree elevator. Moreover the plots of the model outputs are shown in Figure 5.3.

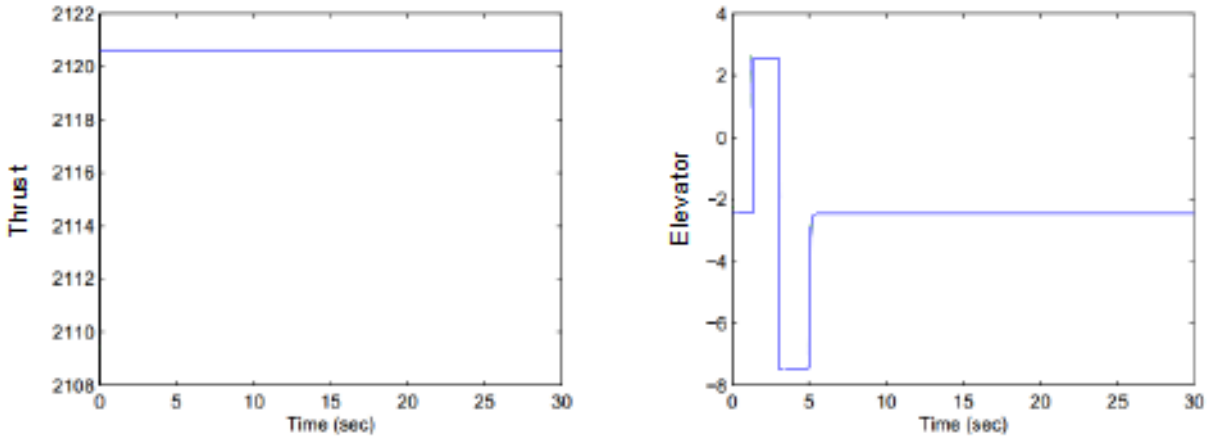

Figure 5.1: *Variation of thrust and elevator as a function of time.*

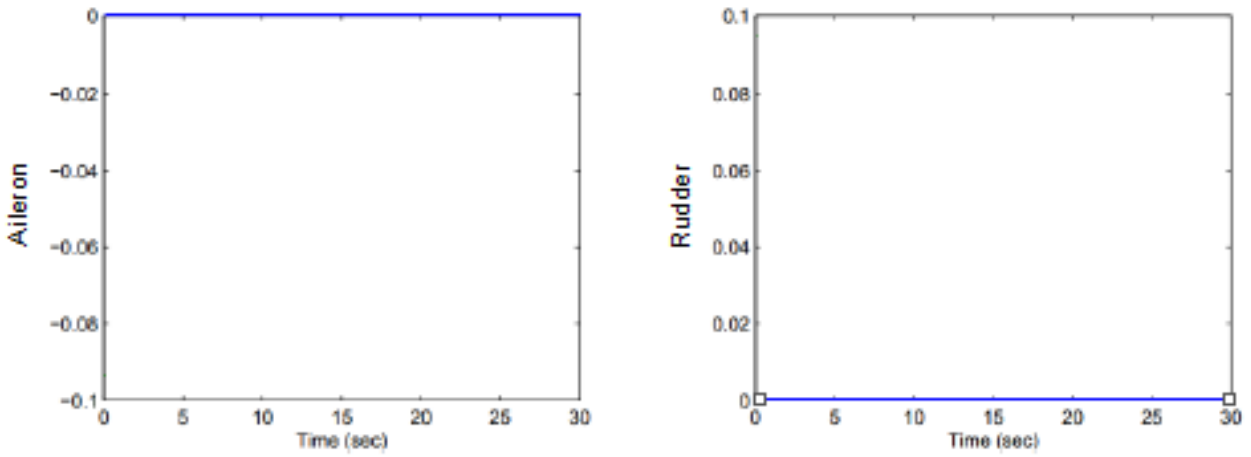

Figure 5.2: Variation of rudder and aileron as a function of time

.

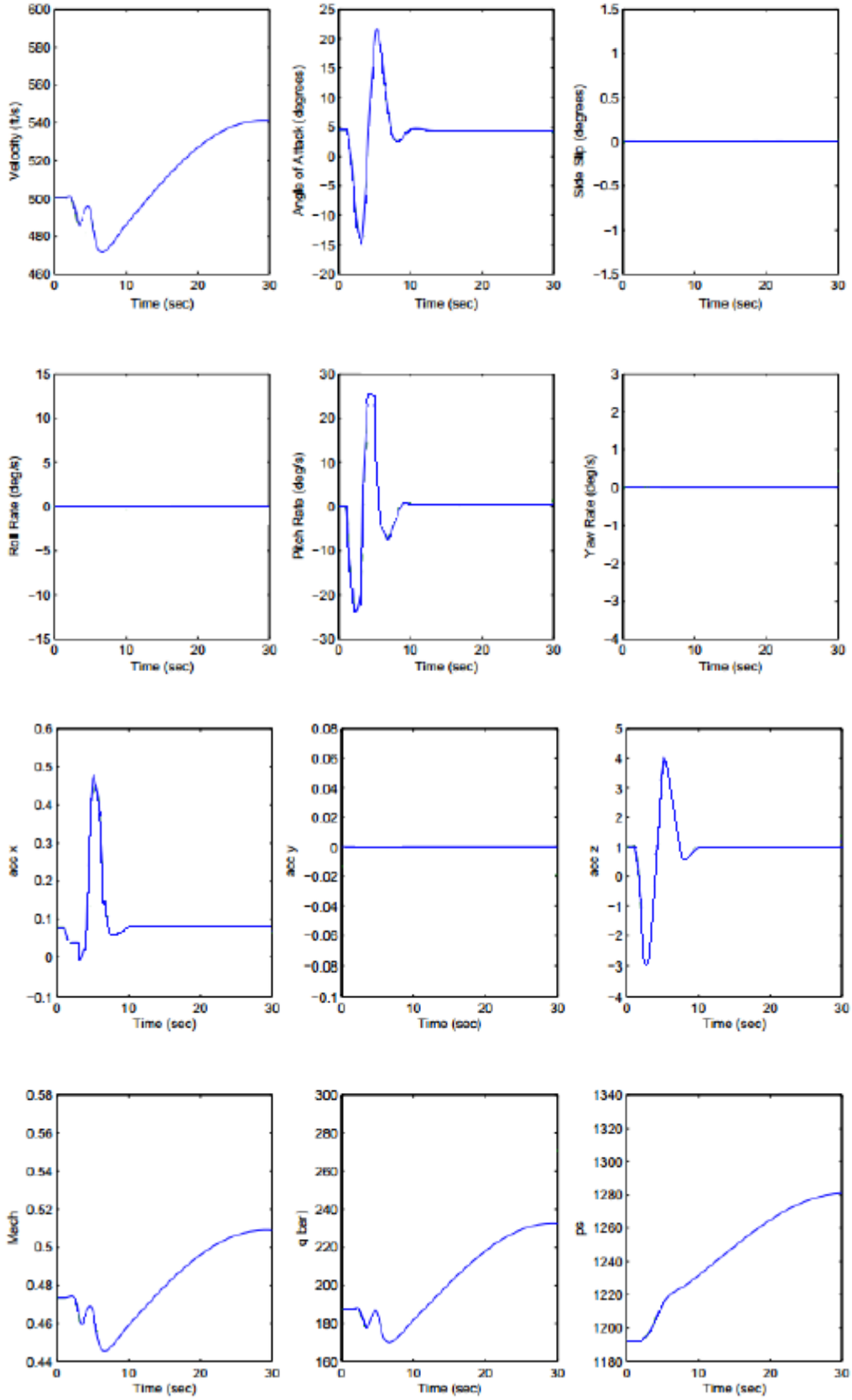

Figure 5.3: *Variation of some non-linear F-16 outputs.*

5.2.1.2 Linear simulation

The non-linear model of F-16 has been linearized as mentioned in the previous chapter around certain trim conditions. The advanced simulation will include the linear decoupled state -space matrices.

The Figures 5.4, 5.5 shows the outputs of the open-loop longitudinal and lateral motions respectively.

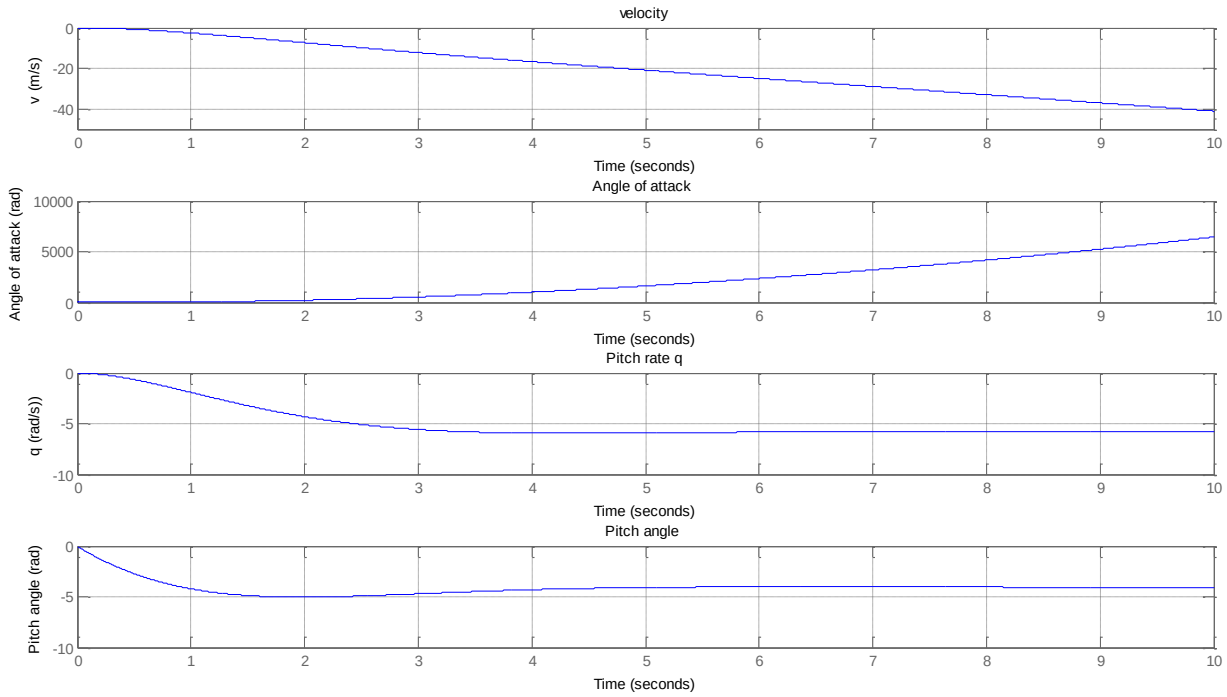

Figure 5.4: *open-loop step responses of the longitudinal motion.*

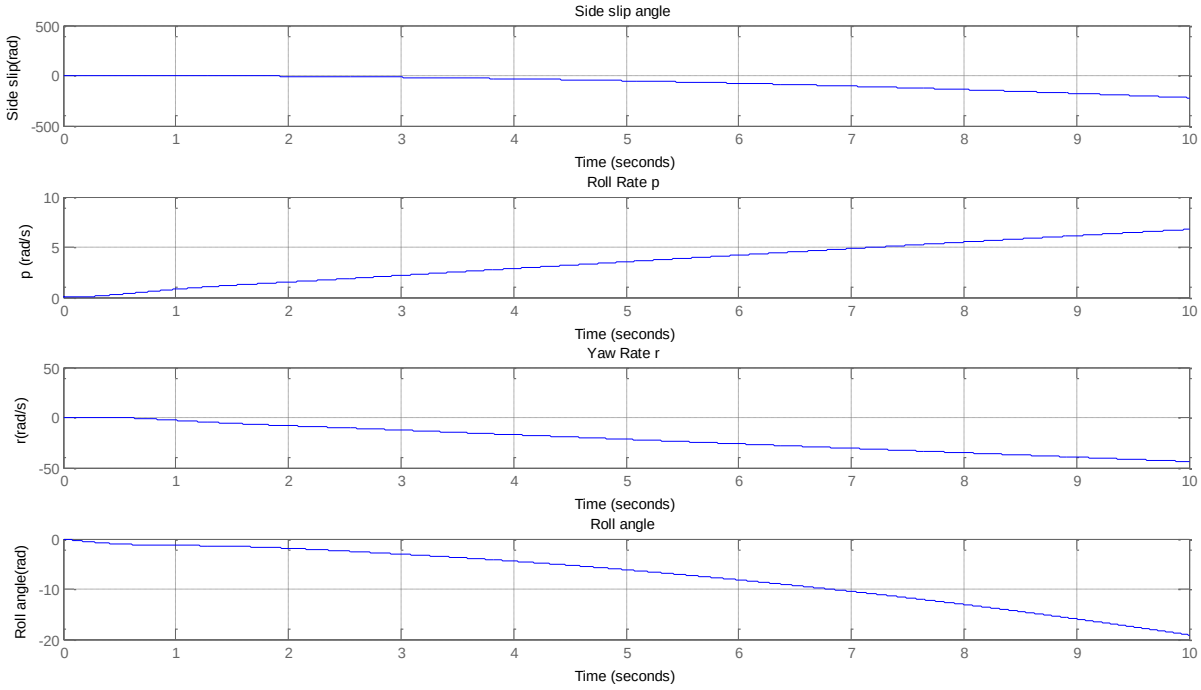

Figure 5.5: *open-loop step responses of the lateral motion.*

According to the simulations results analyzed for the linear decoupled motion. Firstly, the responses outputs of the open-loop systems of both longitudinal and lateral system show instability and a big divergence. However it can be seen that the system is not stable and it is approaching infinity as the time increases. Therefore, a feedback controller needs to be designed in order to stabilize the linear system which will be discussed in the next sections.

5.2.2 LQR/PID control discussion

A Control system for pitch control is simulated using LQR and PID and the results of simulation are analyzed and presented for comparison. We only considered elevator deflection as an input for pitch control. For roll control we considered aileron and rudder deflections. The responses of each controller were plotted in one figure and a step size of one radian is given as elevation reference trajectory and applied to the PID, LQR components.

5.2.2.1 Pitch control

Figure 5.8 shows the response of the pitch control system using PID and LQR respectively.

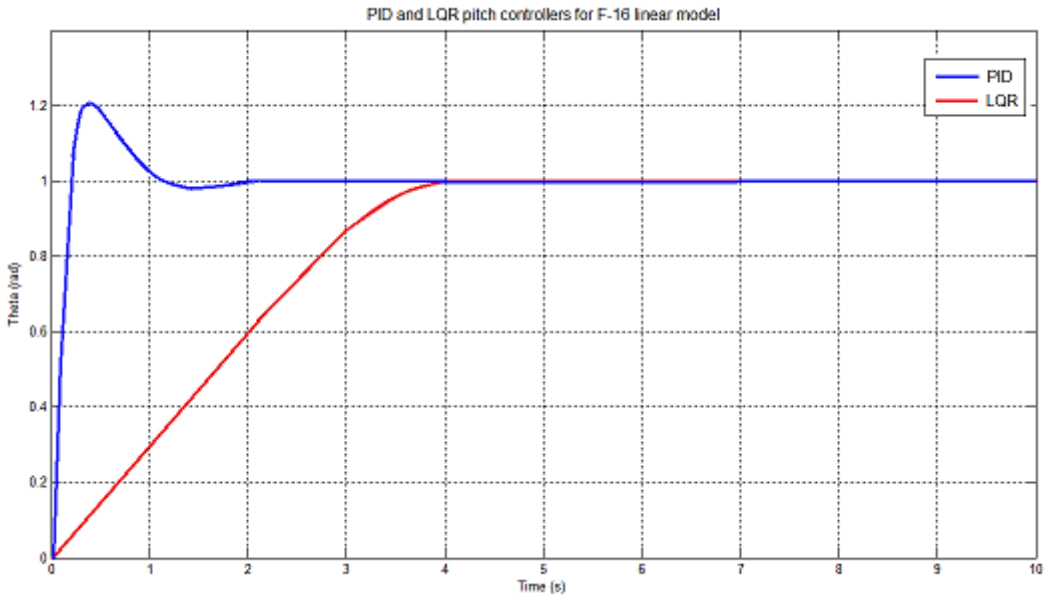

Figure 5.6: *step response of the PID and LQR for pitch control.*

From the above graphs we can analyze the performances of the controllers by specifying the response characteristics as shown in Table 5.1.

Table 5.1: *Comparison of PID and LQR performance for longitudinal motion.*

Performance characteristics	PID (longitudinal)	LQR (longitudinal)
Settling time (s)	2.2 s	4.1 s
Rise time (s)	0.65 s	3.5 s
Peak overshoot (%)	25 %	0 %

By comparing the performance characteristics in Table 5.1, as we can see that the settling time of LQR is higher than the PID by time difference of 1.9 seconds, which is the time required for the response to reach the steady state and stay within the specified tolerance bands around the final value.

The rise time of LQR is slightly larger as compared to PID by a time difference of 3 seconds. On the other hand the peak overshoot for PID is high which represents the deviation of the response at peak time from the step finale value, however the PID's peak overshoot is increased at the start (25 %) then drops remarkably till reaching the desired value, while it remains zero for LQR.

5.2.2.2 Simulation results

Based on the results and the analysis, a conclusion has been made that both of the control method, modern controller (LQR) and conventional controller (PID) are capable of controlling the pitch and roll of the closed-loop linearized system.

Simulation results show that The PID provides a very fast response, whereas the LQR controller is the slowest to reach the desired output. PID controller has better performance compared to LQR controller for settling and rise time.

Further improvement need to be done for both of the controllers for longitudinal and lateral autopilots. PID controller should be improved so that the percentages overshoot does not have very high range as required by the design criteria. On the other side, LQR controller can be improved so that it's settling time might be reduced as faster as PID controller.

5.2.3 Fuzzy logic / PID controllers

5.2.3.1 Discussion

Control system for pitch control is simulated using PID and FLC. The output response of both the PID and FLC is illustrated in Figure 5.10 and a unit step command is required in order for pitch angle to follow the reference value of 0.2 radian =11.5 degree. The summary

for the performance characteristics of the step response for the pitch angle between PID and FLC controller is shown in Table 5.3.

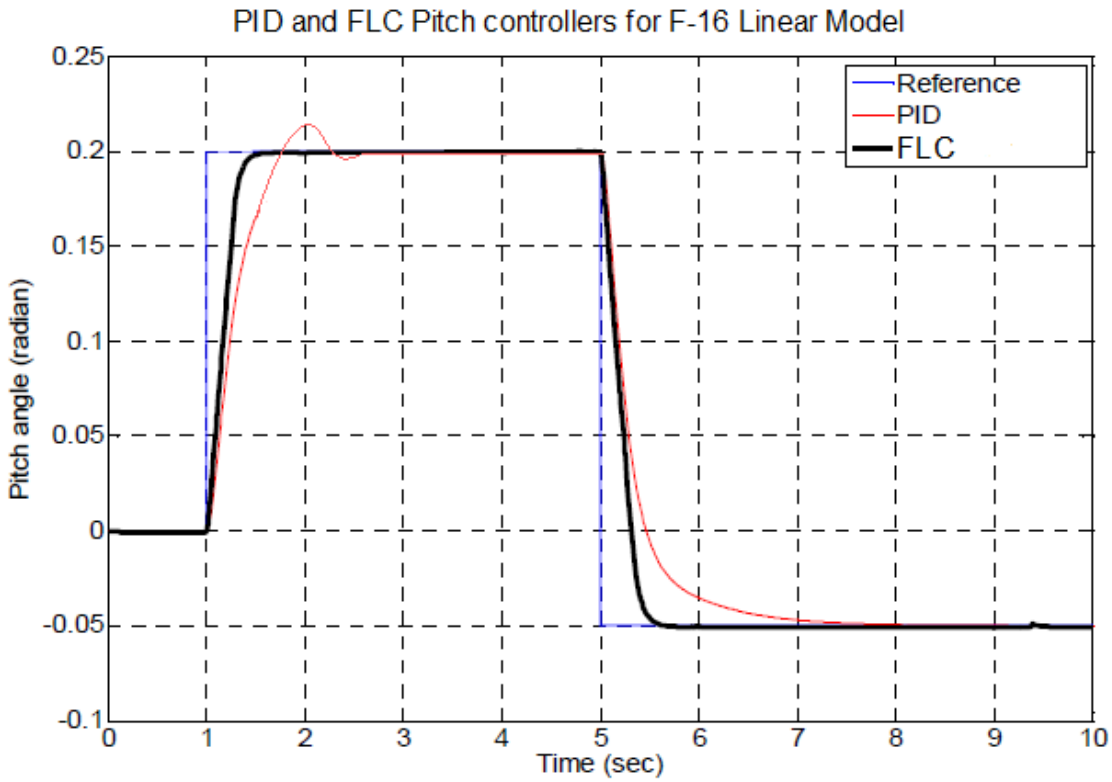

Figure 5.7: *Pitch response with PID and FLC controllers.*

Table 5.2: *Comparison of PID and FLC performance for pitch angle.*

Performance characteristics	PID	FLC
Settling time (s)	3.05 s	1.5 s
Rise time (s)	2.1 s	1.1 s
Peak overshoot (%)	25 %	0 %
Steady-state error (%)	0.001 %	0.001 %

Remark: The steady-state error is computed by comparing graphically the difference between the desired value and the actual value of a system when the response has reached the steady state.

According to the previous results when comparing both of the controllers , the FLC got a faster response with settling time about 1.5 s and rise time about 1.1 s ,the PID with 3.05 s and 2.1 s respectively. The FLC controller is able to give a good response without produce any peak overshoot compared to the PID with 25 % of peak overshoot. Meanwhile, the steady-state error for both controllers is 0.001%.

5.2.3.2 Simulation Results

For comparative assessment, the results clearly shows that FLC controller has the best performance and achieved better tracking response than conventional PID controller and the best controller to enhance the pitch motion of the aircraft. It is indicated from 0% overshoot, faster settling time and faster rising time. At the same time, both control schemes produces the output response with less steady-state error. However, further improvement needs to be done on the FLC controller in order to improve its performance such that it becomes more robust and much better response can be achieved. The limitation in the FLC controller design should be eliminated by adding more membership functions to the controller.

5.2.4 Self-tuning fuzzy PID controller

5.2.4.1 Discussion

The response of the classical PID and the self-tuning fuzzy PID controllers to a step input is shown in Figure 5.8, and the performance characteristics are summarized in Table 5.3

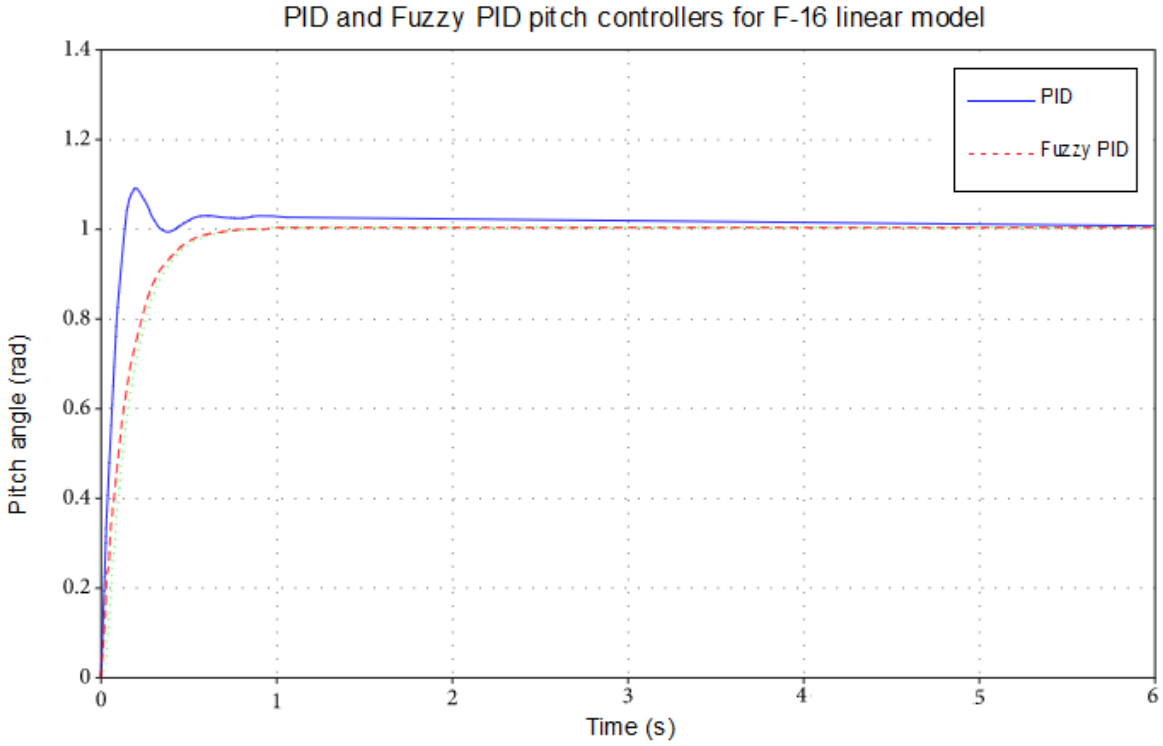

Figure 5.6: *Pitch response with PID and Fuzzy PID controllers.*

Table 5.3: *Comparison of PID and Fuzzy PID performance for pitch angle.*

Performance characteristics	PID	Fuzzy PID
Settling time (s)	1.35 s	0.8 s
Rise time (s)	0.2 s	0.33 s
Peak overshoot (%)	25 %	0 %
Steady-state error (%)	0.002 %	0 %

The result shows better control performance for Fuzzy PID controller than the classical PID controller, without peak overshoot and steady-state error and with a settling time of 0.8s and rise time of 0.33 s, while the PID got a better rise time 0.2 s but with a longer

settling time then the Fuzzy PID about 0.5 s time difference, we also observe a high peak overshoot and a low percentage of steady-state error.

5.2.4.2 Simulation results

The simulation results shows that compared with the traditional PID controller, fuzzy self-tuning PID controller has a better dynamic response curve, performs with better accuracy, it means zero overshoot and zero steady-state error, and settles faster than traditional PID controllers.

The aim of the proposed fuzzy logic-based PID controller is to tune the controller gains automatically to overcome the pitch control and also to eliminate the overshoot without much increase in rise time and eliminate the steady-state error in the response system so that the pitch tracking follows the desired reference.

5.2.5 GA-PID controller

5.2.5.1 Discussion

The results of the implemented Genetic Algorithm PID for pitch controller are shown in Figure 5.9 and the performance characteristics in Table 5.4 above.

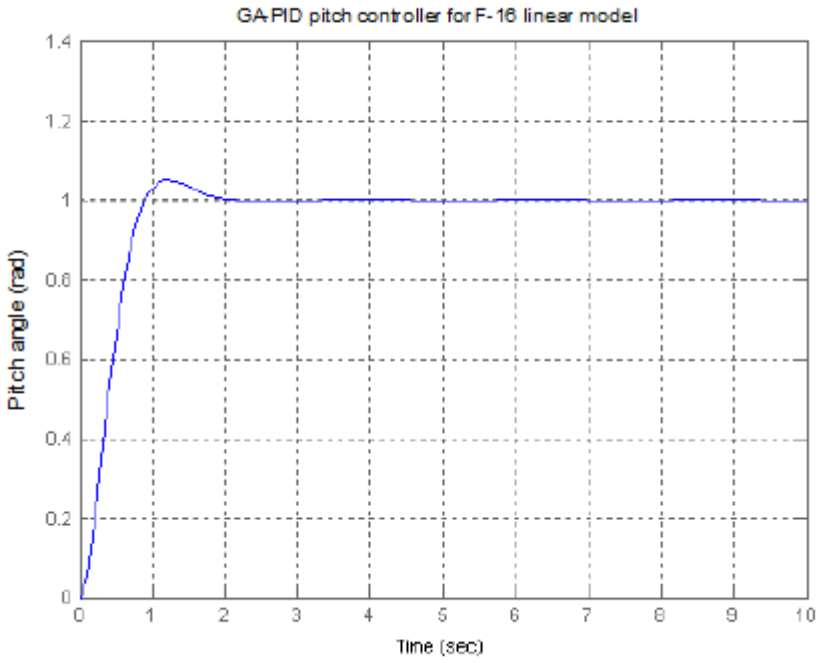

Figure 5.9: *Pitch response with GA-PID controller.*

Table 5.4: *performance characteristics of GA-PID for pitch angle.*

Performance characteristics	GA-PID
Settling time (s)	1.66 s
Rise time (s)	0.592 s
Peak overshoot (%)	12 %
Steady-state error (%)	0.002 %

From one look, the above response is definitely much better than the classical PID tuning method as shown in the previous simulations. In this response, the overshoot value has improved. The settling time has reduced from 2.2s (as shown in Table 5.1) to 1.66 s. The rise time has improved slightly that is 0.592 s as compared to 0.65 s.

5.2.5.2 Simulation results

The simulation response had showed to us that the designed PID with GA has much faster response than using the classical method. Moreover we can add that the GA designed controller has a significant improvement with a much impact in the system optimization over the PID designed controller. The improvement has implication on the efficiency of the system performing the faster response to research stability in the pitch control motion.

5.2.6 H_2/H_∞ with pole placement constraints controller

5.2.6.1 Discussion

The Simulink response implementation of the mixed H_2/H_∞ with regional pole placement controller is shown in Figure 5.10, we used the step response of the LQR for pitch angle for comparison.

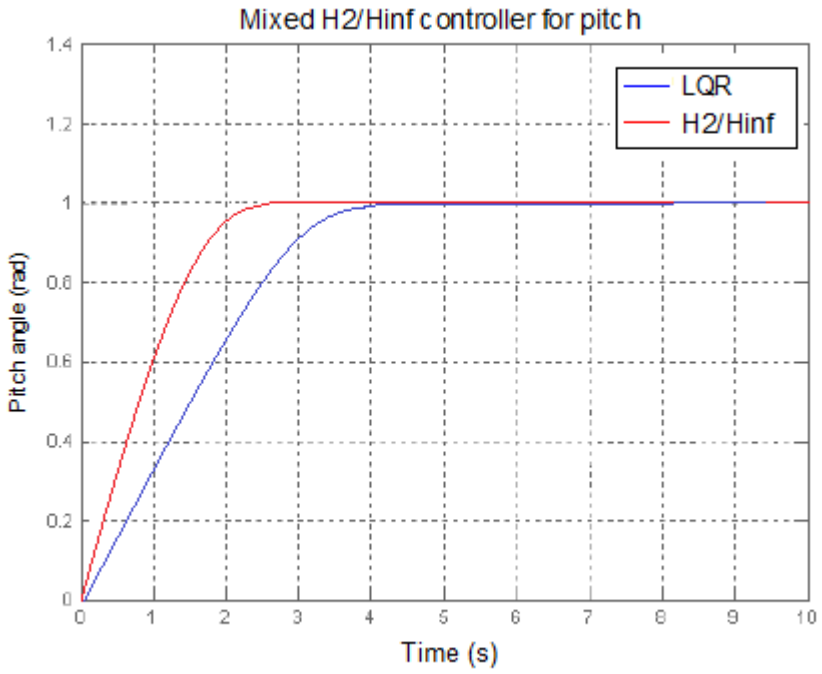

Figure 5.7: *Pitch response with mixed* H_2/H_∞ *and LQR controllers.*

We summarize the performance characteristics in Table 5.5 below:

Table 5.5: *performance characteristics of mixed* $\boldsymbol{H_2/H_\infty}$ *controller for pitch angle.*

Performance characteristics	H_2/H_∞ (longitudinal)	LQR (longitudinal)
Settling time (s)	2.6 s	4.1 s
Rise time (s)	0.65 s	3.5 s
Peak overshoot (%)	0 %	0 %

From the results observed from the Table 5.5 and Figure 5.10 , the step response of the mixed controller have no overshoot and faster settling time and rise time comparing to the classical controller LQR.

5.2.6.2 Simulation results

Mixed H_2/H_∞ control has been developed such that the closed-loop poles are located in a class of regions in the complex plane. The simulation results enhance that the pitch control has improved using the mixed controller H_2/H_∞ output feedback controller based on the LMI method comparing to the LQR. The H_2/H_∞ controller could attenuate the desired response at least 1.5 s faster than the traditional LQR which gives better performance for controlling pitch angle.

5.3 Summary

The non-linear and linear control of the F-16 aircraft has been implemented within simulation environment in MATLAB/Simulink. However from both of the non-linear and linear models simulations presented, we clearly observed instability, particularly in the non-linear model due to the non-linearity which led to instability.

The development and investigation of the proposed controllers for the longitudinal motion control has been evaluated. The proposed controllers consisted of three classical controllers and three mixed controllers schemes. Performances of the controllers have been studied in term of time domain response characteristics specifications. The comparison of controllers considered the aspects of settling time, rise time, overshoot, and steady-state error for some controllers. The comparison results obtained can be summarized in the Figure 5. 11.

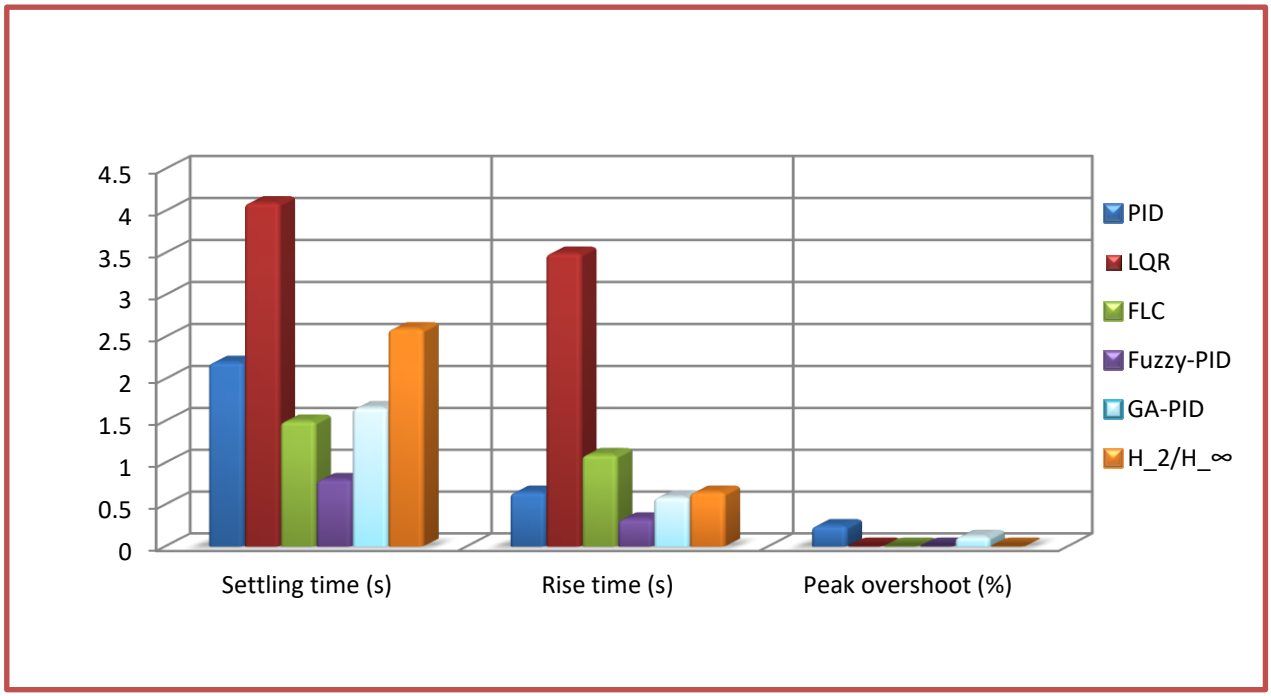

Figure 5.8: *Histogram of the controllers performance characteristics.*

General Conclusion

The emphasis of this thesis is to constitute a basis for the ongoing research on intelligent controllers in the aim of augmenting the pitch control to avoid deep stall conditions of the F-16 fighter aircraft. Therefore, our study consisted of moving from aircraft mathematical modeling included a full non-linear model and a linearized model to the controllers' techniques and concepts designs.

After completing the design process of both types of controllers, a comparative analysis has been examined and compared in terms of settling time, rise time, peak overshoot, steady-state error. The results had showed to us that the mixed controllers had better characteristics performance and much faster response than using the classical ones. The classical method is good for giving us as the starting point of what are the PID values or LQR gain.

However, an optimized algorithm was implemented in the system to see and study the system response. Thus the results obtained through the comparative study are as follows: that fuzzy PID controller generally outperforms the conventional PID controller by eliminating the overshoot; the GA designed PID is much better in terms of the rise time and the settling time; the mixed H_2/H_∞ response was very fast and robust comparing to the LQR it has improved the settling time and rise time with zero overshoot. All this developments led to enhance the pitch control by keeping it following the desired tracking.

On the other hand, it must be emphasized that these mixed types of controllers are not exactly comparable; in fact, it is generally impossible to have exactly the same conditions for a fair comparison of these controllers. The point to make here is that as long as for example fuzzy PID controller work for some control problems on some systems and processes where the conventional PID controller does work or does not work so well. As a consequence that is not to claim that all the methods discussed will replace existing technologies, but the new intelligent controllers achieved good results and therefore they merit and should be further developed and applied.

Finally this project has knowledge in control engineering and its contribution to the improvement of the reliability, safety and security of flight. I hope this work will be of benefit to future students, and I will leave the door of this research open for further developments.

Appendix A

Appendix

A.1 Longitudinal and lateral derivatives

A.1.1 Longitudinal derivative

W-derivatives:

X_w	$-\frac{(C_{D_\alpha} - C_{L_0})QS}{mu_0}$
Z_w	$-\frac{(C_{L_\alpha} - C_{D_0})QS}{mu_0}$
Z_w	$C_{m_\alpha}\frac{(QS\bar{c})}{u_0 I_y}$

$\dot{W}$- derivatives:

$X_{\dot{w}}$	$C_{x_{\dot{\alpha}}}\frac{\bar{c}}{2u_0}\ QS/(u_0 m)$
$Z_{\dot{w}}$	$C_{z_{\dot{\alpha}}}\frac{\bar{c}}{2u_0}\ QS/(u_0 m)$
$M_{\dot{w}}$	$C_{m_{\dot{\alpha}}}\frac{\bar{c}}{2u_0}\frac{QS\bar{c}}{(u_0 I_y)}$

q-derivatives :

X_q	$C_{x_q}\frac{\bar{c}}{2u_0}\ QS/(m)$
X_q	$C_{z_q}\frac{\bar{c}}{2u_0}\ QS/(m)$
M_q	$C_{m_q}\frac{\bar{c}}{2u_0}\frac{QS\bar{c}}{(I_y)}$

α and α̇ derivatives:

Z_α	$u_0 Z_{\dot{W}}$
M_α	$u_0 M_w$
$Z_{\dot{\alpha}}$	$u_0 Z_{\dot{W}}$
$M_{\dot{\alpha}}$	$u_0 M_{\dot{W}}$

A.1.1 Lateral derivatives

β derivatives:

Y_β	$\frac{QSC_{y_\beta}}{m}$
N_β	$\frac{QSC_{n_\beta}}{I_z}$
L_β	$\frac{QSC_{l_\beta}}{I_x}$

β derivatives:

Y_p	$\frac{QSC_{y_p}}{2mu_0}$
N_p	$\frac{QSb^2C_{n_p}}{2I_z u_0}$
L_p	$\frac{QSb^2C_{l_\beta}}{2I_x u_0}$

r derivatives:

Y_r	$\frac{QSC_{y_r}}{2mu_0}$
N_r	$\frac{QSb^2C_{n_r}}{2I_z u_0}$
L_p	$\frac{QSb^2C_{l_r}}{2I_x u_0}$

Appendix B

Appendix

B.1 MATLAB programs

B.1.1 F-16 non-linear model

The following code presents the function to find the trim conditions for straight and level flight at given velocity and altitude.

B.1.1.1 find-trim function code

```
%%%%%%%%%%%%%%%%%%%%%%%%%%%%%%%%%%%%%%%%%%%%%%%%
%F-16 non-linear model
%Code to find intial trim conditions
%--------------------------------------------------------------------------------%
clear all
clc
%%default initial conditions chosen : V=152.4 m/s , h=1500 ft , xcg=0.3

function [ state_trim, control_trim ] = find_trim( velocity, altitude, xcg )

%---- flight constraints --------------------------
global climb_angle; % rate-of-climbing constraint
% climb_angle = input( 'Input the climb angel(deg)' );
climb_angle = 0.0;
global coordi_turn; % coordinate turn constraint
coordi_turn = 0;
global stab; % stability-axis roll constraint
stab = 0;
global skid_turn; % skidding turn constraint
skid_turn = 0;
global rad_gamma; % flight path angle gamma in radian
rad_gamma = 0;
global phi_r; % reference phi
phi_r = 0;
global roll_rate; % reference roll rate
roll_rate = 0;
global pitch_rate; % reference pitch rate
pitch_rate = 0;
```

```
%---- data --------------------------
rtod = 57.29577951; % radian to degree

no_step = 5000; % no. of iteration steps for trimming
disp('  ');
read_no = input('Please input the # of trim iterations ( default =
5000 ):  ');
if read_no == []
no_step = read_no;
end
disp('  ');
disp('-----------------------------------------------------');
disp('Please wait while computing the trim data ......');
disp('-----------------------------------------------------');
epsilon = -1.0;

%---- initial condition ----
x0 = [ velocity
     a. 0.0
     b. 0.0
     c. 0.0
     d. 0.0
     e. 0.0
     f. 0.0
     g. 0.0
     h. 0.0
     i. 0.0
     j. 0.0
     k. altitude
     l. 90 ];

u0 = [  0.73
     a. -1.0
     b. 0.0
          i.  ];

%---- define initial simplex --------------------
s = [ u0(1); u0(2); x0(2); u0(3); u0(4); x0(3) ];
ds = [ 0.2; 1.0; 0.02; 1.0; 1.0; 0.02 ];

%---- simplex algorithm -----------------
init_cost =  cost_f16( x0, u0, s, xcg );
[ s_trim, f_final ] = simplex( s, ds, x0, u0, no_step, epsilon, xcg
);

%---- output the trim result ------------
control_trim = u0;
control_trim(1) = s_trim(1);
control_trim(2) = s_trim(2);
control_trim(3) = s_trim(4);
control_trim(4) = s_trim(5);
state = x0;
state(2) = s_trim(3);
state(3) = s_trim(6);
final_cost = cost_f16( state, control_trim, s_trim, xcg );
```

```
state(13) = tgear( control_trim(1) );
state_trim = constraint( state );
control_trim;
```

B.1.1.2 cost_f16 function code

```
%%%%%%%%%%%%%%%%%%%%%%%%%%%%%%%%%%%%%%%%%%%%%%%%
%Cost function
%This is to define & compute the cost of the current simplex where the states are constrained by different flight condition
function cost = cost_f16 (state, control, s, xcg )

% state   - states before constrained
% control - current control
%  s      - current simplex

control = [ s(1); s(2); s(4); s(5) ];
state(2) = s( 3 );
state(3) = s( 6 );
state(13) = tgear( control(1) );
%---- constraints -------------------------------
state_constr = constraint( state );
time = 0;
% global xcg;
[ xd, an, alat, qbar, amach, q, alpha ] = f16_dynam ( time, state_constr, control, xcg );

cost = xd(1)^2 + 100 * ( xd(2)^2 + xd(3)^2 ) + ...
               1. 10 * ( xd(7)^2 + xd(8)^2 + xd(9)^2 );
```

B.1.1.3 simplex function code

```
%%%%%%%%%%%%%%%%%%%%%%%%%%%%%%%%%%%%%%%%%%%%%%%%%%%%%%%%%%%%
%Simplex function this is to set up a function minimization algorithm( simplex search )to determine a steady-state trim
function [ s_trim, y_low ] = simplex( s, ds, x0, u0, no_step, epsilon, xcg )

% ---- construct the simplex 'vertices' ----
vertices = [];
for i = 1 : 6
for j = 1 : 7
   a. vertices( i, j ) = s( i );
   b. vertices( i, i+1 ) = s( i ) + ds( i );
end
end
% -------------------------------------------------
%    compute the cost at the vertices of the
%    initial simplex and sort them to get the
%    'best' and the 'worst' vertices.
% -------------------------------------------------
y = []; % Here y represents the cost value
y0 = cost_f16( x0, u0, s, xcg ); % initial cost
```

```
y(1) = y0;
for j = 2 : 7
y(j) = cost_f16( x0, u0, vertices( :,j ), xcg );
end
k = 7;
y_high = y(1);
y_low = y(1);
no_high = 1;
no_low = 1;
for j = 2 : 7
if y(j) > y_high
   a. y_high = y( j );
   b. no_high = j;
elseif y(j) < y_low
   a. y_low = y( j );
   b. no_low = j;
end
end
% ------------------------------------------------
%    compute the second 'worst' vertices at which
%    f = max(f(s(i))) for i ~= no_high. f here is
%    computed for later comparison with the
%    reference point s_ref.
% ------------------------------------------------
if no_high == 1
y_temp = y( 2 : 7 );
else
y_temp_1 = y( 1 : no_high-1 );
y_temp_2 = y( no_high+1 : 7 );
y_temp = [ y_temp_1'; y_temp_2' ];
end
y_second = y_temp(1);
for j = 2 : 6
if y_temp(j) > y_second
   a. y_second = y_temp( j );
end
end

% ------------------------------------------------
%    compute the standard deviation to
%    set up the iteration terminate criteria.
% ------------------------------------------------
y_sum = y(1);
for j = 2 : 7
y_sum = y_sum + y(j);
end
y_mean = y_sum / 7;
deviation = 0.0;
for i = 1 : 7
deviation = deviation + ( y(j) - y_mean )^2;
end
devia_stand = sqrt( deviation / 7 );

%-------------------------------------------------------
%  simplex search algorithm
%-------------------------------------------------------
while k <= no_step & devia_stand > epsilon
s_centroid = [];
s_ref = [];
%---- compute the centroid point ----
for i = 1 : 6
```

```
      a. s_centroid(i) = 0.0;
      b. for j = 1 : 7
            i.  if j ~= no_high
           ii.  s_centroid( i ) = s_centroid( i ) + vertices( i, j );
          iii.  end
      c. end
71 s_centroid(i) = s_centroid(i) / 6;
72 end
73 %---- compute the reflection point ----
74 for i = 1 : 6
      a. s_ref(i) = 2 * s_centroid( i )- vertices( i, no_high );
75 end
76 y_ref = cost_f16( x0, u0, s_ref, xcg );

77 %---- compute the new point for the simplex ------------------
78 if y_ref < y_low         %---- case I   ----
      a. s_exp = 2 * s_ref - s_centroid;
      b. y_exp = cost_f16( x0, u0, s_exp, xcg );
      c. if y_exp < y_ref
            i.  s_new = s_exp;
      d. else
            i.  s_new = s_ref;
      e. end
79 elseif y_ref < y_second    %---- case II  ----
      a. s_new = s_ref;
80 else                       %---- case III ----
      a. if y_ref >= y_high
            i.  s_new = 0.5 * ( vertices( :, no_high )' + s_centroid );
      b. else
            i.  s_new = 0.5 * ( s_ref + s_centroid );
      c. end
81 end
82 %---- form the new simplex with the max point no_high
83 %     replaced by the new point derived above ------------------
84 vertices( :, no_high ) = s_new';
85 %---- upgrade step k -----------
86 k = k + 6;
87 % ------------------------------------------------
88 %    compute the cost at the vertices of the
89 %    new simplex and sort them to get the
90 %    'best' and the 'worst' vertices.
91 % ------------------------------------------------
92 y = []; % Here y represents the cost value
93 y0 = cost_f16( x0, u0, vertices( :, 1 ), xcg ); % new cost
94 y(1) = y0;
95 for j = 2 : 7
      a. y(j) = cost_f16( x0, u0, vertices( :,j ), xcg );
96 end
97 y_high = y(1);
98 y_low = y(1);
99 no_high = 1;
100      no_low = 1;
101      for j = 2 : 7
      a. if y(j) > y_high
            i.  y_high = y( j );
           ii.  no_high = j;
      b. elseif y(j) < y_low
            i.  y_low = y( j );
           ii.  no_low = j;
      c. end
102      end
```

```
103       % ------------------------------------------------
104       %    compute the second 'worst' vertices
105       % ------------------------------------------------
106       if no_high == 1
      a.  y_temp = y( 2 : 7 );
107       else
      a.  y_temp_1 = y( 1 : no_high-1 );
      b.  y_temp_2 = y( no_high+1 : 7 );
      c.  y_temp = [ y_temp_1'; y_temp_2' ];
108       end
109       y_second = y_temp(1);
110       for j = 2 : 6
      a.  if y_temp(j) > y_second
            i.  y_second = y_temp( j );
      b.  end
111       end
112       %---- calculate the standard deviation again ----
113       y_sum = y(1);
114       for j = 2 : 7
      a.  y_sum = y_sum + y(j);
115       end
116       y_mean = y_sum / 7;
117       deviation = 0.0;
118       for i = 1 : 7
      a.  deviation = deviation + ( y(j) - y_mean )^2;
119       end
120       devia_stand = sqrt( deviation / 7 );
121       end

122       epsilon = devia_stand;
123       no_step = k;
124       % terminate_text = [ ' The iteration is terminated successfully
   at step = ',...
125       %             num2str(k-1), ' and the standard deviation
   epsilon = ' num2str(epsilon) ];
126       % display( terminate_text );
127       y_low = y( no_low );
128       s_trim = vertices( :, no_low );
```

B.2.1 F-16 linear stability analysis

B.2.1.1 Longitudinal stability

```
1  %%%%%%%%%%%%%%%%%%%%%%%%%%%%%%%%%%%%%%%%%%%%%%%%%%%%
2  %F-16 Linear Model Stability Analaysis
3  %F-16 longitudinal model
4  clear all
5  clc
6  A_long = [0 0 0 1; -32.1 -0.013 -2.66 -1.18; 0 0 -0.67 0.93; 0 0 -
   0.57 -0.87];
7  B_long = [0; 0.0387;-0.0014;-0.1188];
8  C_long =[57.2958 0 0 0; 0 1 0 0;0 0 57.2958 0; 0 0 0 57.2958 ];
9  D_long = [0;0;0;0];
10 poles = eig(A_long)
```

B.2.1.2 Lateral stability

```
%%%%%%%%%%%%%%%%%%%%%%%%%%%%%%%%%%%%%%%%%%%%%%%%
%F-16 Linear Model Stability Analaysis
%F-16 lateral model
clear all
clc
A_lat = [0 0 1 0.078; 0.064 -0.202 0.078 -0.99; 0 -22.92 -2.25 0.54;
0 6.00 -0.04 -0.31];
B_lat = [0 0; 0.0002 0.0005 ; -0.4623 0.0569; -0.0244 -0.0469];
C_lat =[57.29 0 0 0; 0 57.29 0 0;0 0 57.29 0; 0 0 0 57.29 ];
D_lat = [0 0;0 0;0 0;0 0];
poles = eig(A_lat)
```

B.2.2 PID optimal function

```
%%%%%%%%%%%%%%%%%%%%%%%%%%%%%%%%%%%%%%%%%%%%%%%%
%F-16 Linear Model Stability Analaysis
%F-16 linear model
%GA-PID controller design
close all
clear all
clc
function [J] = pid_optim(x)
s = tf('s');
pitch=(-6.8067*s^3-4.6033*s^2-
0.0587*s)/(s^4+1.553*s^3+1.133*s^2+0.0145*s); % Pitch Angle
Kp = x(1);
Ki = x(2);
Kd = x(3);
cont = Kp + Ki/s + Kd * s;
step(feedback(pitch*cont,1));
dt = 0.01;
t = 0:dt:1;
e = 1 - step(feedback(pitch*cont,1),t);
J = sum(t'.*abs(e)*dt);
```

B.2.3 Mixed H_2/H_∞

```
%F-16 Linear Model
%Mixed H2/Hinf code
% clear all
% clc
A_long = [0 0 0 1; -32.1 -0.013 -2.66 -1.18; 0 0 -0.67 0.93; 0 0 -0.57 -
0.87];
B_long = [0; 0.0387;-0.0014;-0.1188];
C_long =[57.2958 0 0 0; 0 1 0 0;0 0 57.2958 0; 0 0 0 57.2958 ];
D_long = [0;0;0;0];
Pp=pck(A_long,B_long,C_long,D_long);
P = ss(Pp);% plant
LeftRealPart = -5;
```

```
RightRealPart = -3;
region = [-2*RightRealPart + 1i 0 1 0;
           0 2*LeftRealPart + 1i 0 -1];
ncont = 1;%Number of control signals,
nmeas = 1;%Number of measurement signals
Nz2 = 1 ;%Number of signals subject
Wz = [0 0];%Weights for H? and H2 performance, specified as a 1-by-2 vector
[K,CL] = h2hinfsyn(P,nmeas,ncont,Nz2,Wz,'Region',region);
pole(CL)
CL = lft(P,K);%Closed-loop system with synthesized controller, returned as
a state-space (ss) model
step(CL(4))% closed-loop step response of pitch
```

Bibliography

[1] Eric Hehs, F-16 Designer Harry Hillaker , code one journal , Posted 15 April 1991.

[2] MANUAL, LOOKHEED MARTIN, F-16 A/B MID-LIFE UPDATE THE PILOT'S GUIDE to new capabilities & cockpit enhancements, US, 15 March 2000.

[3] FRANK L. LEWIS , AIRCRAFT CONTROL AND SIMULATION Third Edition, by John Wiley & Sons, Canada, 2016.

[4] Brian L. Stevens, Frank L. Lewis, Aircraft Control and Simulation, John Wiley & Sons, Inc. 1992

[5] L.T. Nguyen, et al., Simulator study of stall/post-stall characteristics of a fighter airplane with relaxed longitudinal static stability, NASA Tech. Pap. 1538, NASA, Washington, D.C., Dec. 1979.

[6] Michael Cook, M.V., Flight dynamics principles: a linear systems approach to aircraft stability and control, Butterworth-Heinemann, 2012.

[7] Richard S. Russell , F-16 Manual ,University of Minnesota, version 1.0, 22 June 2003.

[8] Robert C. Nelson, Aircraft Stability and Automatic Control, Second edition, McGraw-Hill, New York, 1998.

[9] Charles A. Anderson, General Dynamics Corporation. Convair Aerospace Division, Fort Worth Operation, New York, 16 June 1979.

[10] ETKIN, B. Reid, Dynamics of Flight Stability and Control. John Wily and Sons, New Jersey, 1996.

[11] Sadraey, Mohammad H, Aircraft Design: A Systems Engineering Approach. Chichester, West Sussex, U.K.: Wiley, 2013.

[12] BRIAN D. O. ANDERSON JOHN B. MOORE, Optimal Control LINEAR QUADRATIC METHODS

[13] Dul, F.A.; Lichota, P.; Rusowicz, A. Generalized Linear Quadratic Control for a Full Tracking Problem in Aviation. Sensors 2020, 20

[14] Labane Chrif, Z. M. Kadda, “Aircraft Control System Using LQG and LQR Controller with Optimal Estimation-Kalman Filter Design,” Elsevier, Proce-dia Engineering, 2014.

[15] Svrcek, William Y., Mahoney, Donald P., Young, Brent R. A Real Time Approach to Process Control, 2nd Edition. John Wiley & Sons, Ltd.

[1]Ogata, Katsuhiko. System Dynamics, 4th Edition. Pearson Education, Inc.

[16] PID Controllers , Theory , Design and Tuning K. ÅSTRÖM AND T. HÄGGLUND, 2ND EDITION .

[17] Michael A. Johnson and Mohammad H.Moradi, PID Control New Identification and Design Methods, Nottingham, UK, 2005.

[18] K. M. Passino and S. Yurkovich, Fuzzy Control. Boston, MA, USA: Addison-Wesley Longman, Inc., 1997.

[19] Fuzzy logic toolbox, user's guide," 2017a. The MathWorks, Natick, MA, USA.

[20] H.-J. Rong, S. Han, and G.-S. Zhao, \Adaptive fuzzy control of aircraft wing-rock motion," Appl. Soft Computing J., vol. 14, pp. 181{193, Jan. 2014.

[21] N. Beygi, M. Beigy, and M. Siahi, \Design of fuzzy self-tuning PID controller for pitch

control system of aircraft autopilot," CoRR, vol. abs/1510.02588, Oct. 2015.

[22] Y. Ma, Y. Liu, and C. Wang, \Design of parameters self-tuning fuzzy PID control for dc motor," in 2010 The 2nd Int. Conf. Ind. Mechatronics and Automation, vol. 2, pp. 345{348, May 2010.

[23] Goldberg, David E. ìGenetic Algorithms in Search, Optimization and Machine LearningîAddison-Wesley Pub. Co. 1989.

[24] Naeem, W., Sutton, R. Chudley. J, Dalgleish, F.R. and Tetlow, S., ì An Online Genetic Algorithm Based Model Predictive Control Autopilot Design With Experimental Verification.î International Journal Of Control, Vol 78, No. 14, pg 1076 ñ 1090, September 2005.

[25] D.-W.Gu, P. H. Petkov, M.M.Konstantinov, Robust control design with MATLAB®, Springer, London, 2014. ISBN: 978-1-4471-4681-0.

[26] Scherer, C., P. Gahinet and M.Chilali , Multiobjective output feedback control via LMI optimization. IEEE Trans. Aut. Control 42(7), 896-911. [Output feedback controller design with pole region constraints and constraints on the H_2/H_∞norm is discussed], (1997).

[27] Changhao Chen ,Research Article Advances in Mechanical Engineering ,Study on mixed H_2/H_∞output feedback control of maglev actuator for microgravity vibration isolation system, Advances in Mechanical Engineering 2019, Vol. 11(2) 1–15